UNCLASSIFIED

AD NUMBER
AD148551
NEW LIMITATION CHANGE
TO Approved for public release, distribution unlimited
FROM Distribution: Further dissemination only as directed by Rome Air Development Center, Griffiss AFB, Rome, NY., 30 Jun 1969, or higher DoD authority.
AUTHORITY
RADC ltr, 18 Nov 1988

THIS PAGE IS UNCLASSIFIED

UNCLASSIFIED

AD NUMBER
AD148551
CLASSIFICATION CHANGES
TO: unclassified
FROM: confidential
LIMITATION CHANGES
TO: Distribution: Further dissemination only as directed by Rome Air Development Center, Griffiss AFB, Rome, NY., 30 Jun 1969, or higher DoD authority.
FROM: Controlling DoD Organization... Rome Air Development Center, Griffiss AFB, Rome, NY.
AUTHORITY
30 Jun 1969, DoDD 5200.10; 30 Jun 1969, DoDD 5230.24

THIS PAGE IS UNCLASSIFIED

AD NUMBER
AD148551
CLASSIFICATION CHANGES
TO
confidential
FROM
secret
AUTHORITY
30 Jun 1960, DoDD 5200.10

RL

148551

Technical Information Agency

ARLINGTON HALL STATION
ARLINGTON 12 VIRGINIA

1 OF 4

SECRET

RADC-TR-58-6
AD-148551

SECRET

PROCEEDINGS

PULSE COMPRESSION SYMPOSIUM

10

148551

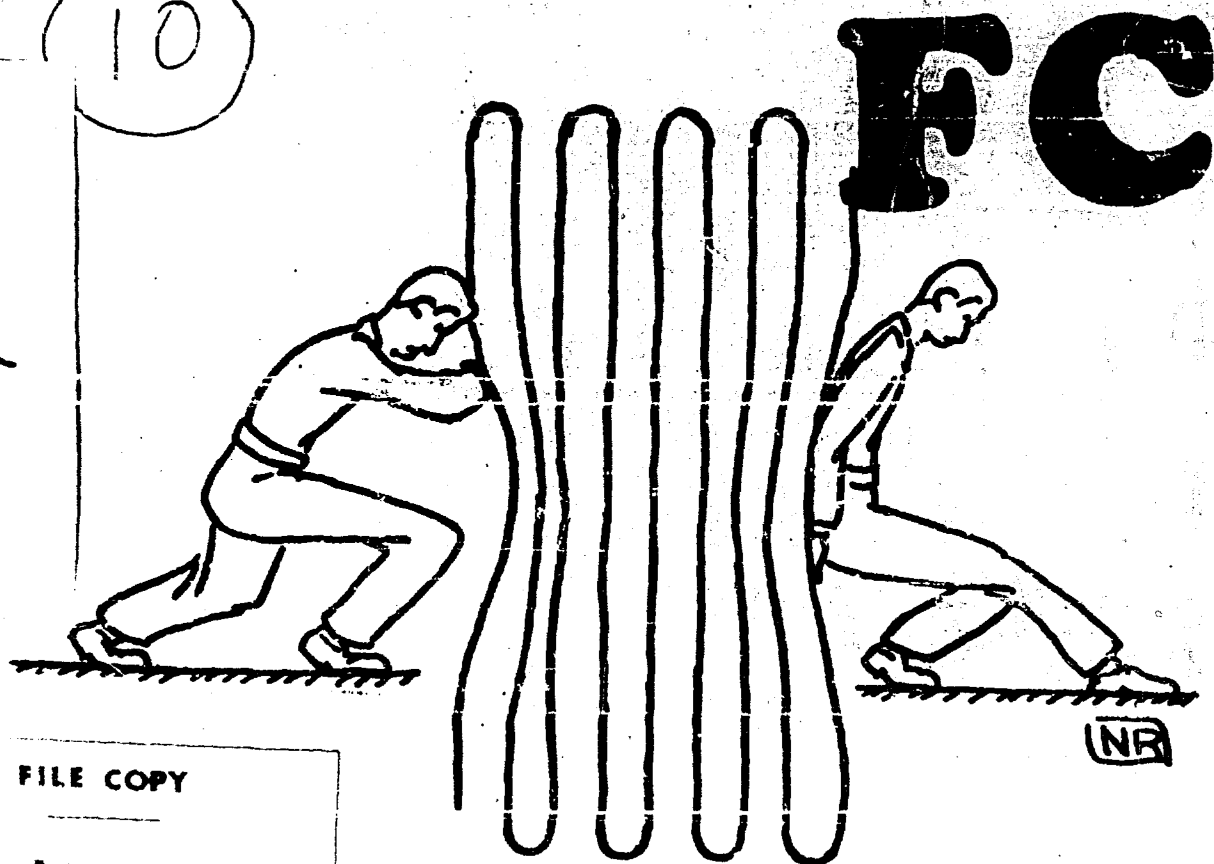

RADAR LABORATORY
ROME AIR DEVELOPMENT CENTER
GRIFFISS AFB ROME, N.Y.
JUNE 25-26, 1957

SECRET

cy 84 of 100 cys
57-9048

UNCLASSIFIED

FOREWORD

A Pulse Compression Symposium sponsored by the Rome Air Development Center was held on 25 and 26 June 1957. Approximately 200 persons from various commercial, educational and government agencies attended this Symposium for the exchange of information concerning recent developments in this field. This technique offers considerable promise in advancing the state-of-the-art in radar and communications.

Fred I Diamond
FRED I. DIAMOND
Chief, Advanced Development Branch
Radar Laboratory

This document is classified SECRET because it reveals pulse compression techniques which are classified SECRET.

APPROVED:

William T. Pope
WILLIAM T. POPE
Chief, Radar Laboratory
Directorate of Control & Guidance

APPROVED:

John S Burgess
for OTTO G. QUANRUD
Colonel, USAF
Director of Control & Guidance

APPROVED:

Harry Davis
HARRY DAVIS
Scientific Director

UNCLASSIFIED

57-9048

UNCLASSIFIED

ROME AIR DEVELOPMENT CENTER
GRIFFISS AIR FORCE BASE, NEW YORK

"PULSE COMPRESSION" SYMPOSIUM

AGENDA

Tuesday Morning, 25 June 1957, 9:30 AM

Welcome Address by Mr. Harry Davis, Scientific Director, RADC

"Waveform Design Considerations", by Messrs. P. W. Howells and S. Applebaum, General Electric Company

"Coded Pulse Theory" by Messrs. W. M. Siebert and R. M. Lerner, Lincoln Laboratory

"LaPlace Transform Treatment of the Modification of a Carrier Envelope by a Linear Network", by Dr. W. R. LePage, Syracuse University

---

Tuesday Afternoon, 25 June 1957, 1:30 PM

"A Matched Filter for Radar" by Messrs. R. C. Thor and E. R. Wingrove, General Electric Company

"A 220 mc/s Distorted Pulse Radar" by Mr. P. D. Hume, Westinghouse Electric Corp.

Lincoln Laboratory Equipment by Mr. L. G. Kraft, Jr., Lincoln Laboratory

"Matched Filter Synthesis Through Phase-Distortion Networks" by Mr. S. Sussman, Melpar, Inc.

An Application of Pulse Coding by Mr. Roger Manasse, Lincoln Laboratory

---

UNCLASSIFIED

57-9048

UNCLASSIFIED

"PULSE COMPRESSION" SYMPOSIUM

AGENDA (CONT'D)

Wednesday Morning, 26 June 1957, 9:00 AM

"Chirp" - A New High Performance Radar Technique" by Mr. A. C. Price, Jr., Bell Telephone Laboratories

"Pulse Compression at S-Band" by Mr. G. P. Ohman, Naval Research Laboratory

"Theory of Matched Filter Pulse Compression" by Mr. R. Schreitmueller, Sperry Gyroscope Company

"Pulse Compression Spectra" by Messrs. C. E. Cook, J. E. Chin and L. R. Sadler, Sperry Gyroscope Company

---

Wednesday Afternoon, 26 June 1957, 1:30 PM

General Discussion Period

UNCLASSIFIED

57-9048

WAVEFORM DESIGN CONSIDERATIONS

Introduction

Our radar defenses are faced with the problem of survival in an environment which becomes continually more demanding. To detect, track, and provide accurate guidance against such targets as supersonic aircraft or hypersonic missiles calls for continual improvements in detection reliability, in the resolution and accuracy of measurement of all target coordinates, and in data rate. Furthermore, such improvements must be achieved in the face of countermeasures which have considerable natural advantage over the radar, in brute force if not in sophistication. To cope with these toughening requirements, there has been a continuing effort to improve radar performance through the development of higher gain antennas, higher power transmitters, more sensitive receivers, and more complicated signal processing. Until recent work by Woodward[1], Elspas[2], Siebert[3], and others, however, little attention has been paid to a factor which puts basic limitations on performance--the radar waveform itself.

The limitations imposed by the radar waveform are well known. Detection reliability or maximum range is limited by the total energy of the signal, range resolution by its bandwidth, and velocity resolution by its time duration. Taking the product of these three factors as a crude figure of merit for the radar waveform, we see that the simple radar pulse is something of a bottleneck. For one thing, its bandwidth-time product is always unity. For another, where the transmitted signal is peak power limited its total energy is proportional to duration, inversely proportional to bandwidth. The designer, then, is always forced to compromise between maximum range and velocity resolution, on one hand, and range resolution on the other. (The velocity resolution referred to here is that achievable on a single-pulse basis.

57-9048

where velocity measurement or clutter discrimination may be performed on a pulse-train basis, as in normal MTI, this is not a limiting factor. However, in many applications involving high-velocity targets, long ranges, or high carrier frequencies, such discrimination may be effectively performed only on a single-pulse basis.)

The target information obtainable with the normal pulse is restricted because it is such a simple waveform. Simple questions elicit simple answers. It seems apparent that to obtain more information we must ask more sophisticated questions, by transmitting long, coded waveforms having a large extent in both the time and the frequency domains. Various codes used with various types of modulation might be employed to produce waveforms having large bandwidth-time products. However, while a large energy-bandwidth-time product is necessary for improved performance, it is not sufficient to guarantee it.

Two problems must be solved. First, a waveform capable of providing the required range and velocity resolution must be chosen. This is a design problem as fundamental to the design of the radar system as the choice of the antenna. Then, a feasible means of processing must be found to encode the signal and decode it in a manner that extracts all the information it contains.

The Matched Filter Approach

A radar is usually required to obtain its target information under adverse conditions, in the presence of noise, countermeasures, or multiple targets. Optimum detection of the signal under such conditions requires receiver filtering which is matched to the radiated signal. It is well known, for example, that with a normal pulse IF bandwidth should be matched to pulse length for best noise performance. Figure 1 illustrates one type of matched filter system in which linear filters are used both to encode and decode a coded pulse signal.

To form the coded signal, a narrow RF pulse is supplied to the encoding filter. Assuming the input pulse spectrum to be flat and linear phase, the coded signal output may be represented by the time response $h(t)$ of the coding filter, or its frequency response $H(f)$. The coding filter cannot, of course, increase the bandwidth of the input spectrum--all it can do is re-arrange it--so the coded signal bandwidth is the same as that of the input pulse. The number and type of coded signals that can be produced in this way are limited mainly by the patience of the filter designer. Long, phase modulated pulses, pulses with linear frequency modulation, even sinusoidal FM signals could be produced by the proper re-arrangement of the impulse spectrum.

The coded signal return from a target is supplied to the matched decoding filter. As shown by North, the requirement on this filter is simply that it have a frequency response which is the complex conjugate of the signal (or the encoding filter). The matched filter characteristic then is $H^*(f)$. Its amplitude response is identical to that of the encoding filter, while its phase or time delay characteristic is the mirror image. This seems reasonable--if the encoding filter has a time delay characteristic which disperses the original pulse, the matched decoding filter should have identical negative delay variations to gather it back together. If the encoding filter emphasized one part of the spectrum more than another, the matched filter should recognize this by weighting the strong part of the signal return more heavily than the weaker, noisier part.

The output of the matched filter is the product of the signal spectrum $H(f)$ by its own frequency response $H^*(f)$. In the time domain, the output is given by the convolution of the signal with the impulse response of the matched filter,

$$A(\tau) = \int h(t)\, h^*(t+\tau)\, dt \qquad (1)$$

Note that this output is <u>not</u> in general the original input pulse. Instead it can be recognized as the autocorrelation function of the coded signal $h(t)$. (It will, of course, be shifted to a time corresponding to target range.) Therefore, we can say that the matched filter cross-correlates the signal return against the transmitted signal waveform, and for good range resolution the coded signal, h(t), should be one having a sharp autocorrelation function in time, with a minimum of "side lobes". Since the minimum effective time duration of the autocorrelation function is the inverse of the bandwidth of the coded signal, it is bandwidth, as stated, which limits range resolution.

The signal-to-noise ratio at the matched filter output has been shown by North to be,

$$S/N = \frac{2E_s}{N_o} \qquad (2)$$

where E_s is total energy in the coded signal return, and N_o is the average noise power per cycle of bandwidth.

This expression leads to two interesting conclusions. First, we may increase the range-velocity resolution of the signal to any desired extent without affecting its detectability, which depends only on its total energy. Second, as the time-bandwidth product of the coded signal is increased, its vulnerability to jamming decreases. For example, assume that the noise power N_o is produced by a jammer which matches the bandwidth (W) and duration (T) of the coded pulse. The total jammer energy competing with the coded pulse is then $E_j = N_o WT$ watt-seconds and Eq. (2) may be re-written

$$S/N = \frac{2E_s}{E_j} WT \qquad (3)$$

If the duration of the coded pulse is fifty times that of the original impulse (but the total energy is the same) it will require fifty times as much energy, on the average, to jam it with a jamming signal that has the correct duration and energy spectrum but is unmatched to the coded signal.

Velocity Resolution

If the coded signal return has suffered a doppler shift due to target velocity, the decoding filter must be shifted in frequency by the same amount, in order to match the shifted signal. When a range of doppler frequencies is expected, a single filter is not enough. A bank of matched filters (or the equivalent) must be provided, one filter for each doppler frequency of interest.

The overall response of such a filter bank to a signal may be explored by considering what happens when a coded signal is supplied to a matched filter tuned off by the difference frequency ϕ. Let the signal still be expressed as $H(f)$. Then, instead of $H^*(f)$, the matched filter frequency response will be $H^*(f+\phi)$, and instead of $h^*(t)$ its impulse response is $h^*(t)\, e^{-j2\pi\phi t}$. As before, the filter output is the convolution of the signal with the impulse response of the filter, or

$$\Lambda(\tau,\phi) = \int h(t)\, h^*(t+\tau)\, e^{-j2\pi\phi t}\, dt \qquad (4)$$

Since this is a function of both range (τ) and velocity (ϕ), it may be called the combined autocorrelation function of the signal. The behavior of this function, as the relative frequency shift is varied, is what determines the velocity resolution capability of the signal.

This point is illustrated in Figure 2. Here, the signal is assumed to be a simple rectangular pulse of duration T, having a sin x/x spectrum whose zeros are spaced at intervals of 1/T cycles apart. The filter bank is assumed to have filters spaced by 1/2T cycles. The bottom filter is tuned to the center frequency of the pulse, so it gives the correct output, the triangular waveform which is the autocorrelation function of the square pulse. The next filter, tuned below (or above) the signal frequency by 1/2T cycles, yields a rounded pulse whose peak is 0.6 that of the correct response. In the presence of noise, this difference might be just perceptible, so the doppler resolution would be 1/T cycles, the spacing between the two filters whose response is perceptibly different from the correct response. As shown in Figure 2, the response of the matched filters tuned further from the signal frequency become successively smaller.

Signal Ambiguity Function

Since the structure of each matched filter is completely determined by the coded signal, the response of each filter to a valid echo depends only upon the form of the coded signal. The time variations of the response from a single filter indicates its range resolution, and the variation in the response with frequency, (that is, from one filter to the next) indicates its doppler resolution. To get a visual picture of the quality of the signal, then, we might construct the surface shown in Figure 3, in which the matched filter responses are plotted vertically on a base plane having range or time as one axis and velocity or doppler shift as the other. The filter bank of Figure 2, of course, provides only the contours of the surface at the fixed doppler frequencies to which the filters are tuned. The complete surface would be described by observing the time response of a single matched filter as it is slowly tuned past a coded signal of fixed frequency (or as the signal is tuned past a fixed filter).

These time responses may be obtained analytically by evaluating Eq. (4) for $A(\tau, \phi)$, using a number of different values for the frequency shift ϕ. Where the signal is more conveniently expressed in terms of its frequency spectrum, the equivalent form,

$$A(\tau, \phi) = \int H^*(f)\, H(f+\phi)\, e^{-j2\pi f \tau}\, dt \qquad (5)$$

may be used.

Either Eq. (4) or Eq. (5), then, provides a complete description of the ambiguity function for a coded signal. The contours of this function parallel to the range-time axis represent the time response of a matched filter to the signal, the time autocorrelation function of the signal for any given value of frequency difference, ϕ. Contours taken parallel to the velocity-frequency axis represent the frequency autocorrelation function of the signal at a given value of time.

Since it is the result of complete matched filter processing of the signal return, this ambiguity function represents <u>all</u> the information that the radar signal contains regarding target range and velocity. It provides a measure of the ability of the radar to resolve targets in these dimensions, in exactly the same way that the antenna pattern indicates its ability to resolve targets in azimuth and elevation. If, for example, a pencil beam antenna explores a point target in space, the shape of the target revealed on an azimuth vs. elevation plot is not the point target, but the shape of the exploring beam. Two targets will be resolved only if they are separated by more than one beam width. Similarly, when we radiate a signal to explore the two-dimensional (range-velocity) target distribution along a given line of sight, two targets will be resolved only if their combined range-velocity separation exceeds the "beamwidth" of the signal ambiguity function. As with the antenna pattern, <u>accuracy</u> in locating a single target may be improved to any desired extent with sufficiently high signal-to-noise ratio. This simply amounts to measuring the location of the peak of the ambiguity function by techniques similar, say, to monopulse antenna techniques. Where targets are to be detected in the presence of noise, jamming, or background clutter, however, it is resolution or beamwidth that counts. Because such signals lack coherence they will tend to sum power-wise rather than voltage-wise, so the ambiguity function should be expressed as the power distribution. $\left[A(\tau,\phi)\right]^2$ in determining resolution.

Superficially, at least, the antenna analogy may be carried somewhat further. The ambiguity function has been compared to the far field pattern of an antenna. A similar comparison might be made between the time-frequency structure of the coded signal and the aperture illumination function of the antenna. And between the time-bandwidth product of the signal and the dimensions of the aperture. The analogy is not exact, of course, but may be helpful in conveying a feeling for the problem.

Radar Signal Selection

The foregoing discussion leads to the conclusion that the radar signal should be designed to provide the desired range-velocity resolution, just as the antenna is designed to provide spatial resolution. Unfortunately, signal design does not appear to be as straight-forward a process as antenna design. In specifying the ambiguity function, for example, it appears that selecting a single contour puts severe restrictions on the entire function. And when the time waveform of the signal is chosen, its frequency spectrum is, of course, determined. At present, selection of the "ideal" waveform requires some intuitive reasoning based on certain ground rules, which may be determined by examining the properties of Eqs. (4) and (5):

(1) Range resolution is largely determined by the frequency structure, doppler resolution by the time structure of the signal.

(2) For a signal duration of T seconds, best doppler resolution is 1/T cycles; for a bandwidth of W cycles, best range resolution is 1/W seconds. This is illustrated in Figure 4a which shows ambiguity function contours for a long and short pulse.

(3) For a given duration, best doppler resolution is obtained with a signal which is flat in time. For a given bandwidth, sharpest range resolution requires a signal flat in frequency. This favors the use of various types of phase modulation. A nearly ideal waveform would be clipped white noise, whose ambiguity contour is shown in Figure 4b. Unfortunately, such a signal must contain a statistically large number of indepedent samples to give a satisfactory approach to the ideal. Matched filter processing equipment for such signals tends to get out of hand.

(4) The power ambiguity function, when normalized with respect to total signal energy, has a peak value of unity and unit total volume. The height and total volume of the ambiguity function for an ideal coded signal is therefore the same as for the simple pulse. However, while the pulse function is a relatively simple main lobe of unit height, 2T seconds total length and 2W cycles width, the "ideal" signal function will be a sharp central spike of unit height, 1/W seconds length and 1/T cycles width, surrounded by low skirts extending out of the limits of 2T seconds and 2W cycles. As the time-bandwidth product of the coded signal is increased from its value of unity for a simple pulse, then, more and more of the total volume is represented by the low extended skirts of the ambiguity function, and less and less by the central spike. Under unfavorable conditions, this may lead to a reduction in "contrast" between a target and its surroundings, since nearby targets will contribute their skirt responses to hide the desired target. At worst, when the entire skirt area (2T, 2W) surrounding a target is solidly filled, both in range and velocity, by clutter, the coded signal will give results no better than a simple pulse. (This is not a weakness against jamming since for a jammer to fill this area solidly would require a large increase in its energy.) Usually, the clutter will occupy a small fraction of the skirt area, and performance will be better than the simple pulse performance by a factor dependent on the bandwidth of the coded signal.

This situation suggests a more "ideal" signal than the clipped noise. As shown in Figure 4c, when a signal is repetitive in time or frequency, its ambiguity function also becomes repetitive. The case illustrated is a train of short pulses, where the "side-lobes" represent the well known blind speed and second-time-around responses. While normal blind speeds tend to fall in the velocity range of interest, the proper use of repetition in the signal code may allow us to push these skirt responses outside this range, thereby allowing increased resolution without introducing harmful skirt response. This is illustrated in Figure 4d.

Dispersed Impulse Coding

Figure 5 shows two examples of a type of signal coding which offers interesting possibilities. Both are generated by dispersing a narrow impulse having a flat spectrum sharply cut off at the edges of the desired band. The flat spectrum is used to provide the best possible range resolution for a given bandwidth.

Linearly Dispersed Impulse - To produce this signal, the impulse is passed through a filter having a square-law phase or linear time delay vs. frequency characteristic. Since the high frequencies are delayed more than the lows, the result is an extended pulse with a duration roughly equal to the maximum delay difference of the filter, and a linear frequency modulation.

The ambiguity function for this signal (Figure 5a) indicates that while it offers some of the advantages of pulse coding, it does not approach the ideal in range-velocity resolution. Its ambiguity contour resembles that of the short pulse, except that its long dimension lies along a diagonal in the range-velocity plane. Targets whose range-velocity separation lies along this diagonal line will be poorly resolved. For single targets and high signal-to-noise conditions, the accuracy of measurement of range and velocity may be improved by using dispersion of opposite sign on successive transmissions.

Sinusoidally Dispersed Impulse - This signal is produced by passing the impulse through a filter having a sinusoidal time delay characteristic. The result is like an extended pulse containing one cycle of sinusoidal FM, except that the time waveform corresponds to the spectrum of normal FM, and the spectrum to the time waveform. The ambiguity function for this signal, shown in Figure 5b, indicates a combined range-velocity resolution which is not far from ideal. Under certain conditions, more than one cycle of "FM" could be used to yield greater resolution at the expense of "side-lobe" responses lying outside the velocity range of interest.

Neither of these signals are ideal in the sense of having a flat time waveform which would allow limiting without some loss of information, but both may be regarded as an interesting base of operations for further exploration.

Matched Filter Equipment

When and if the ideal coded signal for a given application is found, it will be useless unless a practicable means exists for processing it to extract all the information it contains regarding target range and velocity. As suggested in Figures 1 and 2, one such means is a bank of matched filters, with each filter tuned to a different velocity. It is not necessary, in this scheme, to completely duplicate the complex matched filter structure for each velocity--much of the structure may be common to all. The system output appears in a number of parallel velocity channels, requiring separate detectors for each channel, or some means of combining the outputs that retains velocity information and does not involve a penalty in S/N performance.

One such means would be a sampler which rapidly scans the outputs of the matched filter bank. Providing that a complete velocity scan occurs in a time equal to or less than one range resolution cell (the inverse of signal bandwidth), no information is lost in the sampling process. Range of a target is indicated by the scan on which its peak occurs, while its velocity is given by the location of its peak inside that scanning interval. The sampler output might be regarded as the result of a television-raster scan of the range-velocity plane. Displayed as video on an orthogonal range-velocity scan, this output will generate a brightness image of the range velocity plane, showing target ambiguity functions in their proper locations.

Conclusions

The considerable recent interest in coded signals for radar is seen to be solidly based on a number of potential advantages:

Maximum Range - Signal detectability or maximum range depends only on total signal energy. While the coded signal does not offer a fundamental advantage over the simple pulse, its lower peak power may be of practical advantage.

Combined Resolution - Unlike the simple pulse, the coded signal allows independent control of range and velocity resolutions. The combined resolution figure of merit for any signal is tis time-bandwidth product. For the simple pulse, this product is unity, but with coded signals, products in the order of 100 are within the realm of possibility.

Sub-Clutter Visibility - The improved resolution of the coded signal may be used to obtain improved sub-clutter visibility. It is difficult to state a general figure of merit, because each different target-clutter environment implies a different criterion for the design of the coded signal. The signal design should ensure that the clutter ambiguity function is very low in the velocity range occupied by targets.

Anti-Jam Capability - A figure of merit indicating the AJ capability of a signal is its energy-time-bandwidth product. Again, the coded signal may have a figure of merit as much as 100 times that of a simple pulse, for equal energy. This figure of merit is a measure either of the increased energy required in a simple jammer, or the increased complexity of a sophisticated jammer which determines and matches the signal code. Matched deceptive jamming may, of course, be countered by changing the code from pulse to pulse.

These potential advantages depend on the ability to design an ideal signal waveform for a given environment. Work in this direction seems quite promising. Processing equipment for coded signals also seems to be within the reach of present techniques. While this equipment is undeniably complex, it produces some results which cannot be achieved with simple pulse systems, and others which might be considerably more expensive to obtain by brute force. If the field of coded signals lives up to its early promise, we should see a gradual obsolescence of the simple pulse as a radar waveform.

Acknowledgment

This paper has been an attempt to present the salient features of pulse coding theory, as developed by Woodward, Elspas, Siebert et. al., in a manner lending itself to physical and visual understanding of the important concepts. With minor exceptions, no claim is laid to originality, except possibly in the case of errors made by the authors.

References

[1] P. M. Woodward, "Probability and Information Theory, with Applications to Radar", Chapter 7, Pergamon Press Ltd., London, 1953

[2] Bernard Elspas, "A Radar System Based on Statistical Estimation and Resolution Considerations", Stanford University, Applied Electronics Laboratory, Technical Report # 361-1, August 1955

[3] W. M. Siebert, "A Radar Detection Philosophy", IRE Trans. on Information Theory, Volume IT-2, No. 3, pp 204-221, September 1956.

P. W. Howells
S. Applebaum

April, 1957
njl

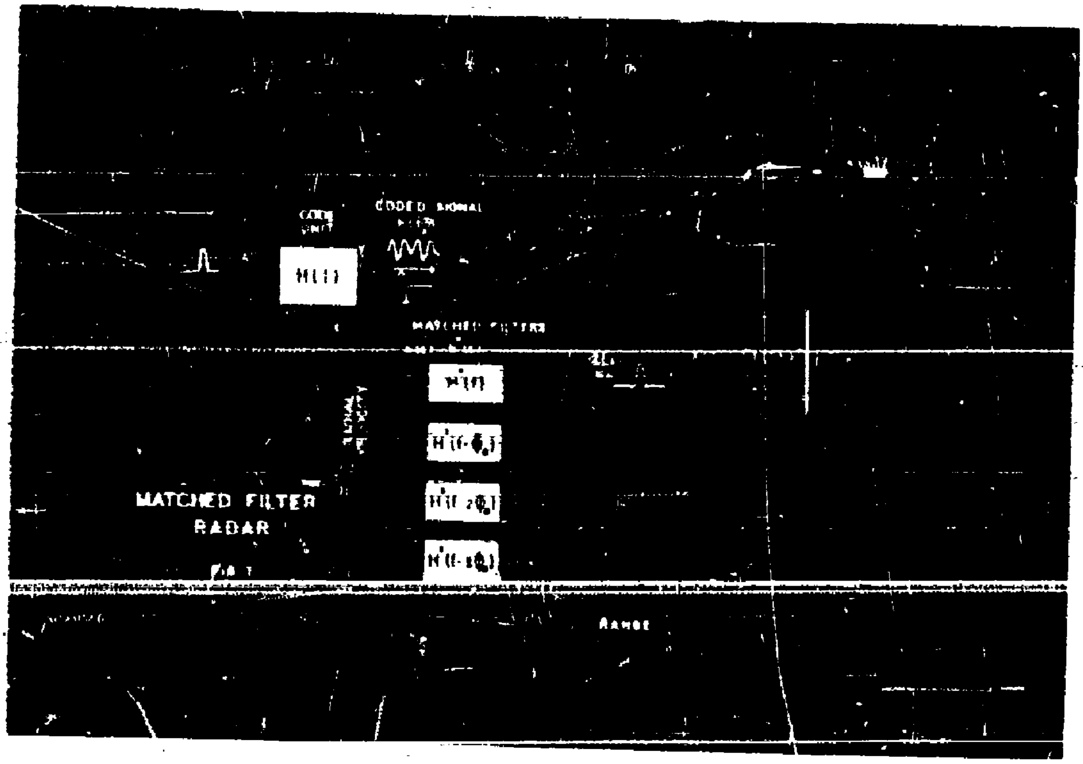

01

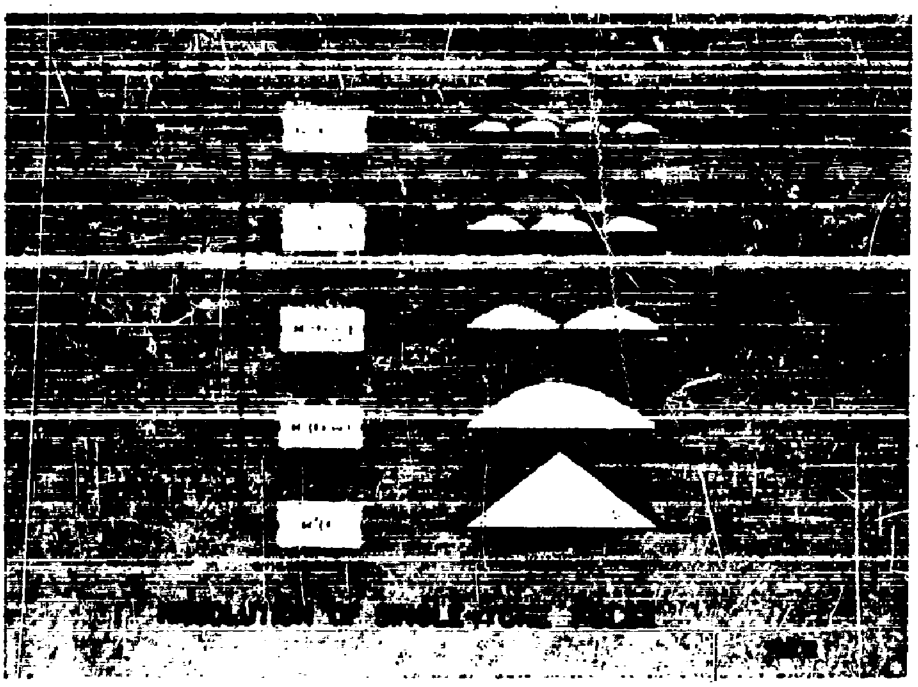

AMBIGUITY FUNCTION OF
[illegible]
FIG 3a

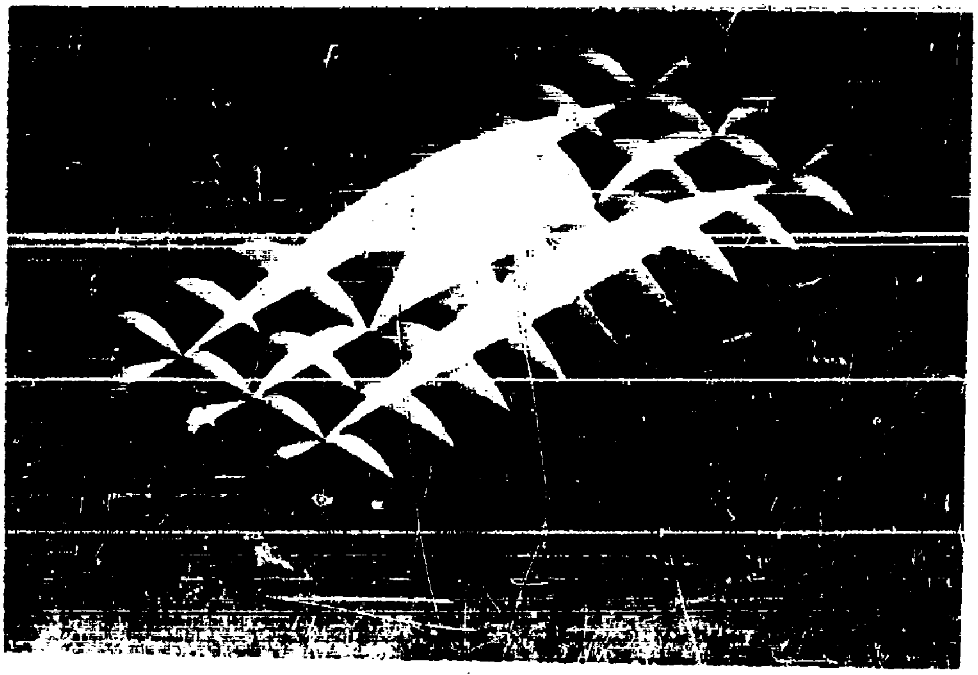

AMBIGUITY FUNCTION OF
SINGLE TONE PULSE
FIG 3a,b,c

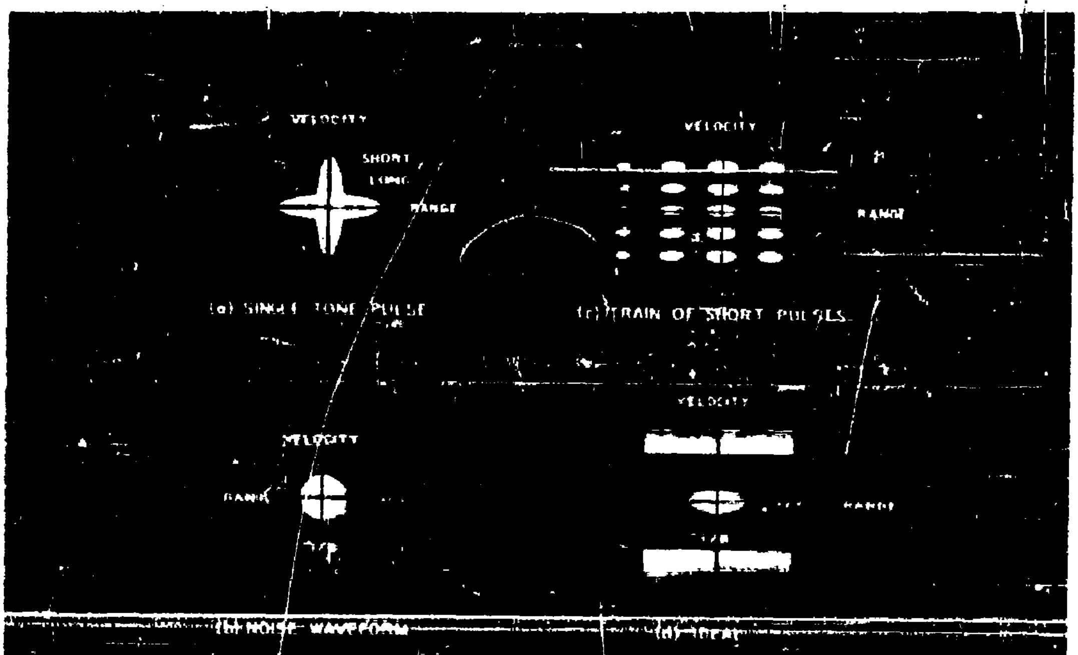

AMBIGUITY DIAGRAMS

FIG. 4

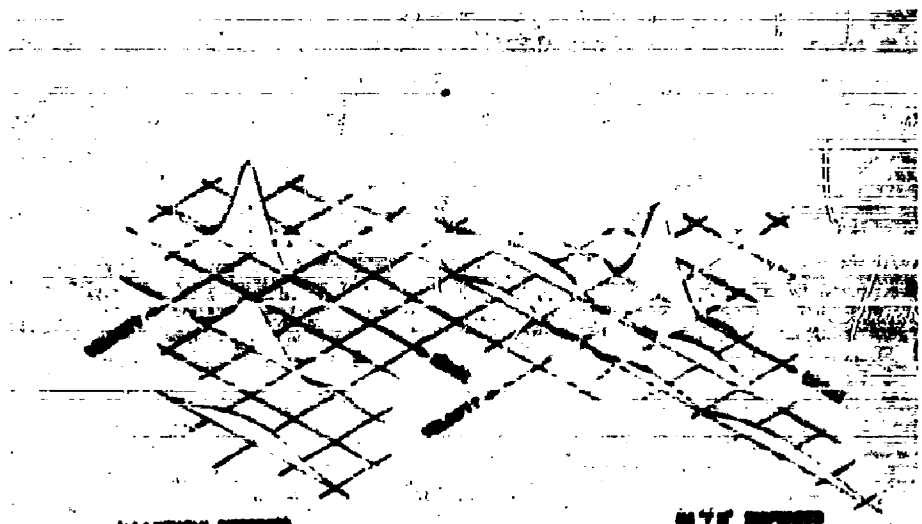

POWER AMBIGUITY FUNCTION

FIG [illegible]

Laplace Transform Treatment of the Modification of a Carrier Envelope by a Linear Network

Wilbur R. LePage, Consultant, Sylvania
Chairman, Dept. Electrical Engineering,
Syracuse University

When a modulated carrier $f(t) \cos\omega_0 t$ passes through a network described by the system function $H(j\omega)$ it is customary to use the spectrum of $f(t)$ obtained by the Fourier transform. This spectrum is shifted to a center at ω_0, with its image at $-\omega_0$ usually being neglected. This is a useful technique for many purposes. However, where explicit response formulas are required, or where phase functions are violent functions of frequency, the Fourier transform loses much of its force.

The Laplace transform formulation gives an alternate treatment which, in some cases, may be more useful. It is found that the envelope of the response is approximately proportional to

$$r_1(t) \quad \overline{r_1(t)}$$

where $r_1(t)$ is a complex function of real t, and $\overline{r_1(t)}$ is its conjugate. The complex function $r_1(t)$ is obtained from the inversion integral with kernel $F(s)k(s)$. $F(s) = \mathcal{L}[f(t)]$ and $k(s)$ is a function derived from $H(s)$ by throwing out half its poles and making a translation in the S-plane. An estimate of the error is obtained in terms of a second function $r_2(t)$ which is the inverse Laplace transform of $F(s) = k^*(s + j2\omega_0)$ where the asterisk implies a conjugate function of k (meaning all poles and residues replaced by their conjugates). An example is worked out, applying the theory to the case of an all-pass non-minimum-phase network.

A MATCHED FILTER FOR RADAR

(Unclassified Title)

by

R. C. Thor and E. R. Wingrove

Often a radar system design is limited in range not by the average power capabilities of the transmitter, but by the peak power in some part of the transmitter-antenna system. If the range must be increased, ordinarily the only possibility is to increase the system duty cycle and accept the resulting loss in range resolution. However, the system to be described permits increase of the duty cycle up to the limit set by the average power capability of the transmitter, without sacrificing range resolution.

Basically, the operation of the system consists of the following steps. A pulse having the desired range resolution is passed into a network having a flat amplitude response over the pulse bandwidth and a special phase response. The output of the network is a lengthened pulse giving the desired transmitter duty cycle. This long pulse is transmitted, reflected from targets present, and received in the usual manner. In the receiver, the long pulse in effect passes through another network again having flat amplitude response, but with a phase response which is inverse to that of the original network. This restores the components of the long pulse to their initial phase relationships, and the short pulse is recovered at the output of the network.

A mathematical analysis giving a theoretical explanation of the operation of the system is presented. Experimental equipment using conventional circuitry giving an increase in duty cycle of 50:1 is described. Spurious side lobes accompanying the recovered short pulse are down 30 db.

57-9048

SECRET

SECRET

A 220 Mc Distorted Pulse Radar

Summary:

Reasons for pulse distortion are briefly covered. The paper then outlines some methods of pulse distortion and leads up to the dispersive all pass lattice filter which is used in this Radar Set. Some advantages of this distortion technique are noted.

A detailed description of the dispersive filter theory is then presented. Some idealizations are necessary as an aid to calculation, but the results presented are shown to be borne out in practice. A simple method of understanding the mode of action of dispersion and recombination results in an approximate graphical analysis. The theoretical performance limits are pointed out, and lead to a choice of system parameters.

The paper then goes on to describe a bread broad model radar set using these parameters and details the engineering considerations for incorporating pulse distortion into a Radar System so that all the theoretical advantages may be realized. It is demonstrated that although problems may arise they may be overcome by existing circuit techniques.

Peter D. Hume 57-9048

Peter D. Hume, Sr. Engr.
Advanced Development Sub-Div.
April 18, 1957

SECRET

A 220 MC DISTORTED PULSE RADAR

1. Reasons and Methods for Pulse Distortion.

In this paper we shall consider distortion as meaning a specific operation on a time function before transmission as a radar signal.

On reception an inverse or complementary operation is performed, such that certain system advantages will result.

These advantages can result in:

1.1 Higher average power, with a corresponding increase in range,

1.2 Secrecy, and

1.3 Improved anti-jam performance over a conventional radar set.

The increased average power is realised since the distortion of the radar pulse can be arranged to lengthen it. Output power being usually restricted to a certain peak value, due to voltage breakdown etc., a longer transmitted pulse results in a better output duty cycle.

Improvements in the duty cycle by increasing the PRF or by using merely a longer pulse of the normal pulsed C.W. type are seen to result in reduced range or reduced resolution respectively. A useful distortion technique must not incur these disadvantages, and three cases known to the writer result in a longer output pulse without loss of range or resolution to any large extent.

In one instance a short pulse is lengthened by successive reflections up and down a delay line. The original and its images are then added and used for transmission. The addition may not occur in the most obvious manner, depending on various considerations of resolution etc.

The pulse on reception is now decoded by a similar series of reflections and additions, and in theory it is possible for the successive images to suffer such numbers of passes over the line that they all add up at one particular point and time and produce a replica of the original pulse. In this system the limiting case is that where the transmitted signal is virtually C. W. but has phase discontinuities corresponding to successive reflected samples. Decoding is done in a passive network, but the encoding may be performed by active switching techniques.

The output pulse (long pulse -- we may call it) of this system is lengthened in effect by addition to its original copies obtained after certain discrete time delays.

These delays may be made continuous by using a network which has different propagation times for different components of the original signal (the short pulse). Reception decoding is now performed by passing the long pulse through a network having a complementary continuously varying delay.

The difficulty here is one of obtaining complementary delay networks with smooth delay variations.

A different approach using smooth variations at the receiving end uses active circuit techniques to generate the long pulse signal for transmission. In effect a radar signal is a modulated carrier and the required time function may be generated by time bases and frequency modulators with almost limitless possibilities. The active devices are designed to provide a signal which may be decoded and compressed into a pulse compatible with the system bandwidth. The compression decoding is done in a passive network, so that one requires the active devices to maintain their adjustment relative to inactive ones.

A third method, which forms the subject of this paper, uses passive networks with smooth delay variations at both the stretching and compressing points. All pass lattice networks are employed, and their design is merely a repeat of one basic element.

The resulting radar signal is a close approximation to a sawtooth frequency modulation over the frequency band consistent with the system range resolution. Very effective use is therefore made of the spectrum bandwidth.

2. The All-Pass Lattice System.

This uses not only passive networks at both receive and

57 9048

SECRET

transmit ends, but furthermore the networks used are identical in all respects. There is even a possibility of using one network for both functions on a time and frequency duplex basis.

2.1. The simple lattice element. (Slide # 1) Fig. 1.

The lattice elements are chosen so that

$$\omega_0 L_1 = 1/\omega_0 C_2 = R_0 = \text{pure resistance}$$

R_0 is the characteristic impedance of the lattice.

This defines

$$\omega_0 = \frac{1}{\sqrt{L_1 C_2}} = \text{Lattice design frequency.}$$

Then it may be shown that if

$$\gamma = \alpha + j\beta$$

is the propagation constant of one section, then

$$\alpha = 0 \quad \text{and} \quad \beta = 2 \arctan \omega/\omega_0$$

where ω is the frequency variable. β is understood as the phase shift of one section. Obviously if identical sections are cascaded and R_0 is left unchanged, the total phase shift is

$$\phi(\omega) = 2n \arctan \omega/\omega_0 \text{ for } n \text{ sections}$$

since the separate phase shifts of the image matched sections will add linearly.

Figure 2 (Slide # 2) shows a plot of the arctan x function.

57-9048

SECRET

Consider now a carrier of frequency ω_1 where $\omega_1 < \omega_0$ with a modulation envelope producing sidebands over the frequency range $(\omega_1 - p_0) < p < (\omega_1 + p_0)$

The modulation will be due to a time function of low pass bandwidth p_0, and we may call this time function $f_0(t)$

Then

$$f_0(t) = \int_{-p_0}^{p_0} A_0(p)\, e^{jpt}\, dp$$

We may assume a symmetrical time function so that $A_0(p)$ becomes real. This is merely a convenience in the explanation. When this time function modulates a cosinusoidal carrier of frequency ω_1 then

$$A_0(p) \quad \text{becomes} \quad \frac{1}{2}\left[A_0(p-\omega_1) + A_0(p+\omega_1)\right]$$

When this signal $f_0(t)$ traverses the lattice the phase characteristic ϕ is impressed onto the signal and the resulting frequency function is proportional to

$$\left[A_0(p-\omega_1) + A_0(p+\omega_1)\right] e^{-j\phi(p)}$$

where

$$\phi(p) = 2n \arctan p/\omega_0$$

and p is now the frequency variable.

Application of the stationary phase principle shows that we may consider this phase characteristic as imparting

57-9048

SECRET

a group time delay proportional to

$$\frac{d\varphi(p)}{dp} = \frac{2n\omega_0}{\omega_0^2 + p^2} \qquad \text{Fig. 3. (Slide \# 3)}$$

This time delay is a function of p and heuristically means that different parts of the signal frequency spectrum arrive at different times. It is noteworthy that over the range

$$.2 < p/\omega_0 < 1$$

this time delay is nearly a linear function of frequency. (Slide # 3. Fig. 3)

If a network of complementary time delay were available, we would expect it to undo the effects just described.

The actual distorted pulse used as a radar signal may be visualized as an envelope obtained by reflecting the frequency function of the signal pulse in the time delay versus frequency graph of the lattice filter. This latter is approximated as the slope of the phase characteristic. This process appears to be valid if the actual time delay variation over the signal bandwidth is large compared with the original signal time duration. This will be so in any pulse stretching scheme of practical interest.

Our system uses 240 identical lattice sections and stretches a 6 μsec pulse to about 100 μsec. Lattice parameters are

SECRET

$R_o = 360\ \Omega$ $\qquad \omega_2/2\pi = .375$ Mc
$L_1 = .367\ \mu h$ $\qquad \omega_1/2\pi = .225$ Mc
$C_2 = 500$ pf.

Only the main lobe of the 6 μsec pulse spectrum is passed by the system.

Fig. 4, Slide 4.

This, when modulated on a .225 Mc carrier, has amplitude zeros in its spectrum at about .075 Mc and .375 Mc.

$\frac{\sin x}{x}$ Between these points the spectrum has the well known form corresponding to a rectangular time function.

Fig. 5, Slide 5 shows the idealized input time function, used for computation.

Fig. 6, Slide 6 shows the output envelope as computed.

Fig. 7, Slide 7 and Fig. 8, Slide 8 are photographs of above 5 and 6 modified by band pass response limits of system. The F.M. nature of the distorted pulse is apparent. We have thus obtained a long pulse by dispersion of a short one. Undispersion is necessary for a complete system. This appears to need a network with a phase characteristic complementary to the dispersing lattice.

We avoid this awkward component by inversion, not of the network, but of the spectrum applied to it. This may be done by heterodyning the signal with a carrier of frequency $2\omega_1$ at some point in the receiver. The frequency function

57 9048

SECRET

now has terms of the form

$$A_0(p-\omega_1-2\omega_1) \qquad A_0(p-\omega_1+2\omega_1)$$
$$A_0(p+\omega_1-2\omega_1) \qquad A_0(p+\omega_1+2\omega_1)$$

each one of which carries the phase function $e^{-j\varphi(p)}$ modified by the appropriate frequency translation.

By filtering we select the terms $A_0(p-\omega_1+2\omega_1)$ and $A_0(p+\omega_1-2\omega_1)$ which are $A_0(p+\omega_1)$ and $A_0(p-\omega_1)$ as in the original carrier borne signal.

The phase characteristics have meanwhile become

$$e^{-j\varphi(p+2\omega_1)} \quad \text{and} \quad e^{-j\varphi(p-2\omega_1)}$$

respectively where

$$\varphi(p+2\omega_1) = 2n \arctan \frac{p+2\omega_1}{\omega_0}$$

and

$$\varphi(p-2\omega_1) = 2n \arctan \frac{p-2\omega_1}{\omega_0}$$

so that the signal frequency function now is proportional to

$$A_0(p+\omega_1)\, e^{-2jn \arctan \frac{p+2\omega_1}{\omega_0}} + A_0(p-\omega_1)\, e^{-2jn \arctan \frac{p-2\omega_1}{\omega_0}}$$

This signal is now applied to an identical lattice to the one used for stretching. The frequency function now becomes proportional to

$$\left[A_0(p+\omega_1)\, e^{-j\varphi(p+2\omega_1)} + A_0(p-\omega_1)\, e^{-j\varphi(p-2\omega_1)}\right] e^{-j\varphi(p)}$$

SECRET

or

$$A_0(p+\omega_1)\, e^{-j\left[\varphi(p+2\omega_1)+\varphi(p)\right]} + A_0(p-\omega_1)\, e^{-j\left[\varphi(p-2\omega_1)+\varphi(p)\right]}$$

When this is demodulated the resulting effect may be considered as a further heterodyning with frequency ω_1 followed by a filtering of the components centered about zero frequency. These components take the form

$$A_0(p)\, e^{-j\left[\varphi(p+\omega_1)+\varphi(p-\omega_1)\right]}$$

The original frequency function has apparently suffered a phase distortion due to the overall phase characteristic

$$\varphi'(p+\omega_1)+\varphi'(p-\omega_1) = 2n\left(\arctan\frac{p+\omega_1}{\omega_0}+\arctan\frac{p-\omega_1}{\omega_0}\right)$$

<u>Slide # 9, Fig. 9</u> shows this phase distortion (now centered about zero frequency) and it is a freak of nature that over a considerable range the departure from a linear frequency variation is very small. The linear phase slope corresponds to distortionless transmission with a time delay, provided the whole system of frequency translations and filtering is a linear circuit.

The theoretical phase distortion due to the lattices may be computed easily if parasitic reactances and losses are ignored. We have found in practice that the wave filters necessary to select frequency heterodyning products introduce more distortion than the stretch and compress operations. Phase equalization is of course possible, but we have not found it necessary in this system to date.

2.2. Choice of system parameters.

It is a distinct advantage that the simple lattice filter meets the requirements of phase characteristic with the ease of construction resulting from having all inductors and capacitors identical. Attendant disadvantages are that shunt capacity in the inductive arms cannot be compensated for and will restrict the filter pass band. Tests were made on sub assemblies of 20 filter sections to determine that the design frequency of .375 Mc was satisfactory. The 6 μsec radar pulse is a prerequisite and may be handled (with some resolution loss) when modulated on .225 Mc. The wide percentage bandwidth here is necessary to realize the maximum of the wanted form of phase distortion with resulting stretch ratio in a practical number of lattice sections.

Fig. 9 shows the overall phase characteristic of the lattice stretching and compressing. A small shift of numbers in practice makes this curve have a slightly wider pass band at the expense of a dip at band center (like a Tchebycheff approximation) with 5° maximum overall ripple.

The pulse envelope of the system so far is not ideal for a high power radar, so the pulse is squared up by amplitude limiting and time gating. This process renders invalid the linear circuit analysis given above, but the effect are not too serious in practice; indeed advantage may be taken of the situation in the receiver, as will be seen presently.

One may note that time gating a stretched pulse corresponds approximately to band limiting in the frequency plane.

For use in a radar the .225 Mc carrier frequency must be heterodyned up several times. The first upward conversion is quite awkward due to the wide percentage bandwidth.

__Slide 10, Fig. 10__ is a block diagram of our distorted pulse radar. Let us consider the numbers involved.

The signal bandwidth is nominally .15 Mc either side of the carrier, be it stretched or unstretched. Going up to .9 Mc avoids the signal second harmonic, and the conversion frequency and its harmonics, so that a mixer filter combination is in theory possible. In practice phase distortion at band limits is a difficulty and balanced square law mixers are used.

Effective gating is necessary and so is limiting to give a square envelope radar pulse. This is done at a low enough frequency to avoid gate leakage and high enough to avoid gate rise time components.

__Slide 11, Fig. 11__ is a photograph of the .9 Mc distorted radar pulse after squaring up and gating.

SECRET

Further mixing up is conventional. The final amplifier is pulsed on the screen in synchronism with the long pulse.

The step sizes at each heterodyne up mixing state after .9 Mc allow more freedom of choice than below .9 Mc. The signal 3rd harmonic is avoided in all cases and balanced square law tube mixers are used. Balance to balance selective filters are used to extract the wanted conversion product. It is emphasized that although the pulse length transmitted is 100 µsec, the signal pass band is designed for the original band limited 6 µsec pulse. This bandwidth is easily accomodated above .9 Mc while securing at least 40 db rejection of unwanted nearby mixer products. Phase linearity in the filters is of more importance than amplitude linearity, particularly since the long pulse envelope has been predistorted by the gate and limiter in the interests of a square transmitted pulse, and is handled by Class C power stages.

2.3. Long Pulse Receiver.

Slide 12, Fig. 12 shows a block diagram of the receiver. This is conventional as far as the 30 Mc I.F. amplifier. The same conversion frequencies as in the exciter are used. But adjacent targets will produce the simultaneous presence of more than one long pulse in the receiver sections ahead of the compression lattice filter. This will result in cross-talk, signal capture, and loss of resolution if the stages are not linear.

SECRET

It is thus necessary to use a minimum of gain ahead of the lattice on this account. After compression, resolution is not marred by nonlinearity and a conventional pulse IF amplifier and demodulator may be used. This latter IF amplifier provides the major part of the necessary receiver gain. The received long pulse is not one which will recombine exactly in the receiver. This is due to the limiting effected in the exciter. The pulse has suffered emphasis of both its low and high frequency components and is essentially a constant amplitude frequency group. The receiver selectivity uses this pre-emphasis to reduce its noise bandwidth. The .9 Mc band pass filter gives 15 db attenuation at the ends of the pass band, while providing low accompanying phase distortion.

Slide 13, Fig. 13 and Fig. 14, Slide 14 show the action of this filter on the pulse envelope. Pulse recombination is improved along with the noise figure by this apparent loss in signal bandwidth.

Sideband inversion is accomplished in going from .9 Mc to .225 Mc.

Slide 15, Fig. 15 shows the input and Slide 16, Fig. 16 shows the output of the compressing lattice. There is a minimum range loss in the system set by the 100 μsec transmitted pulse length. The receiver lattice merely delays the

57-9048

presentation of video information. The received signal seen here is actually duplexer leakage, corresponding to range zero.

The receiver as so far described does not make the most of the anti-jam possibilities. Optional limiting at some controllable level is included in the 30 Mc IF amplifier. In the limit all signals, be they targets or jamming, reach the lattice with the same envelope amplitude. Right signals will build up by 12 db (in theory) on the lattice while wrong ones will be dispersed according to their bandwidth. The gain after the compress filter must be adjusted to take full advantage of this. This 30 Mc limiting is conflicting with the overlapping signal linearity requirement, so in general, there is an optimum limiting level dependent on jamming conditions. The AGC system operates ahead of the limiter to provide this.

Figs. 17 through 19 show some 'A' scope presentations of both the received long pulse at .9 Mc and the compressed pulse at video. These are actual target echoes. The signal to noise build up is clearly illustrated. Fig. 18 shows two targets just resolved at about 60 miles range, while Fig. 19 illustrates this on an expanded sweep. The long pulses are overlapping and are separated on compression.

Fig. 20 is a PPI presentation of some typical targets obtained with an 18° beam antenna. Limiting was adjusted to

 57-9048

SECRET

occur at a low signal level so that noise quieting around each target is apparent.

This radar is due to the combined efforts of many engineers and the writer wishes particularly to give credit to Mr. C. J. Miller, who conceived our use of the lattice filters; Mr. A. Zverev, who built the models, and Mr. E. A. Worrell who did the mathematics.

Peter D. Hume

Peter D. Hume, Sr. Engr.
Advanced Development

57-9048

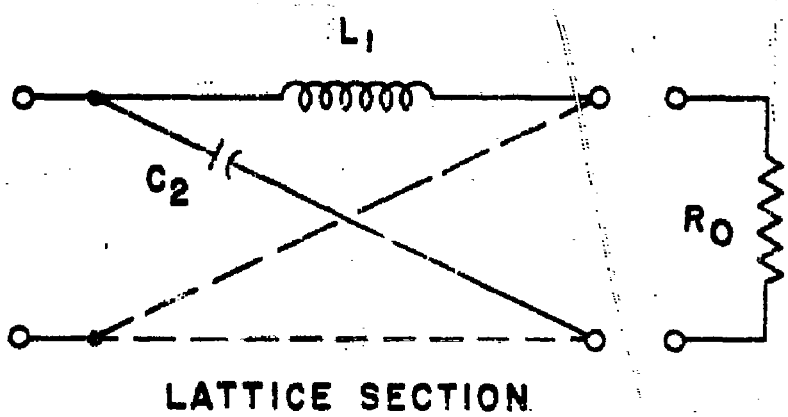

FIG. 1

SECRET

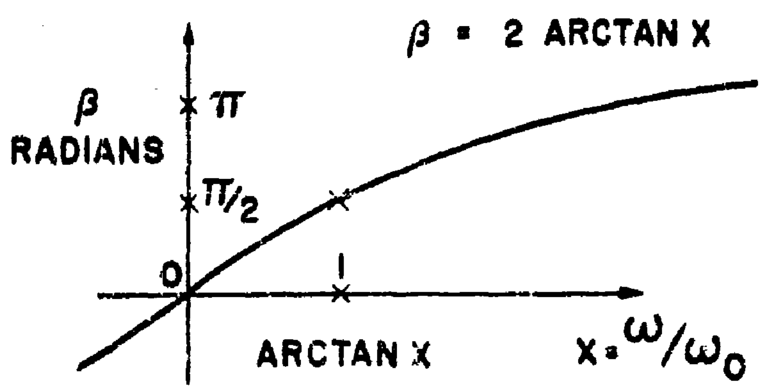

$$\omega_O^2 = \frac{1}{L_1 C_2}$$

$$\omega_O L_1 = \frac{1}{\omega_O C_2} = R_O$$

FIG. 2

SECRET

SECRET 57-9048

SECRET

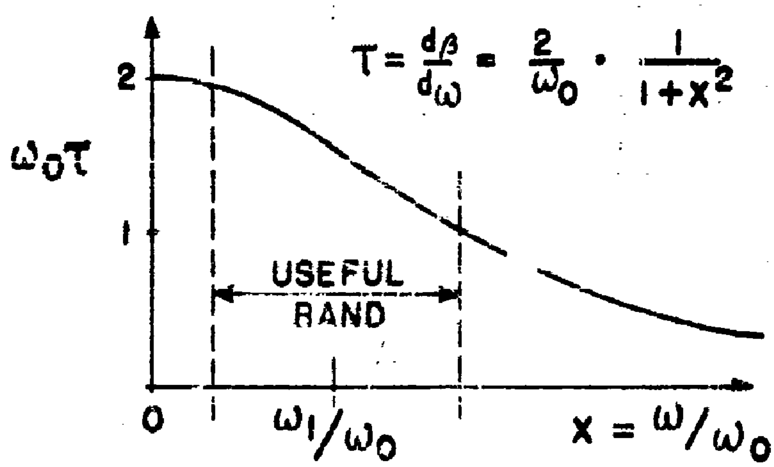

TIME DELAY FOR ONE SECTION.

FIG. 3

SECRET

SECRET

SECRET

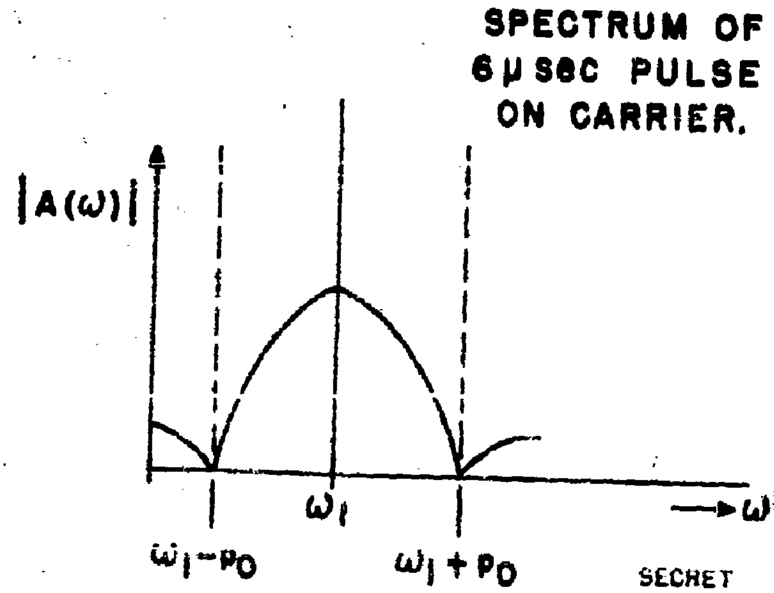
SPECTRUM OF
6 μ sec PULSE
ON CARRIER.
|A(ω)|
ω_1
ω
$\omega_1 - p_0$
$\omega_1 + p_0$
SECRET

FIG. 4

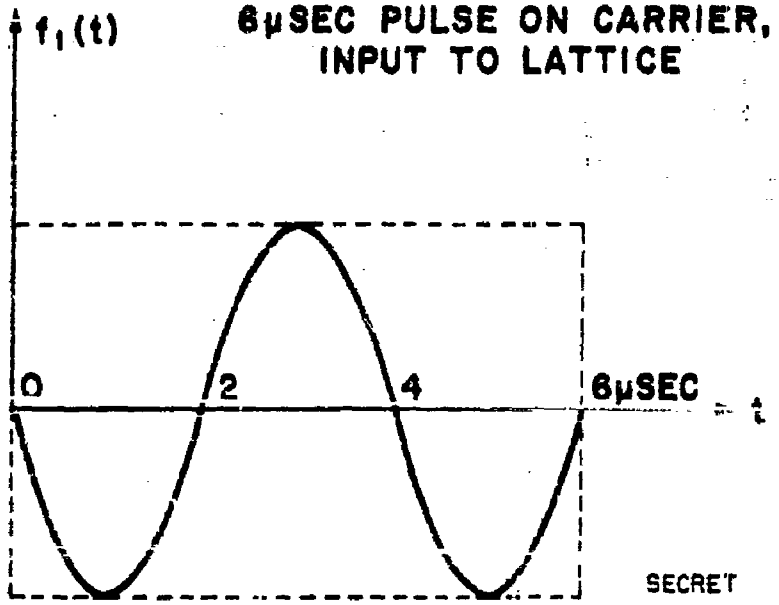

SECRET

FIG. 5

SECRET

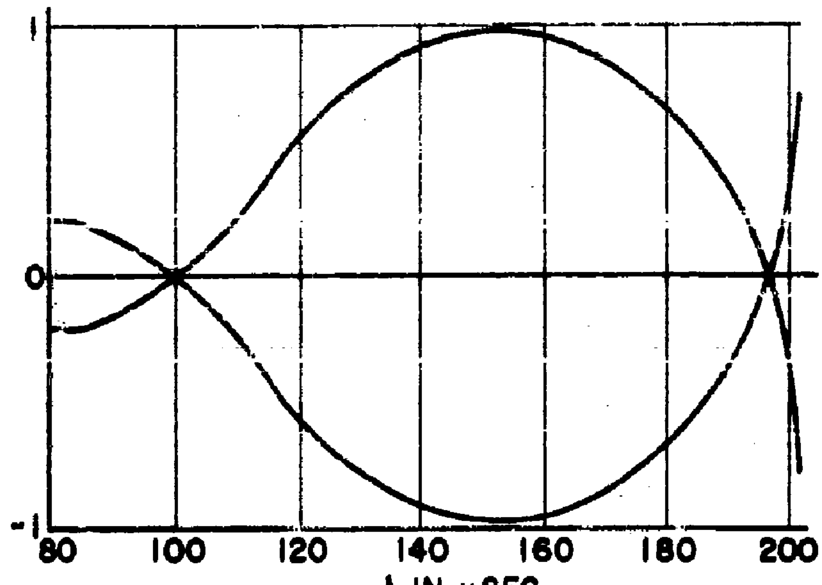

FIG. 6

SECRET

SECRET

52-9018

-3-

SECRET

PHOTOGRAPH OF LONG PULSE

SECRET

FIG. 8

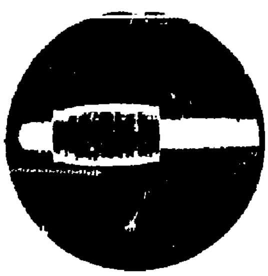

.9 MC LONG PULSE
WITH NOISE AT RECEIVER

SECRET

FIG. 13

SECRET 57-9048

SECRET

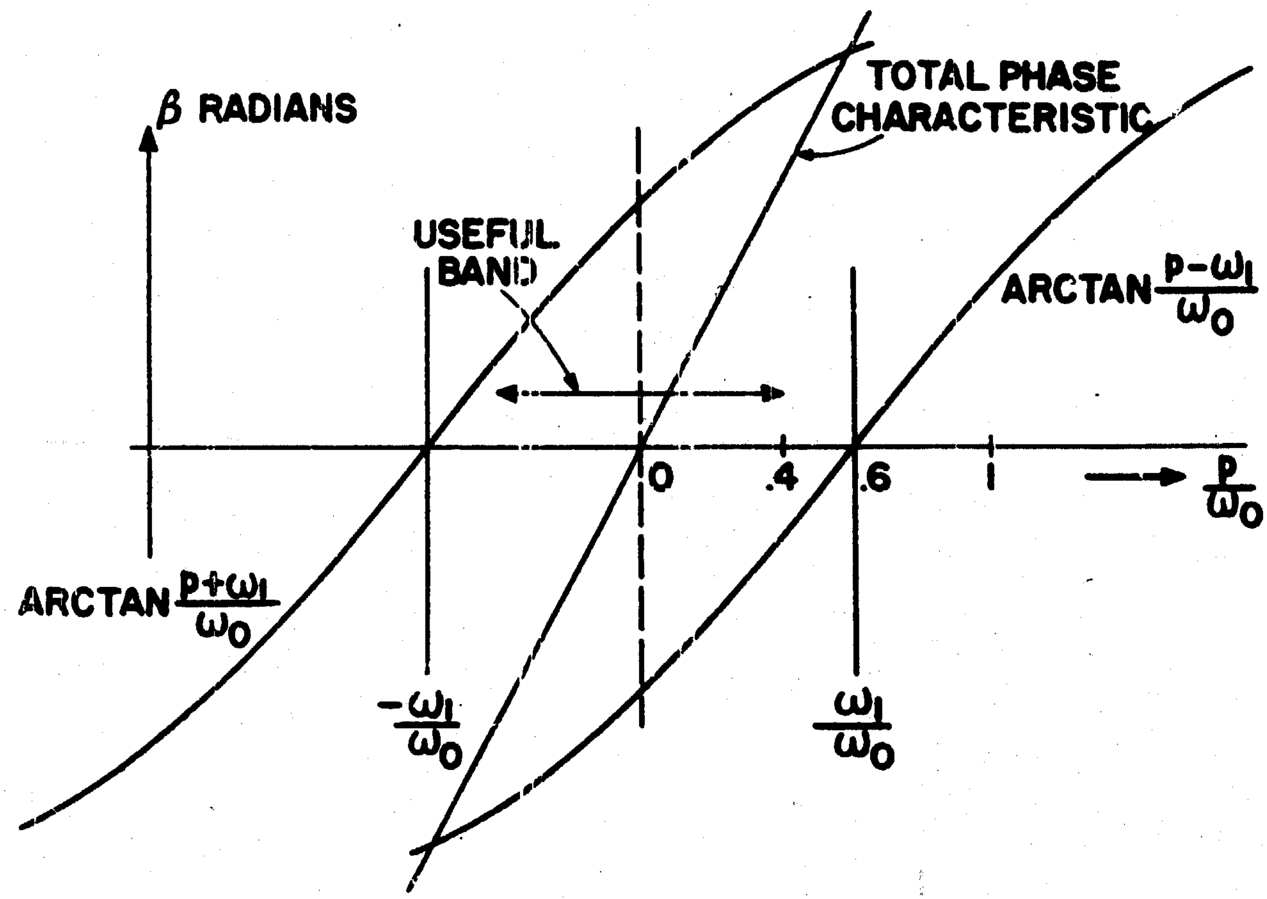

FIG. 9

SECRET

57-9048

SECRET

SECRET

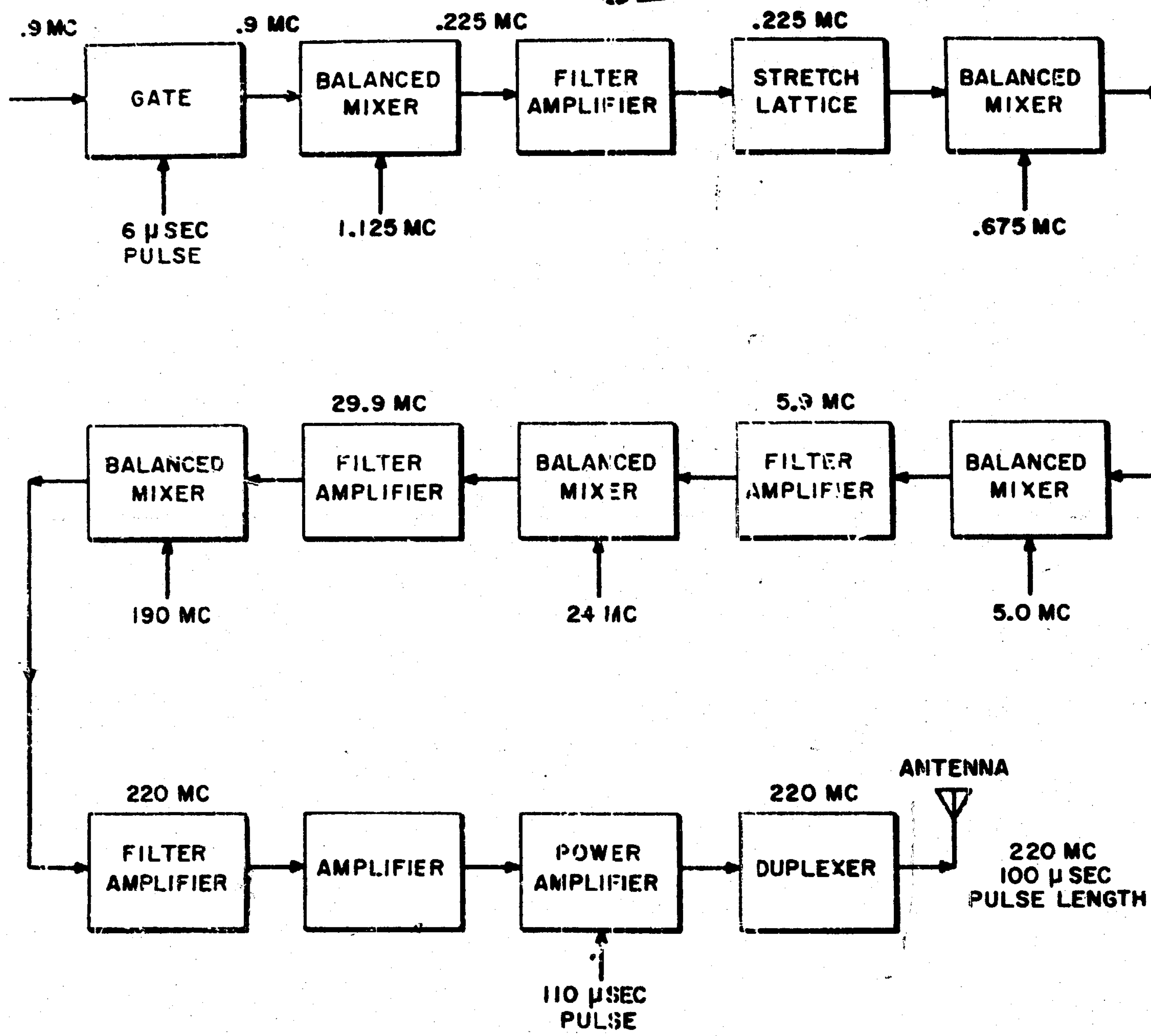

SECRET

FIG. 10

57-9048

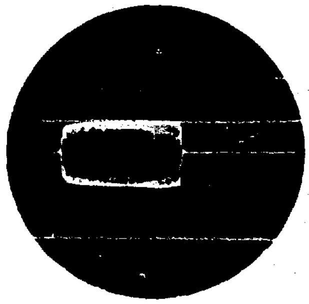

.9 MC LONG PULSE AT EXCITER

SECRET

FIG. 11

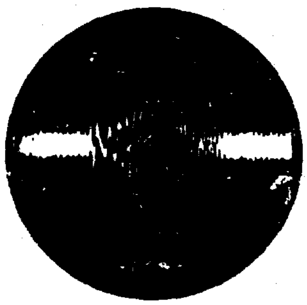

SIDEBAND INVERTED LONG PULSE
AT RECEIVER LATTICE INPUT

SECRET

FIG. 15

57-9048

SECRET

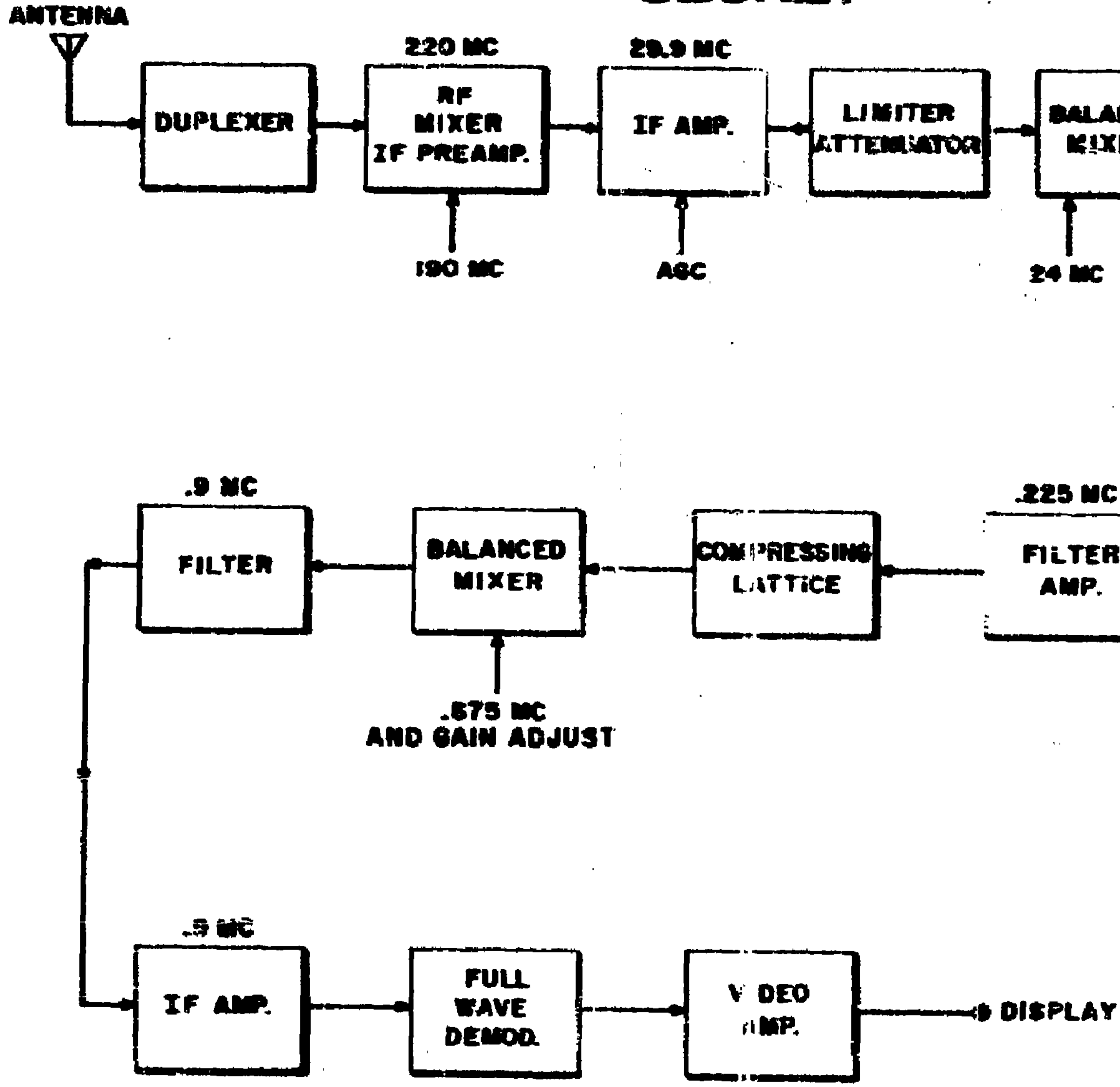

SECRET

FIG. 12

57-4048

.9MC BAND LIMITED LONG PULSE
WITH NOISE AT RECEIVER

SECRET

FIG. 14

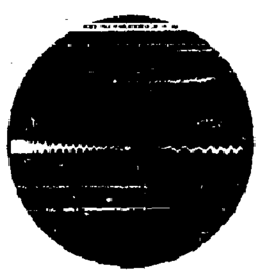

COMPRESSED PULSE AT RECEIVER

SECRET

FIG. 16

SECRET

57-9048

20 MILES (250μSEC) PER cm

SECRET

FIG. 17

20 MILES (250μ SEC) PER cm

SECRET

FIG. 18

01

57-9048

48

SECRET

4 MILES (50 μSEC) PER cm

SECRET

FIG. 19

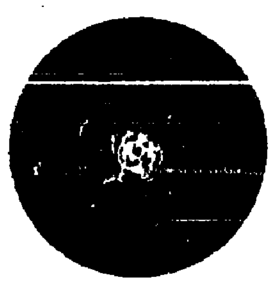

PPI (R.F. LIMITING)

SECRET

FIG. 20

SECRET

57-4048

SECRET

A LINCOLN LABORATORY CODED-PULSE RECEIVER-EXCITER*

(CONFIDENTIAL)

L. G. Kraft, Jr.**

August 1957

* The research in this document was supported jointly by the Army, Navy, and Air Force under contract with the Massachusetts Institute of Technology.

** Staff Member, Lincoln Laboratory, Massachusetts Institute of Technology.

SECRET

57-9048

SECRET

A LINCOLN LABORATORY CODED-PULSE RECEIVER-EXCITER

L.G. Kraft, Jr.

ABSTRACT

A radar receiver-exciter system has been built and tried in which the transmitted pulse waveform is phase-modulated or "coded" during the pulse in order to increase accuracy in range measurement. The reasoning underlying this development is reviewed briefly and the features of the system actually built are described. The early results are mentioned.

INTRODUCTION

In 1954, Professor W.M. Siebert indicated to a symposium of this same nature the possibility of constructing a large high-powered radar for early ballistic missile detection. The essential features he discussed were based on consideration of fundamental principles of detection and parameter estimation. He pointed out the requirements for very large average powers (on the order of 1/2 megawatt), and very large antenna apertures (order of 4000 square meters). These are necessary to achieve the target signal energy required for high probability of detection and low probability of false alarm in the presence of receiver noise.

In addition, he suggested signal parameters which are still reasonable today: a pulse length of two milliseconds; approximately thirty-five pulses per second; and therefore, peak powers of about six megawatts. A unique feature, however, was the suggested departure from a simple pulsed sinusoidal waveform, to a phase modulated signal.

-57-4048

SECRET 306

Shortly after that symposium, an opportunity arose to build and to try such a receiver-exciter system in connection with the RADC-GE FPS-17 program. My purpose here is to describe the significant features of the system which was built together with some of the reasoning behind it and to mention the early results. The emphasis is to be on the feature of coding. The system has become known as the Lincoln Coded-Pulse Receiver-Exciter — and is described in instruction book detail in Lincoln Manual No.12. The ideas and realization of the coded-pulse radar are the work of many, but particular mention should certainly be made of the effort of Prof. Siebert, who directed the project, and Robert M. Lerner, who contributed to all phases of its conception and realization.

OUTLINE OF FUNDAMENTAL PRINCIPLES

I have mentioned that fundamental considerations of detection and parameter estimation underlie the design of this system. There is only time for the briefest outline of the features of this theory: (see ref. 1, 2, 3).

First, most detection criteria lead to the same result — namely, that an "optimum" detector should compute the likelihood ratio and compare it with a threshold. This is true for such criteria as minimum cost of error, minimum information loss, minimum number of errors, and so on. When the criterion is changed, the computation of the likelihood ratio doesn't change, but the particular value of threshold may.

Second, the performance of the system which computes the likelihood ratio can be described by plotting the probability of detection vs. the probability of false alarm. In the case of additive white gaussian noise, the single prime parameter of such a performance description is the ratio of signal energy received to the noise power density present.

On the basis of these facts one can compute the requirements for large antennas, high power transmitters, low receiver noise figures, low system losses, etc., necessary to give, say 95% probability of detection and one false alarm per year, against a one-tenth square meter target at 2500 nautical miles. Given the signal energy and noise power density one specifies the detection performance without regard to the bandwidth, or pulse length, or any other transmitted waveform parameter.

57-9048

Also, if the noise is additive white gaussian, the likelihood ratio computation simplifies to an equivalent computation of the correlation between received signal and expected waveform. One way to compute this correlation is to employ a "matched filter." It can be shown that the linear filter matched to a particular expected waveform has, at a particular time, an output proportional to the correlation between the actual input and the expected waveform.

A third theoretical implication is that if the received signals have parameters such as time delay, doppler frequency shift, etc., then for best detection the correlation must be computed for all values of the parameters involved. The usual practice is to break the receiver into many sections that compute the correlation function at discrete values of the parameters, this results in such familiar devices as range gates, doppler filter banks, narrow beams, orthogonally polarized receivers, etc. Many present receivers are thus correlation computers; the more nearly optimum they are in the presence of additive, white, gaussian noise, the more nearly they must approach being a correlation receiver. The matched filter is a correlation computing device which has the particular property of determining the correlation versus time delay as a continuous function of time. This is very convenient when one of the unknown parameters is the time delay of the signal. An important point to add here is that once having computed the correlation for all the parameters involved, the receiver has all the a posteriori data available not only to make detection decisions, but also to make estimates of the parameters.

Those familiar with the theory will recognize the fourth theoretical implication, namely, that the correlation functions do depend on the particular waveforms which are transmitted and received. Since parameter estimates depend directly on these correlation functions, they are directly influenced by choice of transmitter waveform. Unlike the questions of detection and false alarm probability, which to a first order are measured by signal energy and noise power density alone, the quality of parameter estimates or measurements depends both on signal-energy-to-noise-density ratio, and on the waveform parameters.

For example, it has been shown (ref. 2) that under proper conditions, the optimum accuracy in measurement of time delay and of doppler frequency shift is

57 7048

given by formulas in Figure 1. (Formulas taken from R. Manasse, Lincoln Laboratory Division III Quarterly Progress Report, July, 1956)

where:

δt = r.m.s. error in estimate of time delay in seconds

β = r.m.s. bandwidth of transmitted signal in radians/sec.

E = energy of received signal watt-sec.

N_o = noise power density watts/cps (single-sided spectrum)

δf = r.m.s. error in estimate of frequency in cycles/sec.

τ = r.m.s. time duration of transmitted signal in seconds

T = pulse length of a rectangular envelope signal in seconds

The left-hand formulas apply generally, the right-hand versions are derived for the special case of a rectangular envelope pulse of sinusoid. If one chooses to modulate the transmitted signal in any way that modifies its bandwidth, or its time duration, or its energy content, then the accuracies in estimating parameters such as time delay and doppler shift are influenced in simple cases as indicated above.

The coded pulse receiver-exciter development is a direct effort to improve range measurement accuracy while simultaneously allowing velocity measurement. The actual changes in the system on which the coded-pulse receiver-exciter has been tested included lengthening the pulse to two milliseconds and providing a particular phase modulation internal to the pulse. The longer pulse increases signal energy which improves both detection performance and parameter measurement. The length of the pulse enables a doppler measurement during one pulse only. The phase modulation increases bandwidth and therefore the accuracy of range measurement.

REASONS FOR CODED PULSE

There are a variety of reasons why a phase modulation or coding of the transmit waveform may be useful: coding may improve range measurement accuracy; it may improve certain resolution properties; it may allow longer pulses and more signal energy while maintaining or improving accuracy and resolution; it

57 1048

may influence jamming effectiveness; sophisticated coding may reduce the possibilities of "spoof" jamming; particular waveforms may be used to reduce certain receiver complexities; and there are other possibilities. In the coded-pulse receiver-exciter only the advantage of improved range accuracy was sought.

THE FEATURES OF THE CODED-PULSE RADAR AS TRIED EXPERIMENTALLY

The coded-pulse radar pulse is two milliseconds long. This enables a determination of doppler frequency on one pulse only, to within about 30 cycles per second for a reasonably strong signal ($\frac{2E}{N_0} = 81$). Our hope was for about 100 c/s accuracy when the system errors were all taken into account.

The long pulse is phase modulated in a pseudo-random fashion by breaking it up into one hundred sections or sub-pulses, each of which may be made positive or negative with respect to the others. It is as though a long pulse of sinusoid were modulated by a sequence of one hundred plus or minus ones.

The reasons for selecting such a modulation are first that the properties of the waveform can be made suitable for our purposes and second that generation of the waveform is possible practically. Not only must it be possible to generate the waveform desired for transmitter pulse purposes, it is also required to be able to construct eighteen different matched filters to cover the doppler range of this system.

After juggling the requirements for the many special filters and the somewhat noiselike waveform with the various possible hardware schemes, it was decided to implement a delay line filter bank. A suitable acoustic delay line with one hundred output taps was developed concurrently with the construction of the system — and it worked.

A simplified block diagram of the system shown in Figure 3 indicates how the delay line is used. The conventional parts of the system are shown in simplified form. The selector switch in the right-hand position allows a twenty-microsecond pulse (four cycles of a two-hundred-kilocycle sinusoid) from the pulse generator to be applied to the bandpass delay line. At each of the one hundred taps a delayed version of the pulse is obtained; these may have either positive or negative polarity (each vertical tap line on Figure 3 represents two lines — one plus, one minus — in the actual system). Either positive or

59 9048

negative is connected to the transmit bus shown and finally fed to the remainder of the exciter. The net result is the waveform shown in Figure 2.

Figure 3 also indicates the use of the delay line in forming the matched doppler filters for the receiver operation. In this case, the selector switch is in the left-hand position and the receiver connected to the delay line. As indicated there are adding networks of resistors from the one hundred delay line taps to a number of doppler buses. These resistor networks together with the delay line form linear filters which are good approximations to the desired matched filters. For example, the matched operation of the zero doppler filter may be easily described. Assume a signal like the transmitted signal has been received and fed to the delay line. It is merely necessary to connect all the adding resistors of the zero doppler bus to the positive or negative line taps in such a way as to undo the code — make all one hundred contributions add in phase — and the maximum output is achieved. No other connection can possibly give a larger signal to noise ratio. It should be noted that to make this happen, the plus-minus sequence of the transmit bus connection is simply reversed in time (end for end on the diagram of Figure 3) in forming the zero doppler connection.

The filter for a doppler shifted signal differs first in that two buses are required and second in that the resistances of the adding networks are chosen so as to introduce weighting functions. The weighting functions required and used are cosine on one bus and sine on the second, hence the names on Figure 3.

Consider a doppler shifted signal at the antenna, the doppler effect is one of over-all time expansion or contraction of the waveform. After mixing, which preserves phase shifts, all the phase reversals of the original coding are present and also there are the additional cycles due to the doppler shift. If the doppler shift is five hundred cycles, there is one additional cycle in the two-millisecond pulse length. Such an extra cycle means the zero doppler bus signals are progressively out of phase, and add up to zero. One way to take this phase due to doppler into account would be to use a matrix of phase shifters; set the phase shift to correct for the phase due to the doppler and add the outputs. Seventeen hundred phase shifters at moderate bandwidth looked formidable and the more economical resistor matrix shown was used as a way out.

57-9048

The resistor weighting operation is shown mathematically in Figure 4. The desired impulse response h(t) is expanded into two parts by simple trigonometric expansion. The first term of the result is the same as the impulse response of the zero doppler channel except for weighting by the cosine $[\omega_c(\tau - t)]$ function. Therefore, this part of the desired filter was formed exactly as the zero doppler filter except that the values of the adding resistors are chosen to produce the desired cosine weighting.

To be exact, the sine weighted portion of the filter should have a sine wave carrier instead of a cosine carrier for its impulse response. This might be obtained with quadrature local oscillators and a second delay line; or by seventeen 90° phase shifters on the sine weighted buses of Figure 3. However, for reasonable signal to noise ratios it is possible to avoid the phase shifters by sine weighting the same cosine carrier - detecting envelopes on each bus and adding after detection. This results in roughly one db detection loss and also in inability to separate positive and negative doppler shifts, which were reasonable compromises in this particular system.

THE DELAY LINE

Figure 5 and Figure 6 are photographs of the delay line used in the coded-pulse radar. It was conceived and developed concurrently with the rest of the system. It is an acoustic line of 1/16 inch invar rod made in six sections, having total delay of approximately two milliseconds. There are amplifiers between sections. The input transducer is a piezo-electric barium titanate cylinder approximately 1/4 inch in diameter and 1/2 inch (or 1/2 wavelength at 200 Kc) long. It operates in the longitudinal or piston mode. The magnetostrictive property of the invar is used for output transduction. A center-tapped pick-off coil sandwiched between two coils providing d.c. magnetic biasing responds to changes in magnetic flux caused by mechanical stress in the invar rod. The input operates at about 500 volts peak-to-peak which produces approximately 200 millivolts peak-to-peak across one side of the output coil. Insertion loss is largely in the coupling of the transducers; about 20 db at the input, 40 db at the outputs, and only 2 or 3 db along the line. Bandwidth is approximately 100 Kc, mainly determined by the half-wave input transducer.

57-9046

The resistor matrix is mounted behind the delay line panel. Figure 7 shows one of the three shielded boxes containing 1300 of the required 4000 resistors.

THE OUTPUT SIGNAL

You will recall that the waveform is "de-coded" in the resistor matrix when the long two-millisecond pulse is all present in the delay line. As the acoustic signal moves along, all one hundred outputs do not continue to add in phase and a much lower output results. The output from the ideal matched filter should have the shape of the correlation function for the signal being used. Figure 8 is the correlation function at zero doppler shift for the plus-minus coding used in the Lincoln System.

If the peak value is taken to be 100 units, the "hash" peaks for this particular channel are 12 units as shown. It is because the center peak or "spike" is so narrow that more accurate time delay measurement is possible. An uncoded pulse of pure sinusoid has a triangular-shaped correlation function much wider than the spike of Figure 8. It is because the side "hash" is relatively low, that resolution is improved. The "hash" may be pushed down to a greater extent than shown here by choosing other codes (such as FM, etc.); but reducing the hash in this doppler channel will certainly increase it in some other channel. A search for codes which would maintain low hash in all doppler channels was necessary to avoid ambiguity in the doppler and time delay measurements. The largest hash level in all off doppler channels was experimentally found to be about 30 on the scale of Figure 8.

The actual waveform obtained is shown in Figure 9. The eighteen doppler channel outputs are combined in a diode "or" circuit so that only the largest signal is present at one time. This is called the "greatest-of" circuit. Such a combination is not the ideal integration of the likelihood ratio over the doppler frequencies, but for large signals the approximation is within one db and is a pleasant engineering compromise. In fact it enables one threshold comparison circuit to be used in this system.

When the "greatest-of" signal exceeds the threshold (previously adjusted for an acceptable false alarm rate) the system alarms and begins to photograph the output of three of the likely doppler channels. These outputs are later measured, and with suitable interpolation the doppler frequency may be determined to within about 100 cps.

A sample of one of the film records of an actual missile signal is shown in Figure 10. The outputs of doppler channels zero and one are shown. Square waves are superimposed for time marks (each square wave is about 50 nautical miles long). The square wave without signal is used for calibration purposes. The sweep containing the noise and signal "spike" is centered on a true range of approximately 500 nautical miles. The absence of any noticeable spike in the upper trace (channel one-500 cycles per second) indicates that the doppler shift is very near zero.

RESULTS

The range accuracy in this system has to date been limited by resolution of cathode ray oscilloscope spot size and film read out. Although the theoretical limit is about one microsecond accuracy (for a signal energy to noise-power density ratio of approximately 100), the actual readouts are indicating about 10 μsec variations. Geographical knowledge of actual ranges is good to about the same accuracy, so that fixed or bias errors are at least smaller than 10 μsec.

The doppler frequency measurements have variations which are nearly the computed values. The few test results indicate r.m.s. variations less than 30 cps for strong signals. Two system errors have appeared somewhat worse than anticipated. First, unequal gain in the doppler amplifier channels results in doppler measurements biased as much as 50 cps. Second, at very low signals, the envelope detection has introduced similar bias errors.

ADDITIONAL SYSTEM FEATURES

The Lincoln Coded-Pulse System has a number of additional features which should be mentioned. First, a hard limiter (limit levels set at a fraction of the r.m.s. noise voltage) is included in the receiver, before the matched filter. It has been experimentally determined that such a limiter degrades detection performance of this type system less than one db. It has the advantage of keeping the false alarm rate constant, without other gain control. In addition,

57 4048

the limiting reduces the effects of impulse interference.

In order to reduce the loss in detectability for signals having doppler shifts between two channels, intermediate channels are formed by the artifice of adding outputs from adjacent pairs of the doppler channels described above. These interchannel doppler signals are combined and applied to a threshold circuit which will cause a system alarm when activated.

Since many meteor echoes of short (one pulse) duration were anticipated, the threshold circuits have been arranged to alarm only when a large signal is present in the same 10-mile range interval for two of three successive pulse intervals.

REFERENCES

1. W.W. Peterson, T.G. Birdsall, W.C. Fox, "Theory of Signal Detectability," Part I and II Tech. Report No.13, Electronic Defense Group, University of Michigan, 1953. Also available in 1954, Symposium on Information Theory, Trans. I.R.E., PGIT-4, September 1954.

2. P.M. Woodward, Probability and Information Theory with Applications to Radar, McGraw-Hill, 1953.

3. W. Siebert, "A Radar Detection Philosophy", Trans. I.R.E. PGIT, Vol. IT-2, No.3, September 1956.

4. Lincoln Manual No.12, Vol. I, II, & III – "Coded-Pulse Radar Receiver-Exciter or Radar Set AN/FPS-17," 1 March 1956. (Title: CONFIDENTIAL; Manual: SECRET)

57 9048

LIST OF FIGURES

59-9048

$$\delta t = \frac{1}{\beta\left(\frac{2E}{N_0}\right)^{\frac{1}{2}}} \longrightarrow \frac{\sqrt{2}\,T}{\frac{2E}{N_0}}$$

$$\delta f = \frac{1}{\tau\left(\frac{2E}{N_0}\right)^{\frac{1}{2}}} \longrightarrow \frac{\sqrt{3}}{\pi T\left(\frac{2E}{N_0}\right)^{\frac{1}{2}}}$$

MEASUREMENT ACCURACY FORMULAS

Figure 1

57-9048

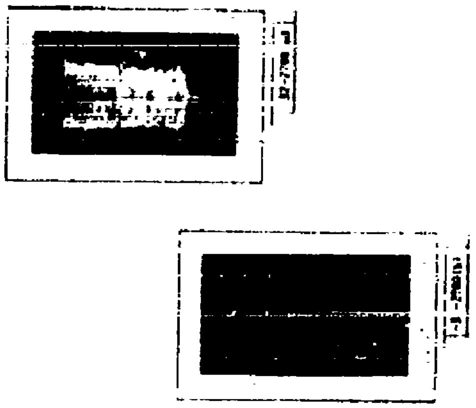

Fig. 2 Transmit pulse at 200 kcps: (a) 2-msec pulse; (b) first 200 μsec coded + + − − + − − + − −.

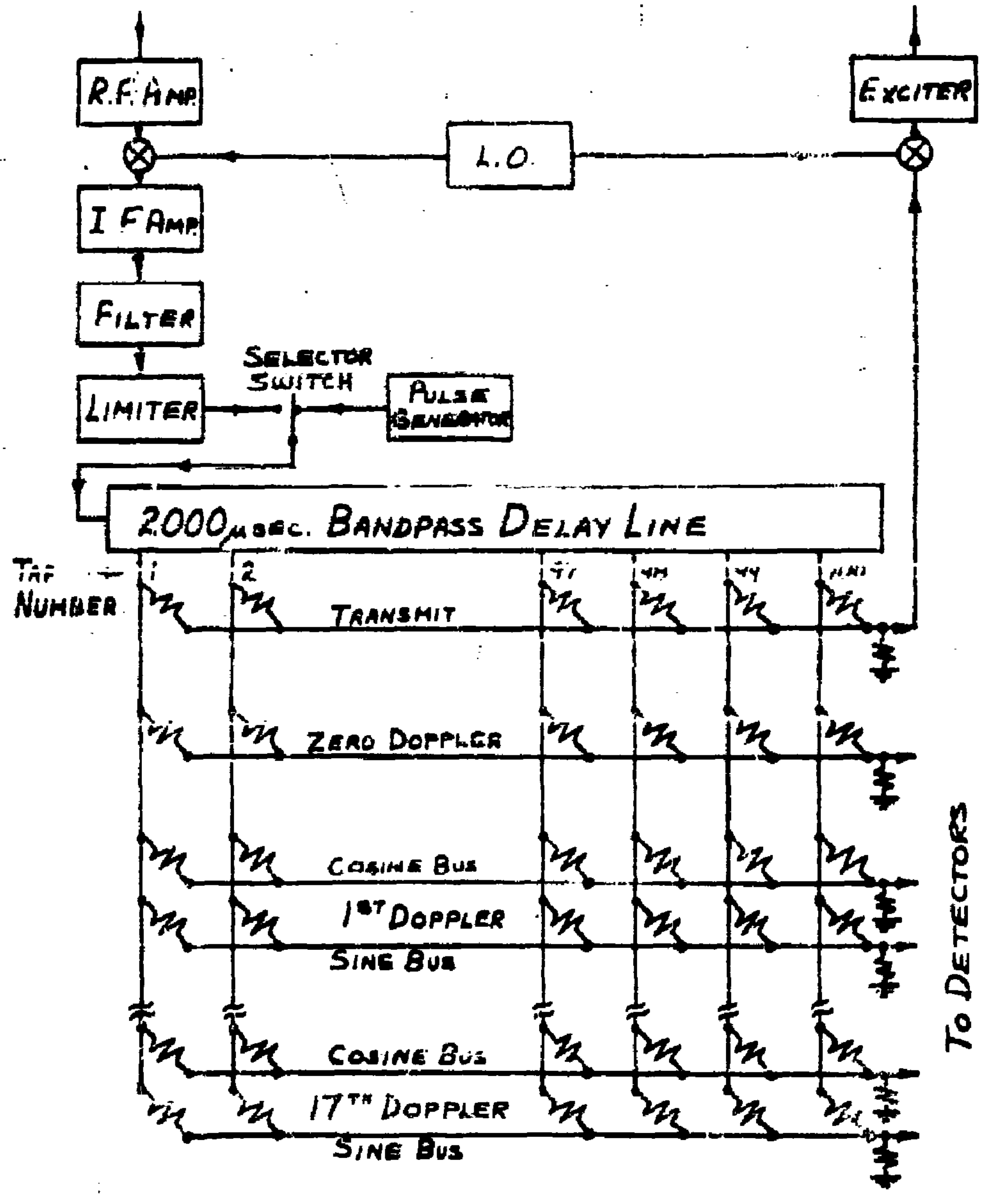

Simplified Block Diagram.

Figure 3

57- 9048

ZERO DOPPLER

$$h(t) = E(T-t)\cos\left[\omega_0(T-t) + \phi(T-t)\right]$$

DOPPLER = ω_D

$$h(t) = E(T-t)\cos\left[(\omega_0 \pm \omega_D)(T-t) + \phi(T-t)\right]$$

$$= E(T-t)\cos\left[\omega_0(T-t) + \phi(T-t)\right]\cos\omega_D(T-t)$$

$$\mp E(T-t)\sin\left[\omega_0(T-t) + \phi(T-t)\right]\sin\omega_D(T-t)$$

DOPPLER CHANNEL IMPULSE RESPONSES
Figure 4

G72-04

57. 9048

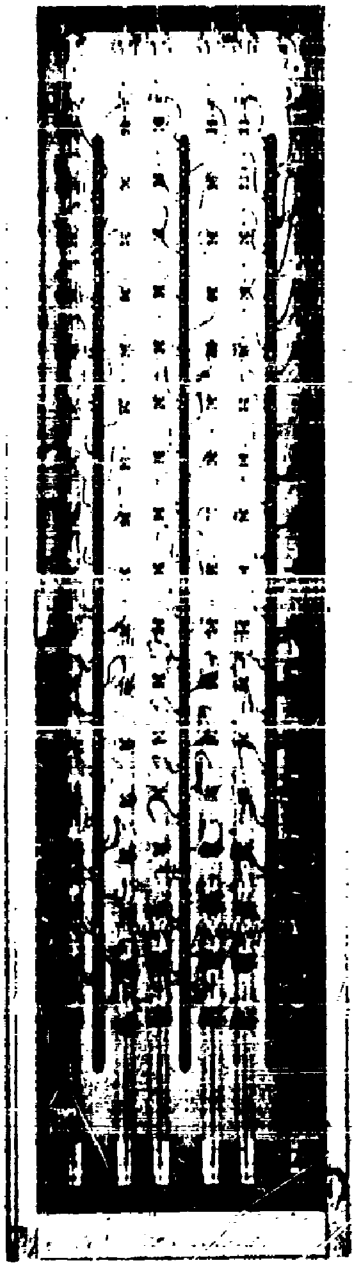

Figure 5

57-4048

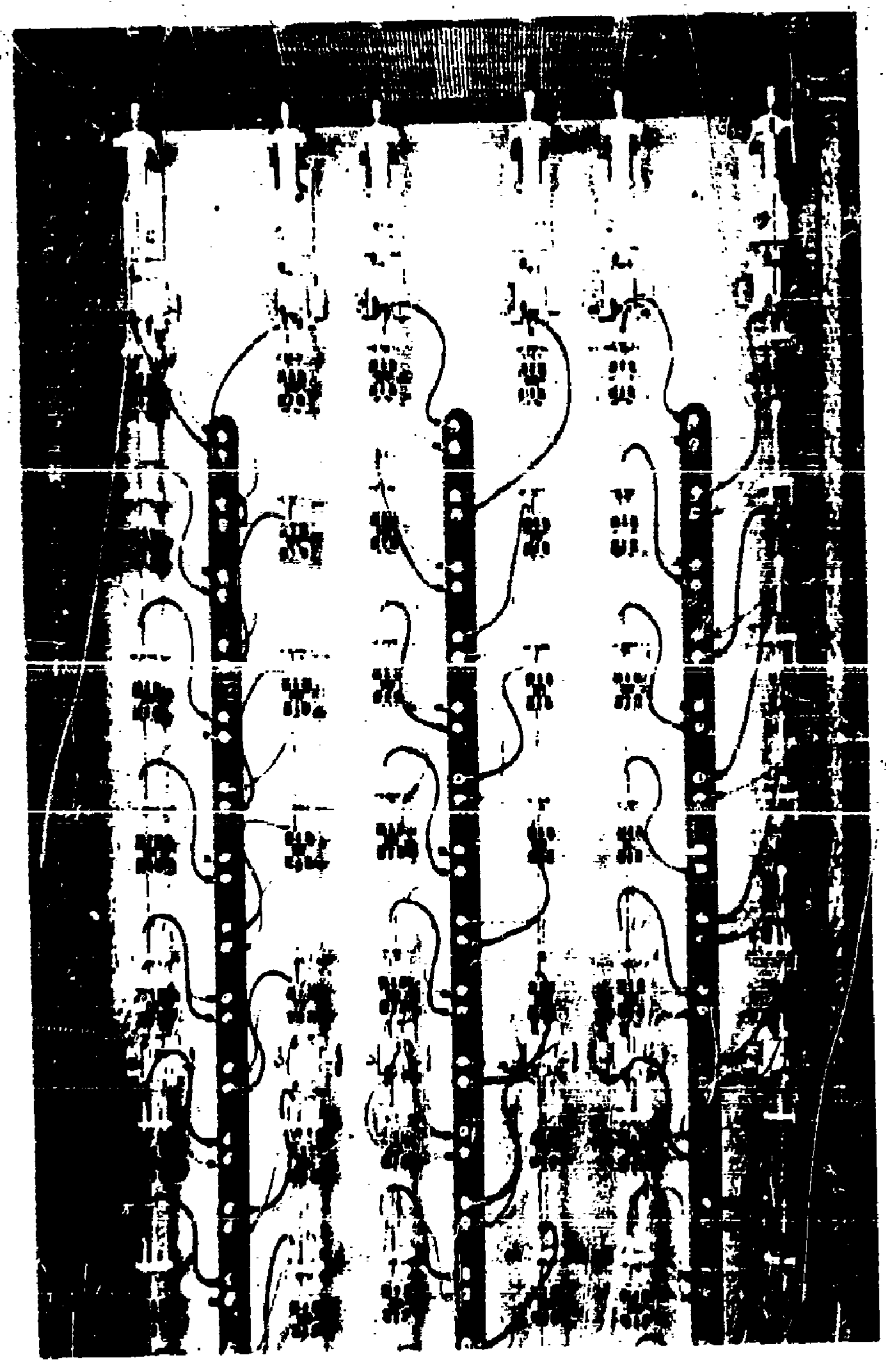

Figure 6

57-9048

SECRET

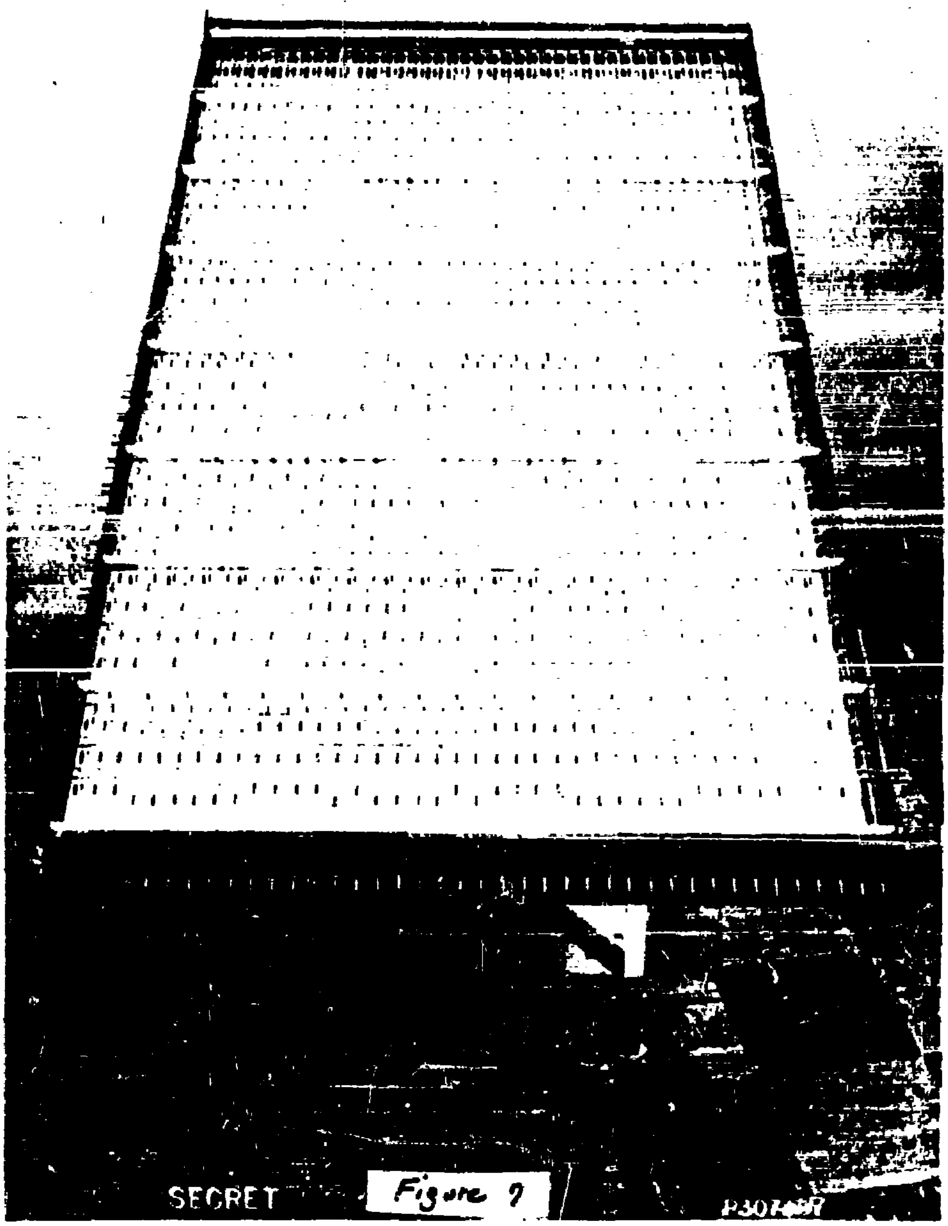

Figure 7

$|\phi_{11}|$ FOR SHIFT REGISTER CODE

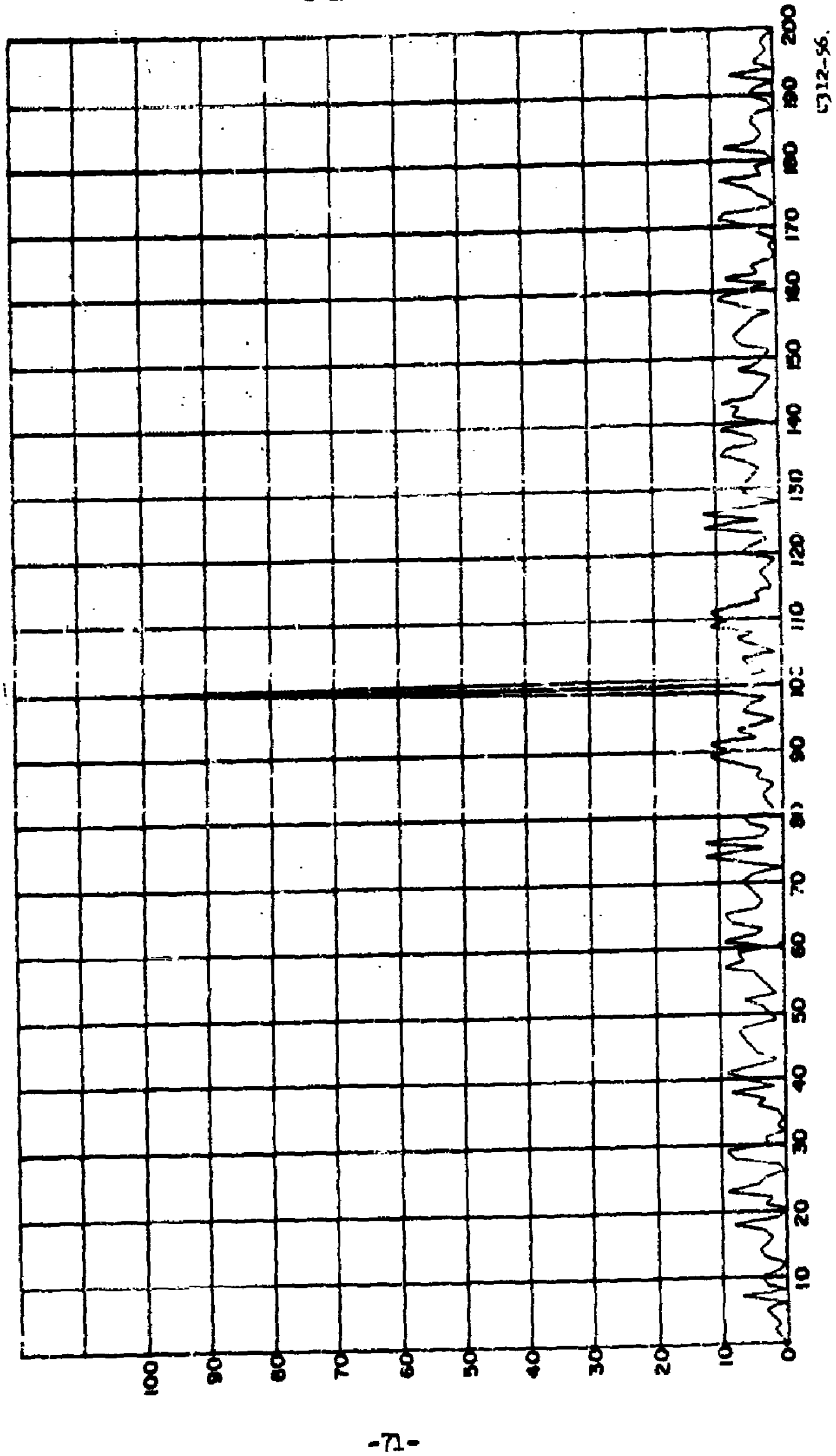

Figure 8

57 90-48

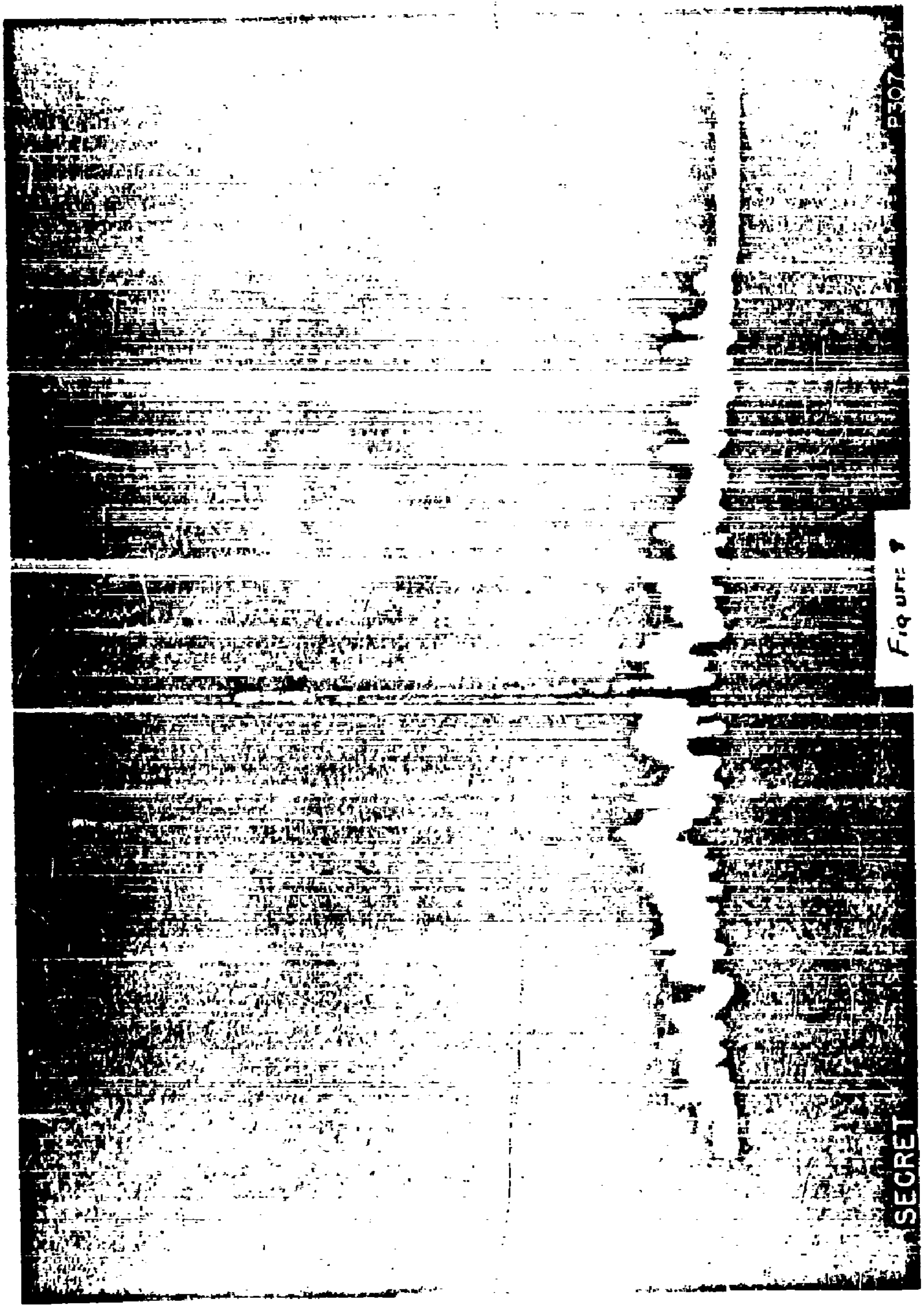

Figure [illegible]

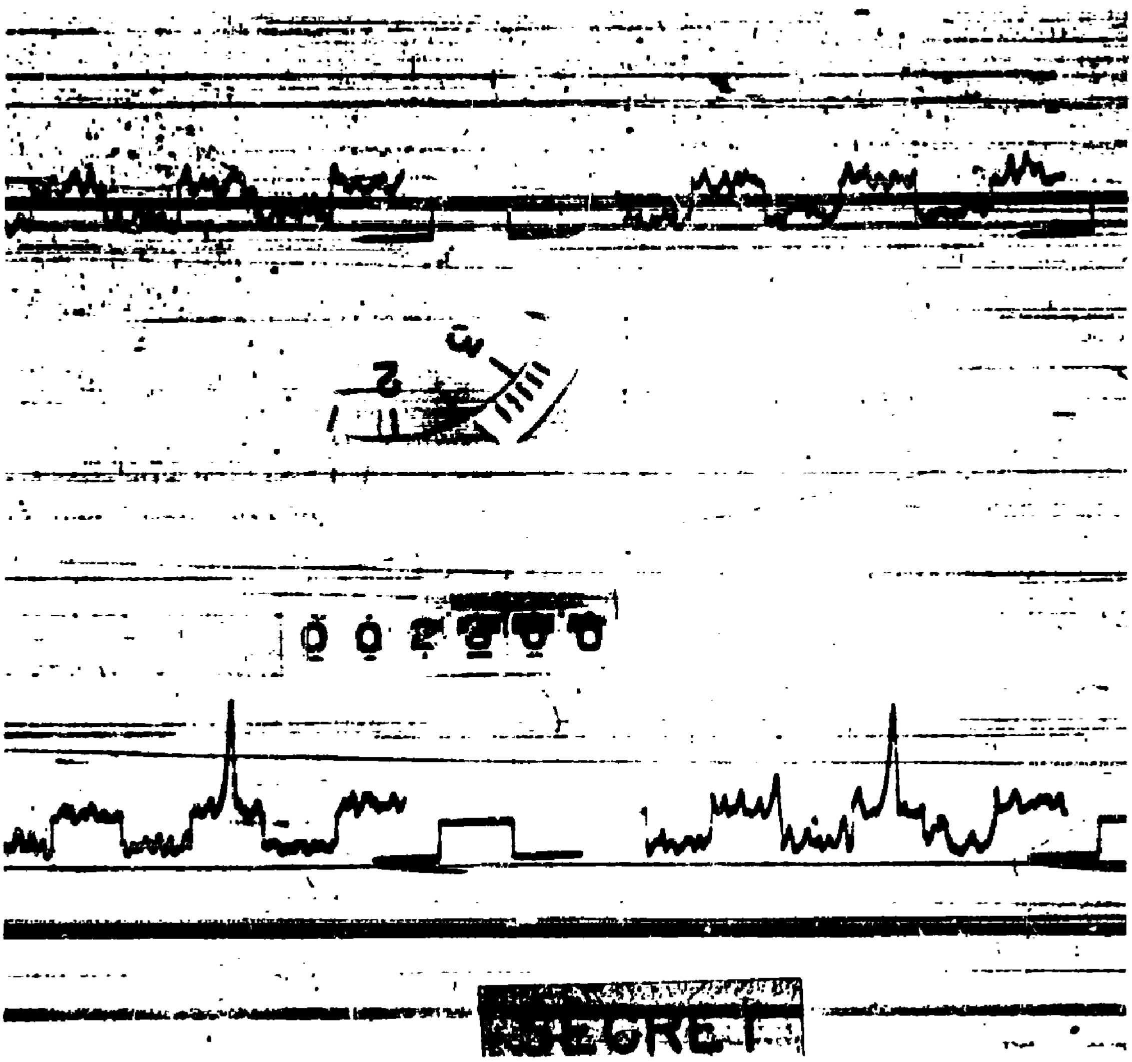

Figure 10

SECRET

Matched Filter Synthesis through Phase-Distortion Networks

by Steven M. Sussman
Melpar, Inc. Research Department

INTRODUCTION

The subject of this paper grew out of one phase of a study contract performed by Melpar for the Signal Corps Engineering Laboratories.* Broadly speaking the problem is the design of matched filters with noise-like impulse responses. The topic will be treated in two parts; the first part relating to some general ideas which lead to a different point-of-view or design philosophy for filters of this type, and the second part dealing with a specific realization which was constructed and tested in the laboratory.

A matched filter is defined in the usual way as a filter whose impulse response is the time-reverse of the applied signal, or in frequency-domain language, the matched filter has a spectrum which is the conjugate of the signal spectrum.

DESIGN CONSIDERATIONS

In our treatment we include, in addition to the matched filter, the generating filter, the one whose impulse response is the desired signal. In short, we are speaking of the situation pictured in Figure 1. N_1 is the generating filter or transmitter and N_2 is the matched filter or receiver.

* A complete description of the system to which the methods of this paper were applied will be given at a Symposium on Electronic Counter Countermeasures to be held at Rome Air Development Center in October 1957.

57-9048

SECRET

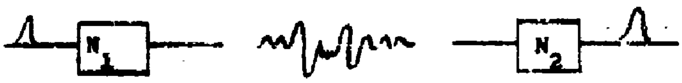

$$H_1(j\omega) = A_1(\omega)\, e^{-j\theta_1(\omega)} \qquad (1)$$

$$H_2(j\omega) = A_2(\omega)\, e^{-j\theta_2(\omega)}$$

Matched Filter Conditions:

$$A_1(\omega) = A_2(\omega) \qquad (2)$$

$$\theta_2(\omega) + \theta_1(\omega) = \omega T$$

Figure 1

The transfer function of the two filters are denoted as in equation (1). In order to satisfy the condition that H_1 and H_2 be conjugate, we require the relations shown in equation (2) for the magnitudes and phases. The magnitudes of the transfer functions must be equal, and the sum of the phases is a linear funtion of frequency. The T in the last expression corresponds to the delay of the system which is necessary to insure realizability. It is apparent from this that the two networks taken together are nothing more than a delay-line whose phase characteristic is split between N_1 and N_2 so as to make the waveform between them have the desired noise-like property.

0|

57-9048

This brings us to the next point: the question of how to define "noise-like" in terms which can lead to network design specifications. We find that a very useful approach is through the TW product, T being the duration and W the bandwidth of the signal, since this is the figure of merit of the pulse compression systems we're dealing with. In tying the T and W measures to the transfer function of the filter we make use of some work of P. M. Woodward on time and frequency resolution. We employ as a measure of bandwidth the inverse of Woodward's time resolution constant and as a measure of duration the inverse of his frequency resolution constant. For the bandwidth measure the pertinent relations are given in equations (3) and (4). $\phi(\tau)$ is the auto-correlation function of the impluse response h(t) and is also given as the Fourier transform of $|H(j\omega)|^2$. The effective bandwidth W_o in equation (4) is seen to be inversely related to the width of the correlation function, since $\phi(\tau)$ is normalized to make $\phi(o) = 1$. W_o can be expressed in terms of $|H(j\omega)|$ as in equation (4) and from this we find, making use of the normalization, that W_o is a maximum when $|H(j\omega)|$ is flat over the available bandwidth. In terms of the networks N_1 and N_2 this maximization condition requires both magnitude functions $A_1(\omega)$ and $A_2(\omega)$ to be constants, i.e. the filters are all-pass.

As for the measure of duration equations (5) and (6) pertain. The complete parallelism with the bandwidth measure is immediately evident. $\psi(\lambda)$ is the complex auto-correlation of the spectrum $H(j\omega)$ and T_e is an inverse measure of the width of $|\psi(\lambda)|^2$. Equation (6) states a relation, whose proof may be found in reference 1a, which holds only for noise-like

01

57-9048

$$\phi(\tau) = \int_{-\infty}^{\infty} h(t)h(t+\tau)\, dt$$

$$= \frac{1}{2\pi} \int_{-\infty}^{\infty} \left|H(j\omega)\right|^2 e^{j\omega\tau} d\omega \qquad (3)$$

$$\frac{1}{W_o} = 2\pi \int_{-\infty}^{\infty} \left|\phi(\tau)\right|^2 d\tau$$

$$= \frac{1}{2\pi} \int_{-\infty}^{\infty} \left|H(j\omega)\right|^4 d\omega \qquad (4)$$

To maximize W_o: $\left|H(j\omega)\right| =$ constant

$$\psi(\lambda) = \frac{1}{2\pi} \int_{-\infty}^{\infty} \overline{H(j\omega)}\; H(j\omega + j\lambda)\, d\omega$$

$$= \frac{1}{2\pi} \int_{-\infty}^{\infty} \left|h(t)\right|^2 e^{-j\lambda t} dt \qquad (5)$$

$$\left|\psi(\lambda)\right| \approx \psi_{RR}(\lambda) = \frac{1}{\pi\sqrt{2}} \int_{-\infty}^{\infty} \mathrm{Re}H(j\omega)\mathrm{Re}H(j\omega + j\lambda)\, d\omega \qquad (6)$$

$$\frac{1}{T_o} = \frac{1}{2\pi} \int_{-\infty}^{\infty} \left|\psi(\lambda)\right|^2 d\lambda$$

$$= \int_{-\infty}^{\infty} \left|h(t)\right|^4 dt \qquad (7)$$

To maximize T_o: $\psi_{RR}(\lambda)$ decays rapidly

0|

57- 9048

SECRET

impulse responses, namely that $|\psi(\lambda)|$ is approximately equal to the autocorrelation function of the real part of $H(j\omega)$. Consequently we can state that the duration T_{ε} will be maximized when $\psi_{RR}(\lambda)$ decays rapidly and remains small with increasing λ. This condition implies that Re $H(j\omega)$ be a "broad-band" function of ω.

We are now in a position to specify more precisely what the networks N_1 and N_2 should be. The all-pass condition has already been mentioned. Using the fact that Re $H(j\omega) = \cos\theta(\omega)$, the wide-band condition on Re $H(j\omega)$ can be met by making the phase a non-linearly increasing function of ω over the frequency band of interest.

In order to get an intuitive picture of these ideas, let us consider a very special phase characteristic for N_1, a concave upward curve as shown in Figure 2; then, in order to satisfy the conjugate relationship, N_2 must have the concave downward characteristic which makes the sum of the two equal to the linear relation giving the delay of the networks. The network N_1 is

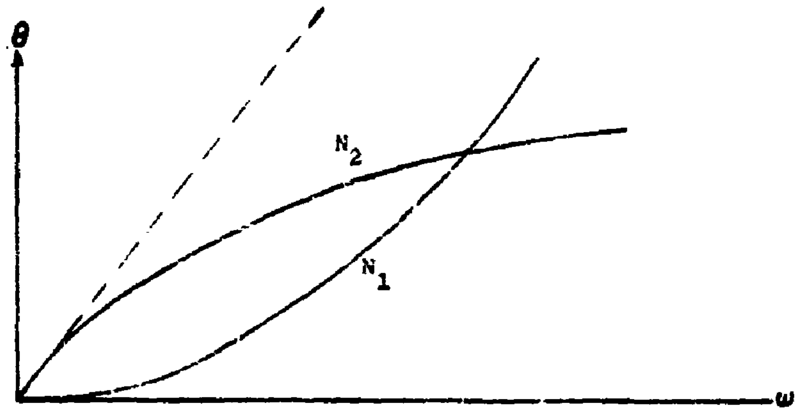

Figure 2 Matched Filter Phase Characteristics

57-9048

SECRET

excited by a narrow pulse which contains all frequencies of interest in essentially equal proportion. Recall now that the slope of the phase characteristic at a certain frequency equals the delay of the frequency group which is a narrow band of frequencies located at that point. Therefore, for the concave phase characteristic the low frequencies are very little delayed whereas the higher frequencies are more delayed. This results in an FM type of impulse response. Conversely for the network N_2, the low frequencies are delayed by larger amounts than the high frequencies and consequently the energy is compressed back into a pulse. In other words the network N_1 spreads the energy of the pulse out in time and the network N_2 brings it back together again. By changing the phase characteristics of the network to a different non-linear form we merely change the order in which the frequency groups appear in time and by making this order random we get the effect of a random waveform.

The general approach to the design of the matched filter is in terms of building-block networks which are cascaded to form the filters N_1 and N_2. We find it convenient hereafter to speak in terms of phase-slope or delay rather than phase. The first graph in Figure 3 shows the phase characteristic of a typical component network section. The derivative of phase or delay is shown in the second graph. The building-block networks are all-pass and they differ one from the other in that their delay characteristics are displaced along the frequency axis. In cascade connections transfer functions are multiplied and delays are additive. By adding a sufficient number of delay curves of the form shown but shifted in frequency one can build a nearly

57-9048

SECRET

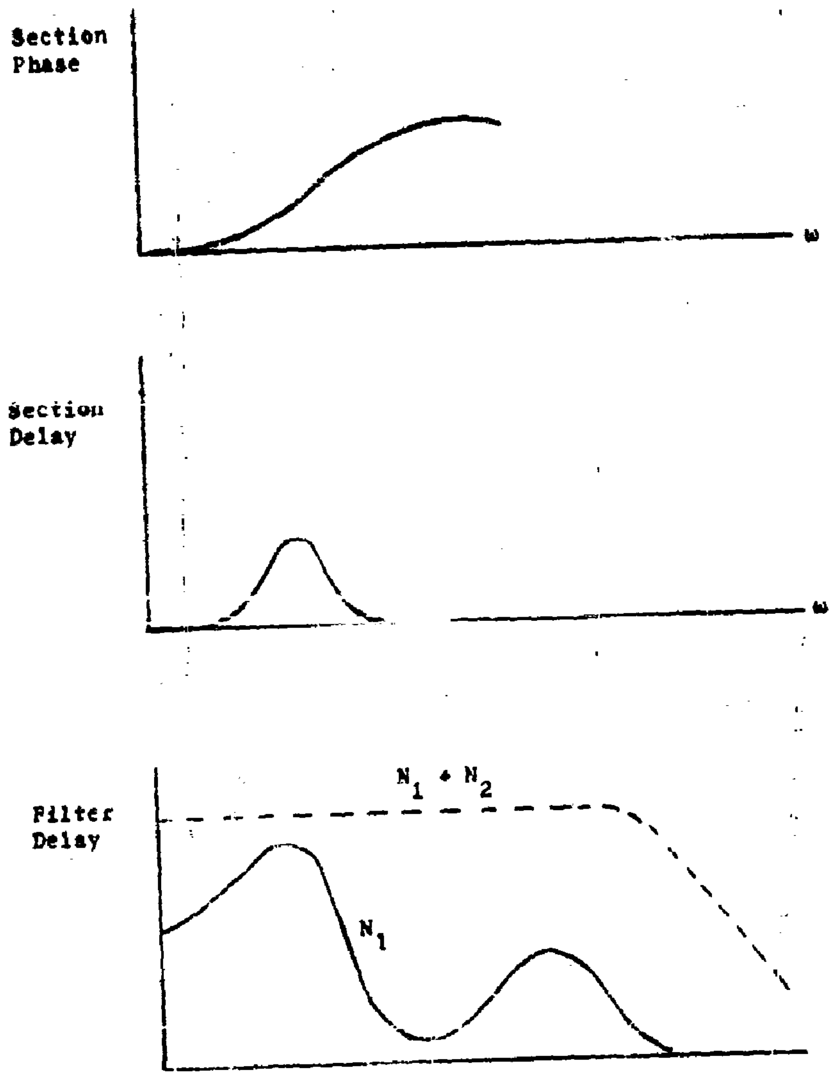

Figure 3 Network Characteristics

57- 9048

SECRET

arbitrary delay function in filter N_1, as, for example in the third graph. Filter N_2 then includes whatever additional component networks are required to make the overall delay uniform over the band of interest. It should be noted that the building blocks need not be made all of the same form although it may be convenient to do so in practice. What is required is sufficient flexibility in the component networks to build up complicated delay functions in N_1 which can be compensated in N_2 to yield a uniform delay.

Several other points are worth noting from the lower graph. First, it can be seen that the useful duration of the output signal is given by the range of the delay curve i.e. the distance between its maximum and minimum points. Secondly we find that the networks act as matched filters for a limited frequency band only as indicated by the constant portion of the overall delay curve. With this design method the delay will always drop near the edge of the band. However, since the filters are all-pass, frequencies within as well as outside the band are passed without attenuation. Therefore, in order to make the system optimum in the presence of noise a sharp-cut-off filter covering the band of constant delay must be inserted.

EXPERIMENTAL MATCHED FILTER

We now turn to a particular realization of the filter which was constructed and tested in the laboratory. The network design is based on the array of poles and zeroes shown in Figure 4 which represents an all-pass delay-line. The system is all-pass since poles and zeroes are equally spaced from the $j\omega$-axis, and the phase is essentially a linear function along the frequency axis. The building blocks in this case are the networks which realize a quadruplet of singularities, for example, those circled in the diagram.

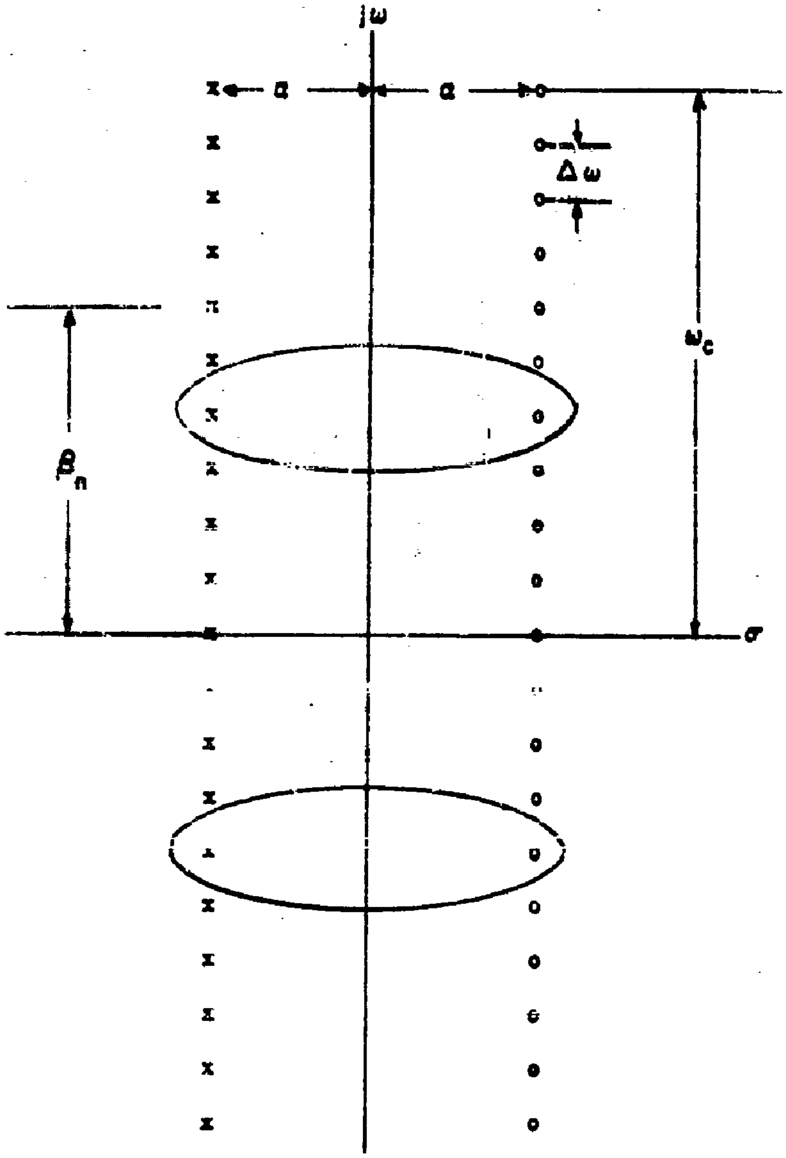

Figure 4 Pole-Zero Pattern

57-9048

It turns out that the spacing between singularities along the $j\omega$-axis is approximately $\frac{2\pi}{T}$ so that the number of network sections required is of the order WT. Each quadruplet can be realized by an all-pass constant - resistance lattice or one of its equivalent forms as shown in Figure 5. These networks may be cascaded directly without buffer stages since the constant-resistance input impedance of one forms the load resistance of the preceeding network. In our experimental model we used the first bridged-T equivalent form since it has only two coils and no mutual inductance.

The experimental model was for a rather modest TW product of 35: a delay of 6 milliseconds over a band-width of 1 to 6.5 kilocycles. Operation was restricted to this low frequency range for reasons to be discussed later. The filter was constructed with toroidal coils and plastic film capacitors of 1% tolerance, and no provisions were made for aligning sections after assembly.

A set of toggle switches was provided for switching each of the bridged-T sections either into the transmitting or the receiving filter. This made it possible to determine the variation of the waveform between the two filters as network sections are switched back and forth. The photographs in Figure 6a show the type of waveforms that were obtained. These waveforms were not hand-picked, but were selected by a random procedure.

The appearance of the signals is noise-like as was anticipated. There is a tendency, however, for the envelope of the waveforms to peak in the center of the interval. This is a result of the random selection procedure which makes delays near the half-way point of the overall delay the most

57- 9048

SECRET

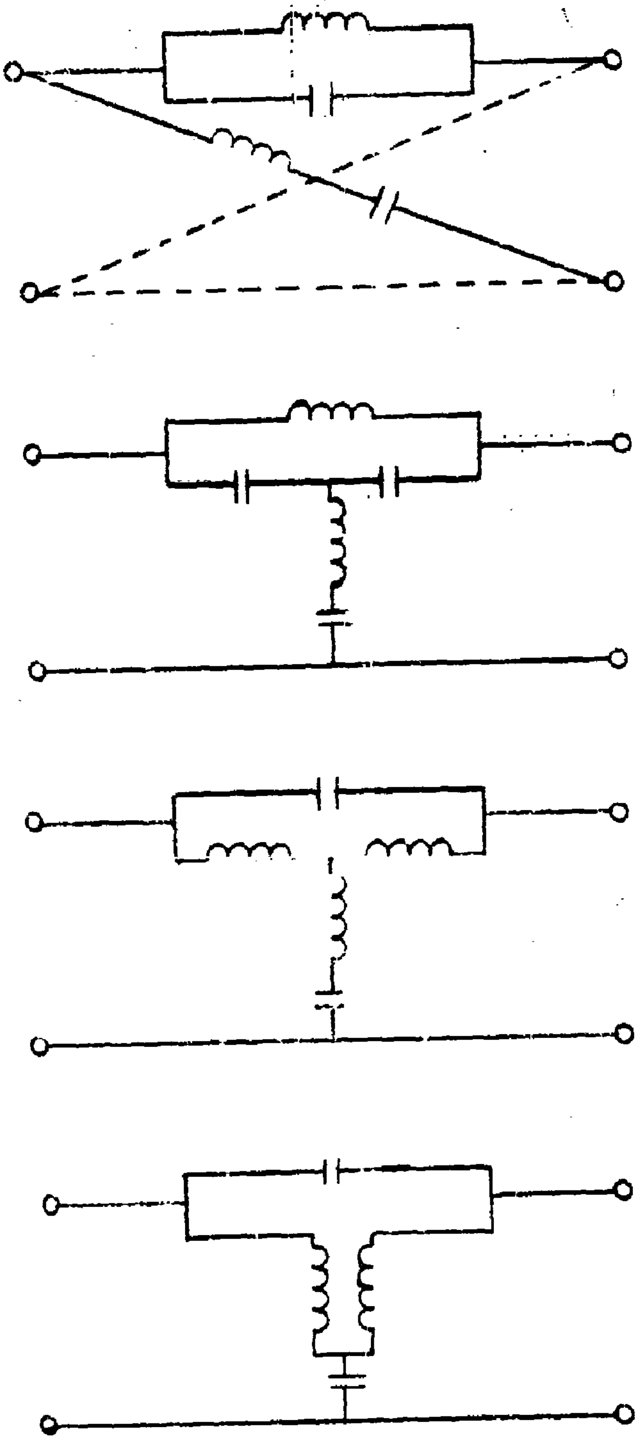

Figure 5 Lattice and Equivalent Networks

57- 9648

SECRET

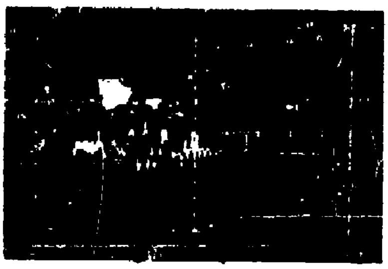

Figure 6a.

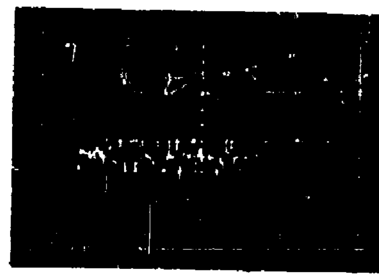

Figure 6a.

Typical Waveforms

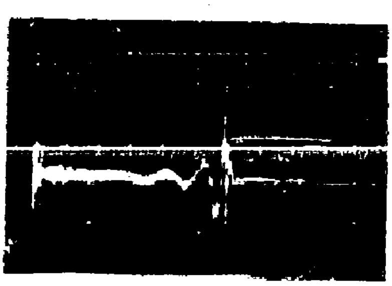

Figure 6b.

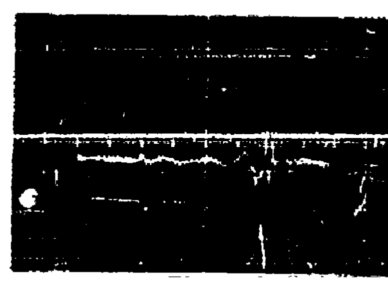

Figure 6c.

Output Pulse

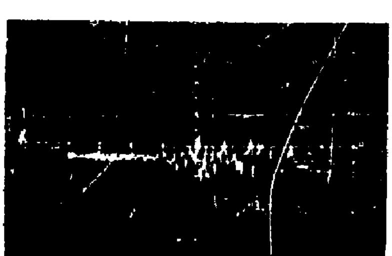

Figure 6d.

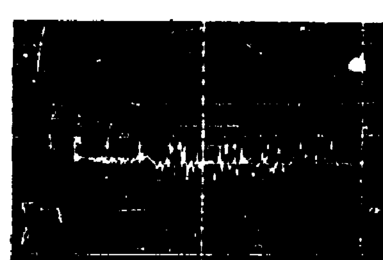

Figure 6e.

Mismatched Output

Scale: 1 millisec/div.

57-9048

likely. In Figures 6b and 6c we show the output pulse from the filter, which, of course, is independent of how the network sections are distributed between transmitter and receiver. We see here the effect of the imperfections in the matched filter which were mentioned earlier. There is both a high-and a low-frequency ripple preceeding the main output pulse. This is due to the fact that the delay drops below the design value near the edges of the pass-band.

Figures 6d and 6e shows the output waveform when a mismatched signal is applied to the receiving filter. In Figure 6d the mismatched signal was especially selected to give small output peaks, whereas Figure 6e shows a mismatched output for which the input waveform was selected at random. The input pulse into the transmitting filter was held constant during these tests, thus permitting a direct amplitude comparison among the waveforms of Figures 6c, 6d, and 6e.

It would be desirable for many reasons to operate a system of this type at higher frequencies rather than in the audio range. However, a limitation is imposed, in this particular design at any rate, by the incidental dissipation in the coils. To see how this comes about let us refer to the pole-zero configuration of Figure 4. Ideally, the poles and zeroes are equally spaced from the imaginary axis. However, the inevitable losses in the components will cause a shift of the pole-zero pair to the left by an amount proportional to the frequency divided by the Q-factor of the coil. This will introduce a dip in the amplitude curve of the network section at the frequency of its singularities, thereby destroying the all-pass nature of the filter.

57-9048

SECRET

From the conjugate conditions on the amplitude, equation (2), we find that the effect works in the opposite direction from what we desire of a matched filter, i.e. at the receiving end we attenuate those spectral bands which are accentuated at the transmitter and vice-versa. In the present design the only way to counter this difficulty is to employ coils with as high a Q as possible. The frequency limitation comes in because the Q requirement goes up in direction proportion to the frequency. We are now operating at the limit of the state-of-the-art in coil-Q at 10 kc. Holding the same shift in the pole-zero pattern at 100 kc implies a Q ten times as great, which is presently not obtainable.

In order to apply the phase-distortion design procedure to an arbitrary frequency-band, different building blocks must be developed. There are two directions in which this can go; the first is to find components with low losses such as crystals or ferrites and determine if it is possible from these to derive a building block with the desired properties, and the second is to design building blocks in such a fashion that the losses appear as a flat attenuation over the whole band of interest without the dip previously mentioned. We are investigating these ideas further so as to increase the usefulness of the phase distortion approach.

ACKNOWLEDGEMENT

We are indebted to Professor E. A. Guillemin of M.I.T. who was employed by Melpar as a consultant on the project, for the particular realization method for matched filter networks described above.

57-9048

SECRET

SECRET

REFERENCES

1. "Study of Variable Optimum Filter System" Melpar, Inc. Contract DA-36-039-sc-63190 a. Second Interim Report 15 July 1955 b. Final Report 15 March 1956.
2. P. M. Woodward Probability and Information Theory McGraw-Hill 1955.

01

SECRET 57-9648

SECRET

THE USE OF PULSE CODING TO DISCRIMINATE AGAINST CLUTTER* (CONFIDENTIAL)

Roger Manasse**

ABSTRACT

This paper considers the use of pulse coding (or pulse compression) in radar to obtain improved detection of targets in clutter. The effectiveness of this technique depends on the differing spatial characteristics of the target and clutter in contrast with the usual MTI which depends on the differing time-varying properties. With the assumptions of a simple clutter model and an appropriately optimized receiver, and with the aid of known results in detection theory, an expression is derived for the single-pulse detection capability of a radar operating in the presence of both clutter and additive white receiver noise. From the expression it is seen that detection performance is simply related to the spectrum of the transmitted signal and, generally speaking, improves as the bandwidth of the transmitted signal is increased. Results for clutter noise only or receiver noise only appear as special cases. The implications of these results for pulse coding (or pulse compression) in radar are discussed.

* The research in this document was supported jointly by the Army, Navy, and Air Force under contract with the Massachusetts Institute of Technology.

** Staff Member, Lincoln Laboratory, Massachusetts Institute of Technology.

SECRET 57-9048

SECRET

I. Introduction

Before proceeding with a theoretical discussion of the applicability of pulse coding to obtaining improved radar detection of targets in clutter, let us consider briefly the connection between the terms "pulse coding" and "pulse compression."

For a radar receiver operating in the presence of additive white gaussian noise, modern statistical detection theory indicates that optimum receiver performance can be obtained with the aid of a linear filter which is matched to the expected radar return, a filter which has a unit impulse response which is simply a time inverted replica of the expected radar return.[1,2,3] The signal $s(t)$ and noise are fed into a matched filter with unit impulse response $h(t) = s(T - t)$.

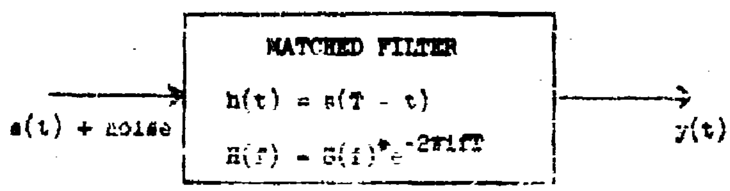

Figure 1

T is an arbitrary time delay factor chosen so that $h(t)$ satisfies the realizability condition

$$h(t) = 0 \qquad \text{for} \qquad t < 0$$

In the frequency domain the filter response is given by the expression shown in Fig. 1, where $H(f)$ and $S(f)$ are the Fourier transforms of $h(t)$ and $s(t)$, respectively. Then the output of the matched filter $y(t)$ is equal to the convolution of $s(t)$ with $h(t)$ plus a noise term.

SECRET 57 9048

$$y(t) = \int_{-\infty}^{\infty} s(z)h(t - z)dz + \text{noise} = \int_{-\infty}^{\infty} s(z)s(T - t + z)dz + \text{noise}$$

$$= \varphi(T - t) + \text{noise}$$

where $\varphi(\tau)$ is the autocorrelation function of $s(t)$. Detection is performed at approximately time $t = T$ where the signal autocorrelation function at the output of the filter reaches its peak.

Under the assumption that the receiving filter always remains matched to a delayed replica of the transmitted signal, the signal pulse at the output of the matched filter will always be the autocorrelation function of the transmitted signal. If, for various reasons, we desire to have (in some sense) an autocorrelation function which is short compared to the transmitted pulse length, it will be necessary to code, i.e. amplitude and phase modulate, the transmitted pulse in order to increase its bandwidth appreciably beyond that for the uncoded pulse.* Pulse compression, a term taken to refer to a process whereby a relatively long low amplitude pulse is converted to a relatively short high amplitude pulse, is brought about automatically by the matched filter when the transmitted pulse has been coded. Thus, for our purposes, the terms "pulse compression" and "pulse coding" are synonymous and the terms can be used interchangeably.

*Recalling that the autocorrelation function is the Fourier transform of of the signal energy spectrum, we see that the requirements on the shape of the output pulse can be expressed in terms of requirements on the shape of the signal energy spectrum.

 57- 9048

SECRET

A number of possible advantages can be cited for the use of pulse compression or pulse coding in radar. Among them we have

1. Increased range capability with the use of longer radar pulses while range accuracy and resolution are maintained or improved over that attainable with a short uncoded pulse.
2. Increased capability against jamming.
3. Increased ability to maintain a constant false alarm rate in the receiver.
4. And, in certain situations, even the ability to obtain reduced receiver complexity when special types of pulse coding are used.

The possibility of [illegible] a radar's ability to discriminate against clutter through the use of pulse compression, which is the subject of this paper, was suggested to the author by Dr. Robert F. Naka of the M.I.T. Lincoln Laboratory.

II. Analysis of the Problem

Let us now consider a conventional pulsed radar in which the doppler shift on a single radar pulse is negligible: That is, the signal pulse reflected from a point target is simply a delayed and attenuated version of the transmitted pulse. On the sweep return from a single pulse, then, we completely ignore the time-varying properties of both the target and the clutter. Following the procedure used by George,[4] the space surrounding the radar, appropriately weighted with the antenna beam pattern, may be

SECRET 57-9048

considered as a linear filter whose transfer characteristic is characterized by a unit impulse response function which is denoted $W(t)$.

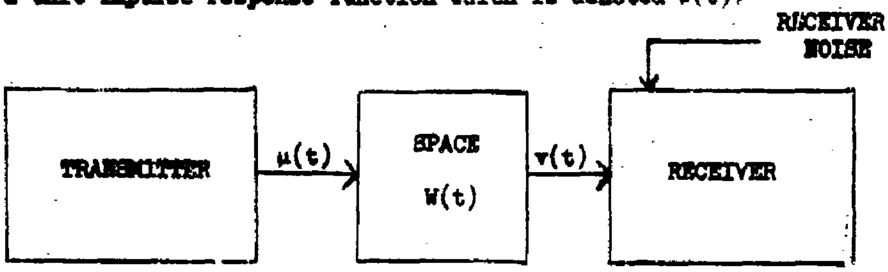

Figure 2

The transmitter generates the transmitted pulse, denoted $\mu(t)$, which is en reflected from objects in the space surrounding the radar. This process is equivalent to passing $\mu(t)$ through the filter $W(t)$ to produce the reflected waveform $v(t)$ which presents itself to the receiver along with receiver noise, where $v(t)$ is given by

$$v(t) = \int_{-\infty}^{\infty} \mu(z)W(t - z)dz$$

We can imagine, without loss of generality, that $\mu(t)$ is generated in the transmitter by sending a spike or δ-function into a filter with impulse response $\mu(t)$, and the above block diagram is equivalent to the following.

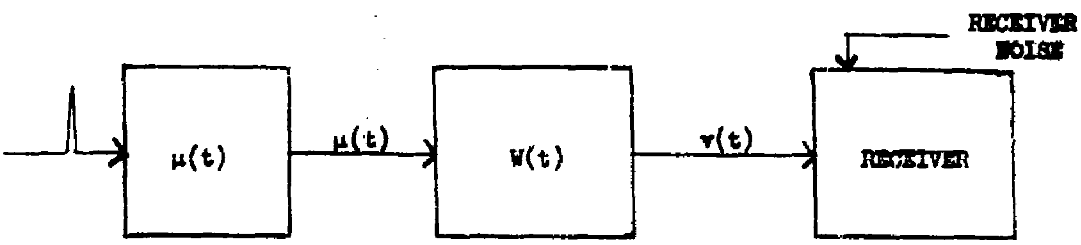

Figure 3

57- 9048

Because the frequency response function of the first two filters taken in series is simply the product of the frequency response functions for the separate filters, these two filters may be interchanged without affecting v(t).

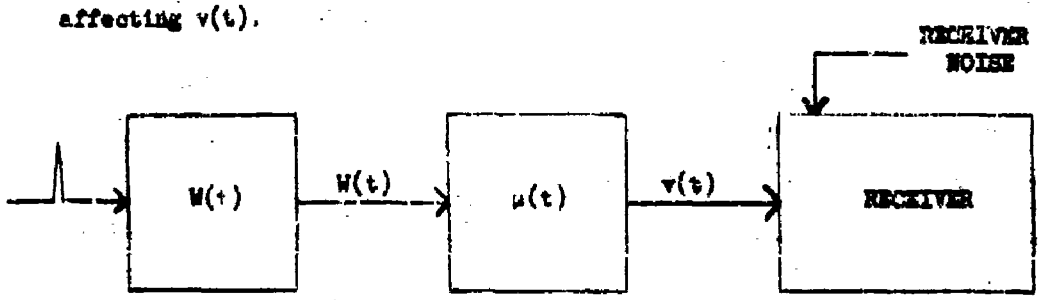

Figure 4

In order to proceed further we must assume a model for the clutter return. We assume for the purpose of analysis that the clutter consists of a large randomly distributed ensemble of very small independent point scatterers. That is,

$$W(t) = \underbrace{A\delta(t - t_s)}_{\text{Signal term}} + \underbrace{\sum_k a_k\delta(t - t_k)}_{\text{Clutter noise term}}$$

The first term is the response of the point target to a transmitted δ-function. The amplitude A is finite, corresponding to the fact that the cross section is finite, while the time delay t_s measures the range of the target. The second term represents the clutter response to a δ-function and is a sum of appropriately amplitude weighted and delayed δ-functions corresponding to the point scatterers of the clutter model.

57-9048

The a_k's and t_k's are taken to be independent random variables. Consider an interval of range, sufficiently small so that the inverse fourth power of range and other geometrical factors can be ignored across the interval. Then the t_k's are uniformly distributed across the interval. Letting our model for clutter approach the limit in which the distribution of t_k's over the interval is infinitely dense and the a_k's are infinitesimal, we obtain a process which is, mathematically, exactly analogous to the shot effect.[5] Thus, the clutter noise at the input to the filter $\mu(t)$ in Fig. 4 is equivalent to white gaussian noise.

Then $v(t)$, which is the output of the $\mu(t)$ filter and is the message presented to the radar receiver, is given by

$$v(t) = \underbrace{A\mu(t - t_s)}_{\text{Signal}} + \underbrace{n_c(t)}_{\substack{\text{Clutter} \\ \text{noise}}}$$

where $n_c(t)$ is the result of passing white gaussian clutter noise through the $\mu(t)$ filter. Because the $\mu(t)$ filter has a spectral transfer function given by $|U(f)|^2$, $n_c(t)$ is simply colored gaussian noise with power spectrum $N_c(f)$ which is proportional to the energy spectrum of the transmitted signal.* That is,

$$N_c(f) = c|U(f)|^2$$

where c is a proportionality constant which depends on the intensity of the clutter. Adding the colored noise from the clutter to the additive

*This fact has been noted by Lawson and Uhlenbeck, reference 6.

white gaussian receiver noise with noise power per cycle $N_o/2$, and noting that these two noises are independent, the result is colored gaussian noise with power spectrum $N(f)$.

$$N(f) = \frac{N_o}{2} + c|U(f)|^2$$

The problem presented to the receiver is that of detecting the returned radar signal $Au(t - t_s)$ in the presence of colored gaussian noise. Dwork[7] and later George[4] have independently extended signal detectability theory to include the case of a known signal in colored gaussian noise. If $S(f)$ is the voltage spectrum of the signal and $N(f)$ is the power spectrum of the noise, they have shown that the transfer function of the optimum filter is given by

$$\frac{S^*(f)e^{-2\pi ifT}}{N(f)}$$

where T is a conveniently chosen time delay. Note that in the white noise case $N(f)$ is a constant and the above expression becomes the transfer function of the usual matched filter. The above filter is really the generalization of the matched filter to the colored noise case. The peak signal-to-noise power ratio obtained with the above filter is given by

$$(S/N)_{opt} = \int_{-\infty}^{\infty} \frac{|S(f)|^2}{N(f)}\, df$$

For our problem

$$S(f) = \int_{-\infty}^{\infty} Au(t - t_s)e^{-2\pi ift}\, dt = AU(f)e^{-2\pi ift_s}$$

57-9048

and

$$|S(f)|^2 = A^2|U(f)|^2$$

Also, recalling that $N(f) = \frac{1}{2} N_o + c|U(f)|^2$ and substituting in the above expression, we have

$$(S/N)_{opt} = A^2 \int_{-\infty}^{\infty} \frac{|U(f)|^2}{\frac{1}{2} N_o + c|U(f)|^2} df$$

The quantity $(S/N)_{opt}$ is a good measure of the single pulse detection capability which is available from the optimum receiver.* Therefore, in order to maximize the detection capability we must choose the parameters of the radar system to maximize $(S/N)_{opt}$. The constants A and c are determined by the nature of the target, the clutter and the geometrical parameters of the system. In this discussion we assume that these parameters are not at our disposal.

*For an exactly known signal, P_D (probability of detection) versus P_F (probability of false alarm) curves given in reference 3 can be used if one replaces $2E/N_o$ by $(S/N)_{opt}$. In practice, the returned radar signal is not exactly known because of unknown parameters such as time delay. For a given P_D these unknown parameters have the effect of increasing the false alarm rate by an amount which may depend on the shape of transmitted signal waveform. However, for the level at which most radars operate the increase in false alarm rate introduced by these unknown parameters does not seriously degrade the signal detectability.

57-9048

It is of great interest to determine the dependence of $(S/N)_{opt}$ on $U(f)$, that is, the dependence of the signal detectability on the transmitted signal waveform. There are several conclusions which are immediately apparent from the expression for $(S/N)_{opt}$.

1. When no clutter is present, that is when $c = 0$, $(S/N)_{opt}$ depends only on the ratio of the signal energy to noise power per cycle at the receiver. Therefore we have the well-known result that the detection capability depends only on the energy of the transmitted pulse and not on its shape.
2. In the limit where internal noise is negligible, that is where $N_o = 0$ (or where the clutter return overpowers the receiver noise), the integrand is a constant and $(S/N)_{opt}$ depends only on the effective system bandwidth. This fact has been pointed out by George and Urkowitz.[4,8] In particular, the detectability does not depend on the transmitted pulse energy.

If there are no restrictions on pulse energy and pulse bandwidth, it is also clear from the above expression that $(S/N)_{opt}$ can be made as large as we please by choosing $|U(f)|^2$ to be sufficiently broad and flat versus frequency.* For the purpose of this analysis, however, the

*This conclusion depends critically on the clutter model which has been assumed. In a practical radar situation the conclusion may not hold because of the discrete or granular nature of the clutter.

requirements on the shape of the transmitted pulse can be derived by maximizing $(S/N)_{opt}$ subject to the requirements that the pulse energy and pulse bandwidth are fixed. That is,

$$\int_{-\infty}^{\infty} u(t)^2 dt = \int_{-\infty}^{\infty} |U(f)|^2 df = E \quad \text{(a finite constant)}$$

and

$$U(f) = 0 \quad \text{unless} \quad f_1 \leq f \leq f_2 \quad \text{or} \quad -f_2 \leq f \leq -f_1$$

where $\Delta f = f_2 - f_1$ is called the available system bandwidth. The maximization of $(S/N)_{opt}$ is a straightforward problem in the calculus of variations which yields a very simple result. It says that the spectrum of the transmitted pulse should be flat over the available frequency band. This result is independent of the constant c, and hence is independent of what fraction of the noise is due to the receiver and what fraction is due to the clutter. Thus, a transmitted pulse which has a flat spectrum over the available system bandwidth is optimum under the assumed restrictions both at short ranges where clutter noise tends to predominate and at long ranges where thermal noise tends to predominate. Parenthetically it may be remarked that the requirements which have been derived on the spectrum of the transmitted pulse are identical to the requirements which would be derived by minimizing $\int \varphi(t)^2 dt$, the integral of the squared autocorrelation function, subject to the same restrictions.

The optimized pulse energy spectrum $|U(f)|^2$ should therefore satisfy

$$|U(f)|^2 = \begin{cases} E/2\Delta f & \text{for} \quad f \text{ in } \Delta f \\ 0 & \text{otherwise} \end{cases}$$

Substituting this in the expression for $(S/N)_{opt}$ we obtain

$$(S/N)_{opt,opt} = \frac{2A^2E}{N_o + cE/\Delta f}$$

The opt,opt denotes the fact that S/N has been optimized both with respect to the choice of receiving filter and shape of transmitted waveform. From this expression the desirability of having large Δf in order to minimize the effect of clutter noise and large E to minimize the effect of receiver noise is evident. For a pulse radar which is peak power limited E will be proportional to the pulse length. These two requirements, large system bandwidth and long pulse length, imply that the transmitted pulse should have large time-bandwidth product. In other words, the transmitted pulse must be coded or phase modulated to produce a time-bandwidth product substantially greater than unity. For the optimized pulse energy spectrum the returned clutter noise spectrum as well as receiver noise will be flat over the signal bandwidth and therefore the optimum receiver filter must be the usual matched filter which results from the assumption of white gaussian background noise. One signal waveform which approximately satisfies the optimum conditions derived here is a pulse with rectangular envelope and a carrier with linearly swept frequency, where the pulse length and frequency sweep are such that the time-bandwidth product of the pulse is much larger than one.

57-9048

It is of interest to ask what are some of the basic limitations on the pulse coding or pulse compression technique as a means for obtaining improved detection of targets in clutter. Aside from obvious practical difficulties associated with obtaining transmitting and receiving electronic components to handle wider bandwidth signals, there are basic limitations due to the detailed properties of clutter and targets themselves. The inherent granularity of the clutter which our model does not take into account will set an upper bound on the system bandwidth Δf which can be utilised in the discrimination against clutter. For finely divided and randomly distributed types of clutter such as precipitation (and to some extent chaff) the useful system bandwidth Δf is probably quite large, but for ground clutter, which is not so well behaved because of the presence of large point scatterers (large rocks, cliffs, buildings, watertowers, etc.), the useful Δf may be much smaller. A second limitation on Δf is due to the fact that the target itself is not a point, but is actually a distributed scatterer. Reasonable target dimensions suggest a useful system bandwidth in the vicinity of 10 mc.

What about the compatibility of pulse compression techniques with pulse-to-pulse integration techniques employing MTI? Provided that the pulse coding does not change from one pulse to the next, pulse phase at the output of the matched filter remains a well-defined quantity which may be compared on a pulse-to-pulse basis. Thus, in principle, pulse compression and MTI are compatible. In pulsed doppler systems range gating or sampling followed by filtering can be employed at the output of

 57-9048

the matched filter, but the number of range processing channels will have to correspond approximately to the effective number of resolvable range intervals. The greater the bandwidth of the transmitted pulses, the greater must be the number of range processing channels. Thus, as a practical matter for this type of data processing, pulse compression will require increased receiver complexity. MTI schemes employing two-pulse or several-pulse cancellation and integration should not have to be significantly modified if the delay lines and associated electronic components in the data processing have sufficient bandwidth to accommodate the coded pulses.

The use of MTI and pulse compression simultaneously to discriminate against clutter appears to present a fortuitous combination. For generally a type of clutter which responds poorly to one technique should respond well to the other. For example, precipitation or chaff which sometimes responds poorly to MTI because of its non-zero velocity should respond well to the pulse coding, while ground clutter which, because of its spatial properties, may respond poorly to pulse coding will respond very well to MTI.

III. Summary

The type of clutter discrimination which we have discussed here is obtained by virtue of the spatial properties of the clutter rather than its time-varying properties, as with MTI. Using a convenient model applicable to finely distributed clutter and proceeding from available results on the detection of a known signal in colored gaussian noise, we have set up an expression for the single pulse detection capability for a

57-9048

radar operating in the presence of both receiver noise and clutter noise. Results for detection capability in the presence of predominantly clutter or predominantly receiver noise appear as special cases of this expression. From the expression we have seen that detection performance is simply related to the spectrum of the transmitted signal. Subject to the requirement of fixed transmitted signal energy and fixed system bandwidth, we have seen that the optimum spectrum for the transmitted pulse is one which is flat over the available system bandwidth and that this optimum is independent of the relative strength of receiver and clutter noise. For a radar whose transmitter is peak power limited, the logical result of these considerations is a pulse with large time-bandwidth product, in other words a coded pulse. We have mentioned that one method of approximately realizing the optimum pulse spectrum is a linearly swept FM pulse with rectangular envelope and large time-bandwidth product. Lastly, it has been pointed out that pulse coding and MTI are not mutually exclusive radar techniques. In fact, when used together they should form a powerful combination for the purpose of obtaining improved detection of targets in clutter.

IV. Acknowledgement

The author is indebted to Dr. Robert F. Naka who suggested the application of pulse coding discussed here. The author is also indebted to Mr. Edwin L. Key for helpful discussions relating to this material.

57- 9048

SECRET

BIBLIOGRAPHY

1. D. O. North, T. R. PtR-6C, RCA Laboratories, Princeton, New Jersey, June 25, 1943.

2. J. H. Van Vleck and D. Middleton, "Theoretical Comparison of the Visual, Aural and Meter Reception of Pulsed Signals in the Presence of Noise," Jour. App. Phys. 17, p. 940, 1946.

3. W. W. Peterson, T. G. Birdsall, and W. C. Fox, "Theory of Signal Detectability," Parts I and II, T. R. No. 13, Electronic Defense Group, University of Michigan, 1953. Also available in 1954 Symposium on Information Theory, Trans. I.R.E., PGIT-4, September, 1954.

4. T. S. George, "Fluctuations of Ground Clutter Return in Airborne Radar Equipment," Inst. Elec. Eng. (London), Monograph No. 22, 1952.

5. S. O. Rice, "Mathematical Analysis of Random Noise," B. S. T. J. Vol. 23, pp. 282-332, and Vol. 24, pp. 46-156, 1945-46. Also available in Selected Papers on Noise and Stochastic Processes, N. Wax (editor), pp. 133-294, Dover Publications, 1954.

6. J. L. Lawson and G. E. Uhlenbeck, Threshold Signals, Radiation Laboratory Series, Vol. 24, p. 297 (McGraw-Hill, New York, 1950).

7. R. M. Dwork, "Detection of a Pulse Superimposed on Fluctuation Noise," Proc. I.R.E. 38, p. 771, July, 1950.

8. H. Urkowitz, "Filters for Detection of Small Radar Signals in Clutter," Jour. App. Phys. 24, No. 8, p. 1024, August, 1953.

SECRET

57-9048

CHIRP, A NEW HIGH PERFORMANCE RADAR TECHNIQUE

Amos C. Price, Jr.

57- 9048

SECRET

Introduction

To achieve high range resolution in a conventional radar, short, high peak power pulses are required. The generation of these pulses is a difficult problem limited by practical considerations. It is believed possible to avoid some of these problems by employing the CHIRP principle. The range performance of a radar is limited by the signal-to-noise capability of the system and hence, is a function of the average transmitted power and the receiver noise figure. In a CHIRP radar, a long, relatively low peak power, frequency modulated pulse is transmitted to obtain high average power. High range resolution, comparable to a very short pulse system, is realized by collapsing the received pulse to a short duration pulse before it is displayed in the indicator.

The CHIRP principle which makes this possible is illustrated in its simplest form by Figure 1. The linear frequency modulated wave shown at the bottom of the figure 1 is applied to a network which has the delay depicted at the top of the figure. Thus instantaneous frequency f_1 is delayed by t_1, f_2 by t_2, etc. The net result is an output shown at the far right of Figure 1. The original long pulse has been collapsed into a shorter, higher amplitude pulse.

This principle and its ramifications can be credited to several people. Among the early patent holders are Mr. Amos Dickey of the Massachusetts Institute of Technology and Mr. Sidney Darlington of the Bell Telephone Laboratories. Although the principle was conceived quite a few years ago, lack of wide band microwave transmitting tubes prevented radar applications from being developed. With the broadening research activity on traveling wave amplifiers in the past few years, radar applications of the CHIRP principle have become a possibility. In mid-1955 Contract AF33(616)-2847 was awarded to the Bell Telephone Laboratories to explore the radar system applications of frequency dispersive techniques. This contract is under the jurisdiction of the Weapons Guidance Laboratory, WCLGG-4, at Wright-Patterson Air Force Base.

57-9048

SECRET

Since the origination of the contract, considerable analytical and experimental investigations have been performed to substantiate early evidence of the practicality of a CHIRP radar system.

Basic Theory

The theory to be presented is a survey of some of the analytical work done on this project. It is not intended to be mathematically rigorous since a general presentation of the principles involved, rather than the pure mathematical mechanics, is thought to be more useful to the audience. Also, much of the detailed analysis is presented in the quarterly engineering reports prepared for this contract.

If a frequency modulated pulse which has the characteristics shown in Figure 2(a), i.e., rectangular envelope and linear frequency modulation during the pulse is impressed upon the input to a lossless network which has the characteristics shown in Figure 2(b); some rather interesting and useful properties are exhibited by the network output pulse shown in Figure 2(c). Basically, all frequencies contained in the input pulse have had their phases rearranged so that they tend to emerge from the network at approximately the same time. Early low frequency portions of the input pulse are delayed longer and are effectively overtaken by the higher frequency portions occuring later in the pulse. The net result is an output pulse which may be made considerably shorter in duration and higher in amplitude. Thus, it is possible to start with a relatively long frequency modulated pulse and, after going through a passive network, have a higher amplitude, shorter output pulse. Some of the interesting properties of the output pulse follow. If the input pulse has a pulse length of $2T$ microseconds and a total frequency swing of Δ megacycles, the output pulse has a pulse length at the -4db points of $\frac{1}{\Delta}$ microseconds and is increased in peak amplitude by a factor of $\sqrt{2T\Delta}$. However, these characteristics are gained at the cost of time or range side lobes on the output pulse. It can be shown methematically that the output of the network under the previously given conditions takes the form of $\frac{\sin \pi\Delta t}{\pi\Delta t}$. The first side lobes on the range pulse are down 13db from the peak.

57-9048

The question arises as to whether side lobes of this level can be tolerated and if not, what can be done to decrease them. In many applications, it is important that these side lobes be decreased as much as possible. Therefore, analytical studies were made to see what could be done to reduce the side lobes to a tolerable level. If one recognizes the analogy between the rectangular frequency modulated input pulse which gives a $\frac{\sin \pi\Delta t}{\pi\Delta t}$ output pulse and the rectangular current distribution in an antenna which gives a $\frac{\sin \Theta}{\Theta}$ spatial far field radiation pattern; some results of antenna theory are very useful. Using this analogy, shaping of the frequency modulated input pulse envelope should give a reduction in the time side lobes on the output pulse. This has been shown to be correct and analytical results have been obtained for various types of shaping networks. This shaping can be performed by passing the CHIRP signal through a phase equalized loss network either before or after it is collapsed. Shaping widens the output pulse but this effect is not serious for a side lobe reduction of approximately 10db which is being considered.

A possible means of using the CHIRP principle just described is shown in Figure [illegible]. This is a simplified block diagram of a CHIRP radar using an active frequency modulated generator. The required frequency modulated pulse is obtained by applying a shaped voltage pulse to the reflector of a klystron or any other suitable device. The delay equalizer is in the receiving branch of the radar. It could also include a shaping network. Thus, a long frequency modulated signal can be transmitted, and a short video signal used in the display.

Certain system considerations have shown the active generation scheme just described to be undesirable for high resolution applications. The following method appears to be a more suitable way to obtain the required CHIRP signal for these applications. Since the delay equalizer is a bi-directional network, what happens if a short pulse is impressed upon the input of the network? As might be suspected, just the reverse of collapsing occurs; the pulse is dispersed by the network. This has been shown both experimentally and analytically. If a short pulse is presented to the delay equalizer input, the output pulse is spread out in time and possesses frequency modulation. For the linear time delay network already described, the frequency modulation is linear with the frequencies which are delayed least (high frequencies) occurring earliest in the network output pulse. This is just the reverse of the frequency modulated signal

57-9048

previously described so the collapsing network must be altered to have an equal, but opposite slope.

A simplified system using passive generation is shown in the block diagram of Figure 4. The frequency modulated transmitter signal is obtained by passing a short pulse through a dispersing delay network and after suitable amplification, it is radiated to the target. The reflected signal is amplified and passed through a collapsing delay network whose slope is equal and opposite to the transmission network's slope. After the signal is collapsed and demodulated, it is presented to a suitable display.

System Status

Early experimental work led to the conclusion that preliminary results would be obtained more rapidly if the required CHIRP frequency modulated signal were generated in a klystron or similar voltage tunable device. A klystron was chosen and work went on to develop or adapt it for use over a 50 megacycle frequency band. A klystron oscillator was built which, by using two coupled cavities, had a bandwidth of 40 some odd megacycles to the 0.1 db power points.

The first delay equalizer design was to have a delay slope of 0.1 microseconds/megacycle with a bandwidth of at least 10 megacycles. Previous design experience indicated that results would be obtained more rapidly if the network were built in the video frequency band. Consequently, the first CHIRP delay equalizer had a bandwidth of 12 megacycles with a center frequency close to 6 megacycles. This network was built to permit early experimental signal analysis. Subsequent delay equalizer designs called for a differential delay of 2 microseconds over a 30 megacycle band. The center frequency chosen is 70 megacycles. Several of these networks have been constructed and tested.

Further experimental and analytical work has shown that it is very difficult to generate a frequency modulated pulse in an active device and retain the same center frequency each time. This is important because the signal goes through a network which transforms frequency instabilities into time jitters by a sloping delay with frequency characteristic. Numerically, if it is desired to hold the output pulse time jitters to less than one-tenth

57-9048

of the contemplated final output pulse length of 30 millimicroseconds which would be obtained with the 30 megacycle bandwidth, the total deviation in the center frequency of the frequency modulated signal generator and the beating oscillator must be held to less than ±22.5kc. To do this, frequency stabilities in the order of a few parts in 10^6 or better are required. To achieve this order of stability it is usually necessary to resort to high Q, narrow band devices which is diametrically opposed to our original aim of wide band electronic tuning.

Fortunately, there is a solution which has other desirable features. The passive generation scheme previously described requires no broad band oscillators. This will be shown in the following discussion. A practical CHIRP system is shown in the block diagram of Figure 5. The short pulse used to drive the transmission dispersion network is obtained from a balanced i.f. modulator which has a crystal controlled 70 megacycle signal as its carrier. After dispersion through the network and i.f. amplication, the CHIRP signal is modulated up to the microwave frequency by a microwave single side-band modulator. This modulator has as its carrier a signal from an ultra-stable microwave oscillator operating at some frequency (f_o). Since the upper sideband is chosen as the output of the modulator, the signal presented to the traveling wave tube amplifier has a center frequency of f_o + 70mc. With the dispersion network characteristic shown, this signal will be frequency modulated starting with high frequencies and linearly dereasing to low frequencies. This is the signal radiated to the target.

After reception, the signal is amplified by a low noise traveling wave tube amplifier. This tube is designed to have a gain of 20-25db and a reliable noise figure of 10 db or less. The received signal is then presented to a microwave single sideband modulator and appears at the modulator output as an i.f. signal. The carrier supplied to this modulator is obtained by beating the second harmonic of the crystal controlled 70 megacycle signal with the output of the ultra-stable microwave oscillator which is at a frequency of f_o. By choosing the upper sideband, a carrier signal frequency of f_o + 140 mc is obtained. With this as the carrier frequency and the received CHIRP signal as the signal input to the receiving modulator, the sidebands will be inverted. That is, the

57-9048

output i.f. signal now has its frequencies inverted so that low frequencies occur first and there is a linear increase in frequency.

This permits the collapsing network to be similar to the transmission dispersion network. In fact, the same network may be time shared by both branches. After suitable amplification and detection, the collapsed pulse is presented to the display.

Since all oscillators in the system may now be operated at fixed frequencies, the oscillator circuits may be made narrow band and high stability may be obtained. In addition, the transmission and reception channels now consist of passive circuits which do not destroy the phase information of the signal; hence, the system can be made coherent by making the oscillator stabilities sufficiently high.

Results

The CHIRP principle has been demonstrated in a closed circuit test. Figure 7 shows the experimental equipment connections used to obtain the waveforms shown in Figure 5. The CHIRP f.m. signal was generated with an X-band klystron modified for wide band operation. This signal was then modulated down to a low intermediate frequency and passed through the 0-12 megacycle delay equalizer whose characteristics are shown in Figure 8. The waveforms of Figure 6 have the correct relative amplitudes for a Δ of 10 megacycles and a 2T of one microsecond. It should be noted that the collapsed pulse length is approximately half the predicted value obtained from the theory. In the case of equalization at low intermediate frequencies, the collapsed pulse does not have enough cycles to completely fill the predicted output pulse envelope. In this particular case, the output pulse has a duration of approximately one-half cycle of the center frequency of 6 megacycles.

Further network development resulted in the design and construction of two delay equalizers, each of which has two microseconds of differential delay over a 30 megacycle band centered at 70 megacycles. The deviations from a linear slope of 0.0683 microseconds per megacycle are less than ±20 millimicroseconds over the desired band. The networks also have a flat loss of about 36 db over the band.

57-9048

More recent results have been obtained with a low power experimental system utilizing network dispersion. The experimental system closely resembles the block diagram of figure 5 and employs two delay networks both centered at 70 MC. The experimental system parameters are:

1. Radar Parameters

   Transmitter Frequency ≅ 9300 MC.
   Transmitter Peak Power = 1 Watt
   Transmitter (Dispersed)
   Pulse Length = 2 μsec
   Receiver (Collapsed)
   Pulse Length ≅ 0.035 μsec

2. IF Delay Network Parameters

   Center Frequency = 70 MC.
   Bandwidth = 30 MC.
   Differential Delay = 2 μsec

The transmitting and receiving delay networks are of identical design; sideband inversion is used to obtain a conjugate relationship between the two.

Some of the experimental waveforms obtained with this system are shown in Figures 9 through 12. Figure 9(a) shows the short video pulse used to modulate the 70 MC. balanced modulator in the transmitter. The 70 MC. counterpart of this pulse is then dispersed in the transmitting delay equalizer. Figure 9(b) is the rectified envelope of the X-band signal after amplification and time limiting has been performed in the transmitting traveling wave tubes. The same time scale has been used in Figures 9(a) and 9(b) to emphasize the amount of dispersion (60 to 1) obtained in this system.

The low power experimental system just described is operating in a laboratory which has a large, radar transparent window which permits scanning of the adjacent terrain. Figure 10 is a picture of the "A" scope video obtained when the system is illuminating a corner reflector target test range. The corner reflectors are located in a radial line centered at the radar antenna. Target separations as small as 12.5 feet can be discerned in the picture thus the collapsing is occurring as anticipated.

57- 9048

Spectrum weighting effects have been investigated both analytically and experimentally. A Taylor weighting function was chosen for the system. Two weighting networks have been built and tested qualitatively. The two networks are designed to give 25 and 34db sidelobes respectively. Figure 11 shows the effects of weighting on the collapsed "main bang". Figure 12 shows the effects of weighting on the radar return from the corner reflector test range. The waveforms corresponding to no external weighting are included in each figure for comparison purposes. Since the detector used in these tests had a power law characteristic, no quantitative comparisons should be made from these photographs. A maximum range of 44,000 feet was obtained with the system parameters previously given. The target at maximum range was a medium sized water tower.

Analysis has brought out certain anti jamming features inherent in a CHIRP system. First of all, the average power, for a given waveguide breakdown, can be greatly increased over a short pulse system with comparable bandwidth and resolution. The system also has an advantage over a conventional radar when short pulse jamming is considered. As has been shown previously, short pulses are dispersed by the receiving delay equalizer with the resultant decrease in amplitude.

Conclusions

Signal-to-noise ratio, and hence range capability of a conventional radar is largely a function of the average radiated power. To get more range, the average power has to be increased. Once the limiting peak power is reached, the only way to increase the average power - if the pulse repetition rate is held fixed - is to increase the pulse length with a resultant loss in range resolution capability. The CHIRP radar has the range capability inherent in a long pulse - high average power radar but combines this with the resolution capability of a short pulse system by using frequency modulation.

A low power experimental radar is being built which will have a 2 (and eventually a 4) microsecond transmitted pulse with 30 megacycles of linear frequency modulation. The video display pulse will be about 35 millimicroseconds long in both cases since the video output pulse length is a function of the amount of frequency modulation alone. This results in collapse ratios of 60 and 120 to one.

57-4048

These collapse ratios are not thought to be the ultimate, but as the collapse ratio increases, component tolerances mount accordingly. Analysis plus experiment will determine the ultimate limit; but for the present, the collapse ratios being contemplated appear reasonable.

In summary the CHIRP principle provides a radar technique which permits the transmission of longer pulses with the resultant higher average power but retains the resolution capabilities of a short pulse system through the proper use of moderate amounts of frequency modulation. This technique also has inherent anti-jamming features.

Att.
Figures 1-12

57-9048

SECRET

FIGURE I
CHIRP PRINCIPLE

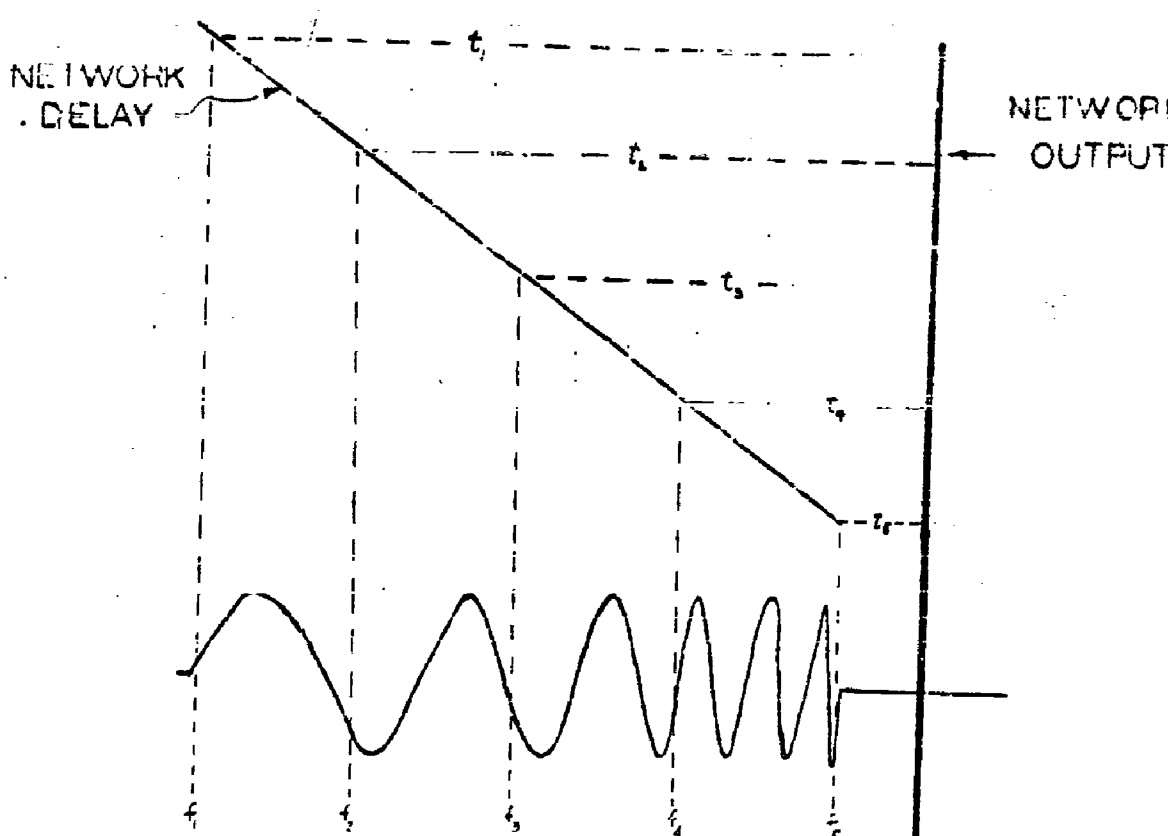

57-9048

SECRET

SECRET

FIGURE 2
CHIRP CHARACTERISTICS

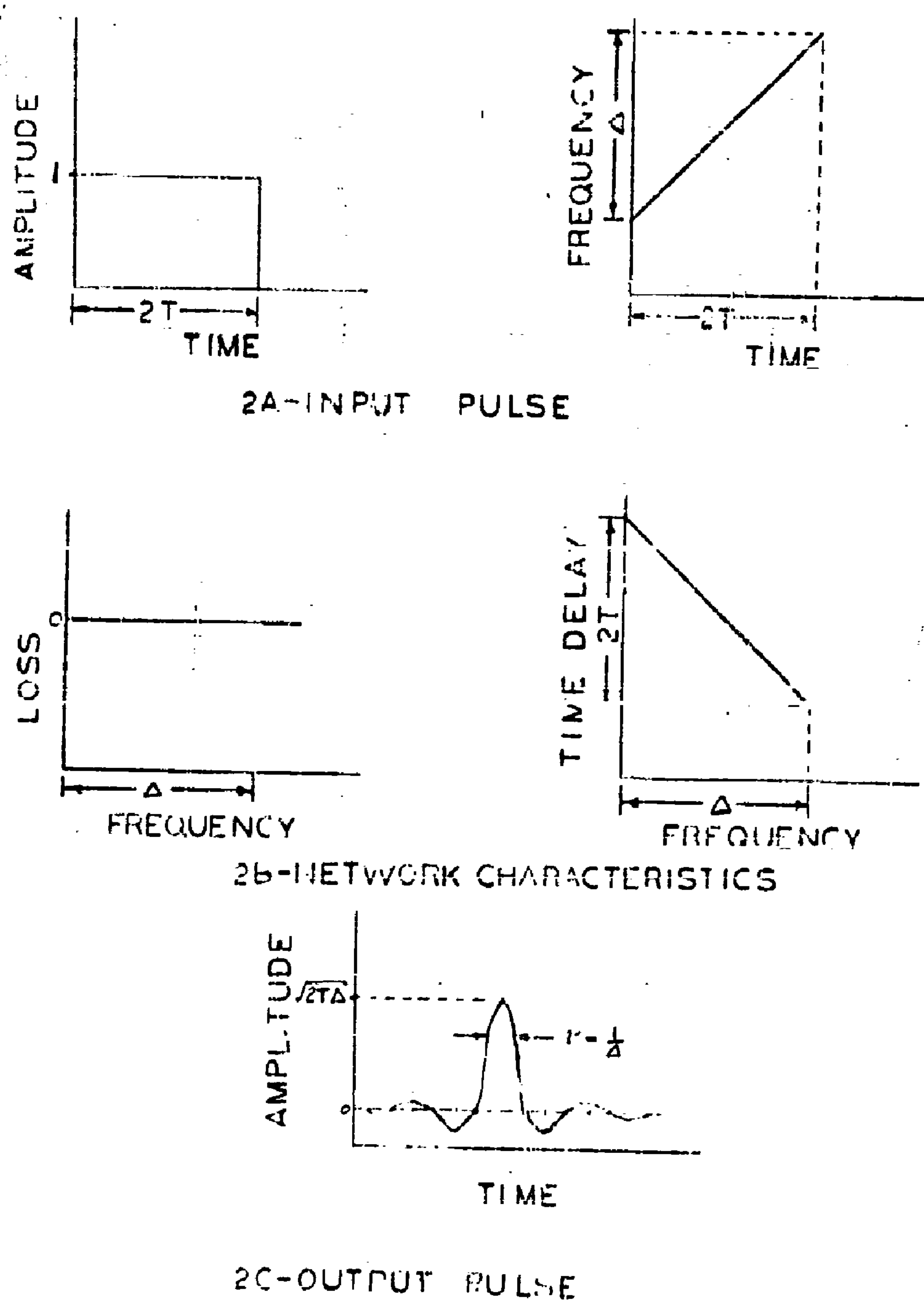

SECRET

57-9048

FIGURE 3

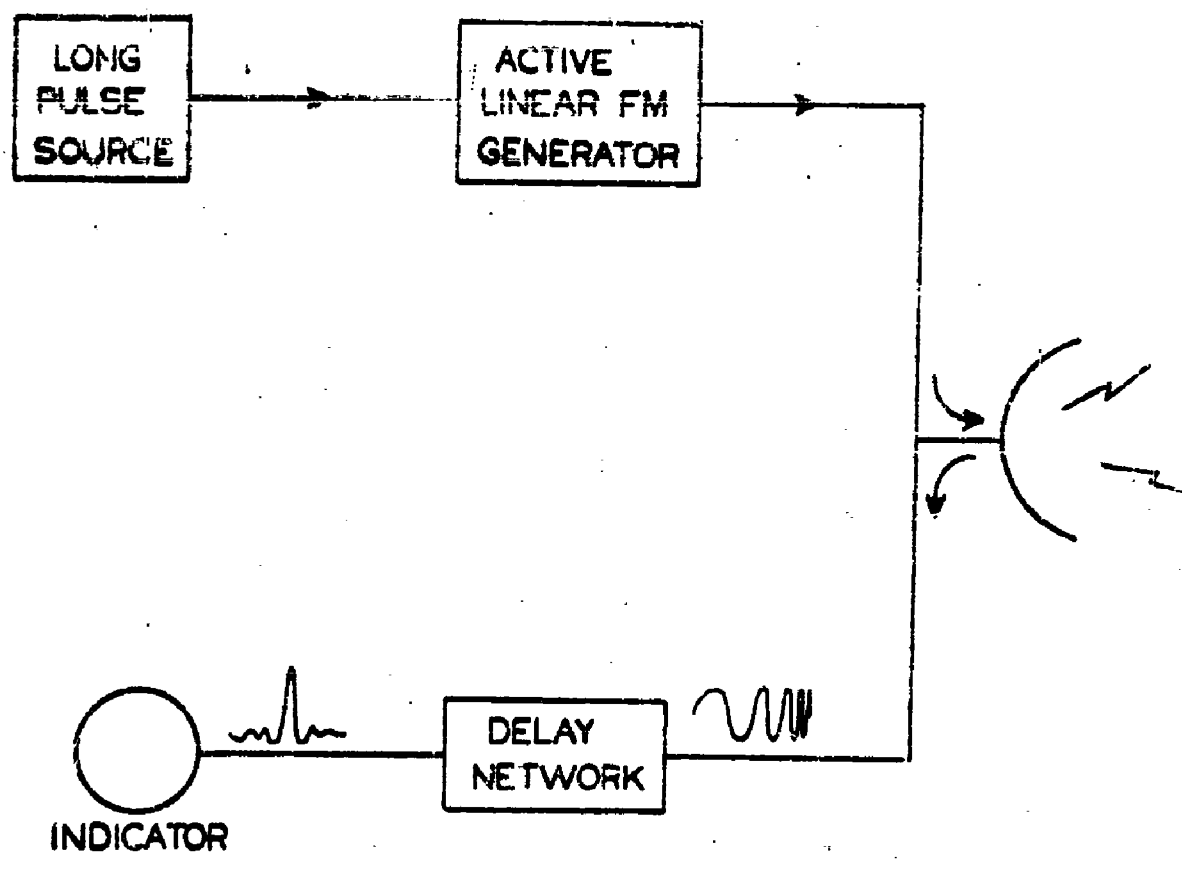

CHIRP RADAR
USING ACTIVE GENERATION

E7- 9048

SECRET

FIGURE 4

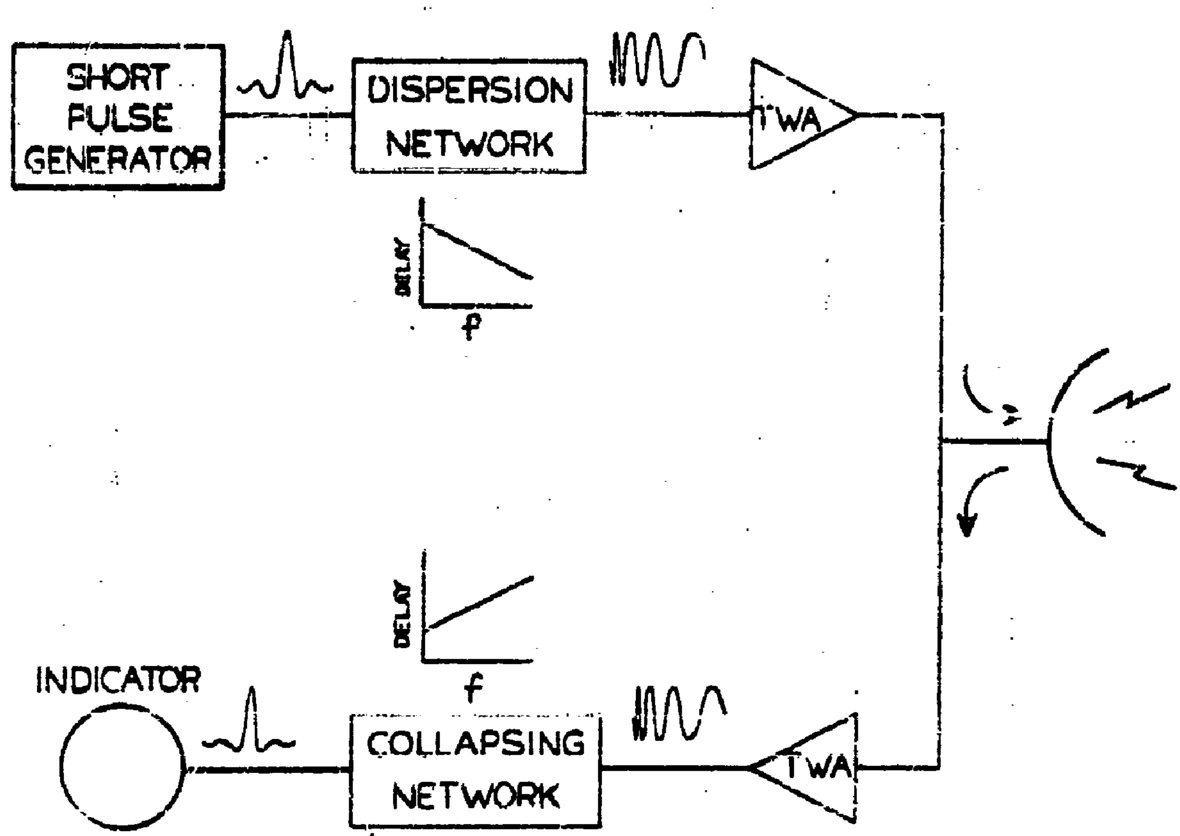

CHIRP RADAR
USING PASSIVE GENERATION

57-9048

SECRET

FIGURE 5
CHIRP SYSTEM BLOCK DIAGRAM

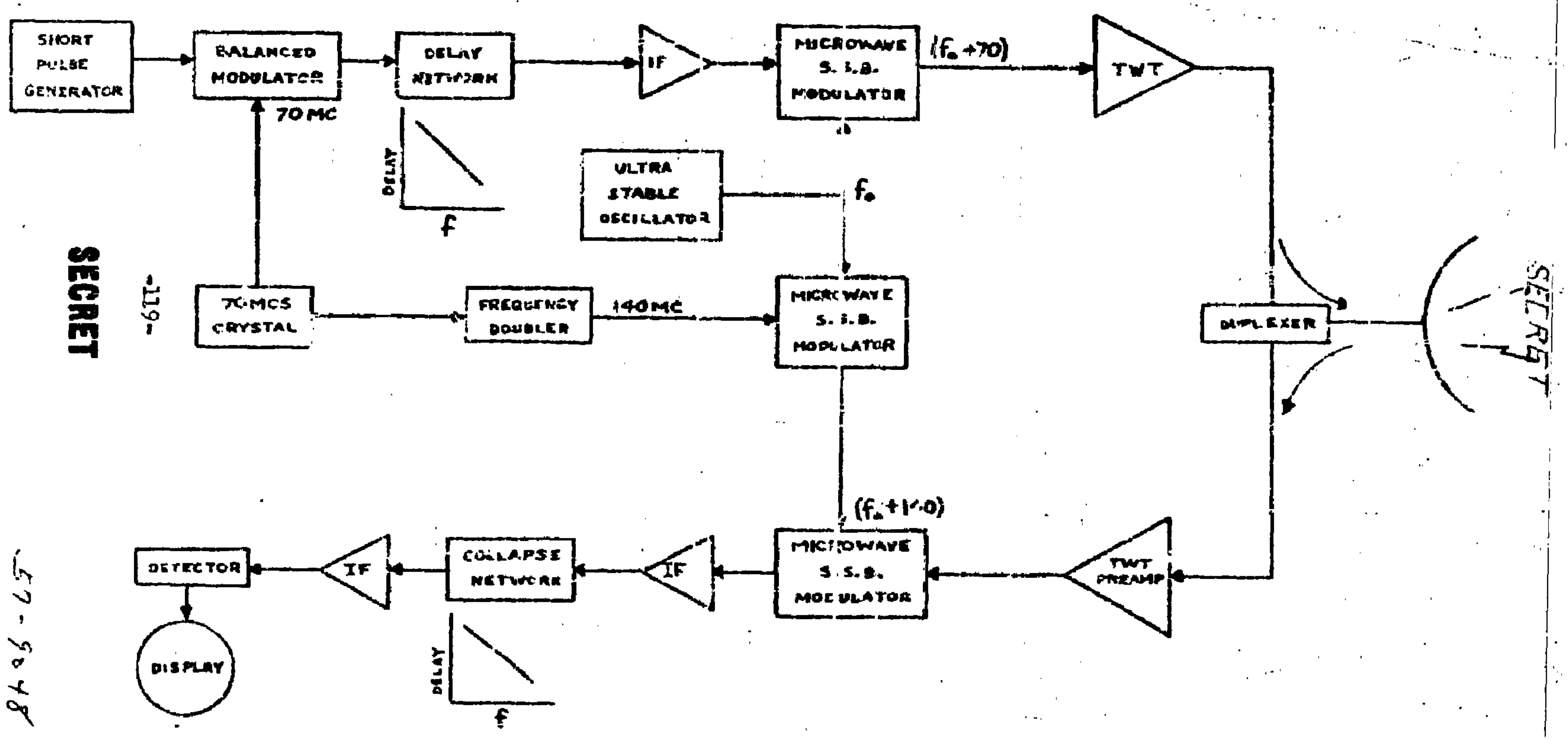

SECRET

SECRET

57-9048

SECRET

FIGURE 6

EXPERIMENTAL CHIRP WAVEFORMS

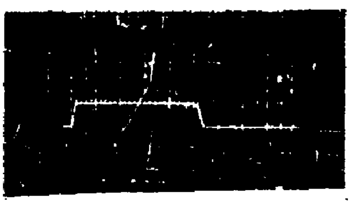

(A) R.F. ENVELOPE*

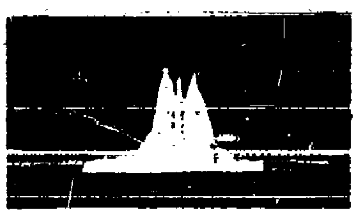

(B) R.F. SPECTRUM

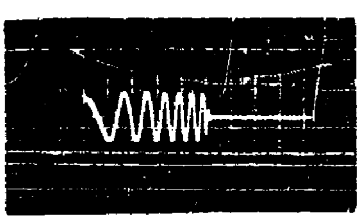

(C) MIXER OUTPUT*

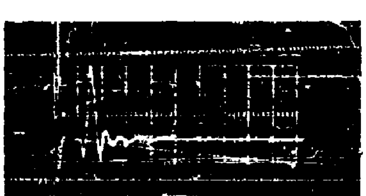

(D) SQUEEZED PULSE*

* HORIZONTAL TIME SCALE - 0.2 MICROSECOND PER DIVISION

SECRET

57-9048

FIGURE 7
EXPERIMENTAL EQUIPMENT

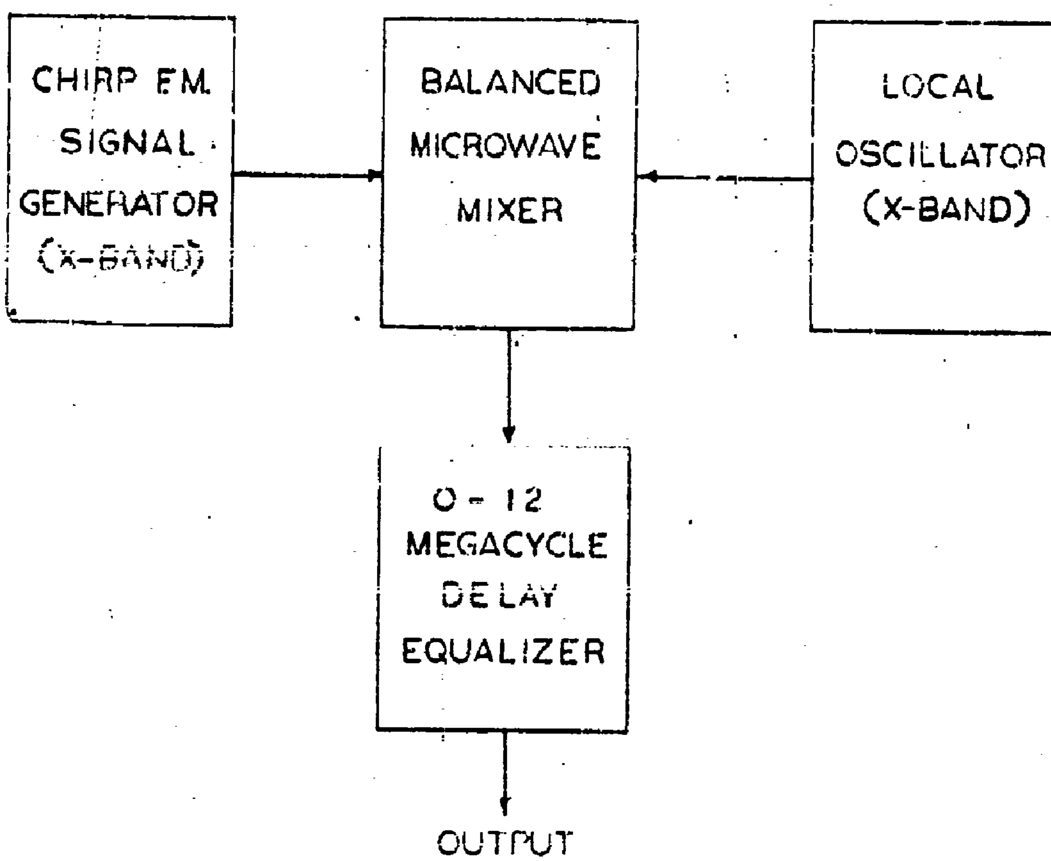

57- 9048

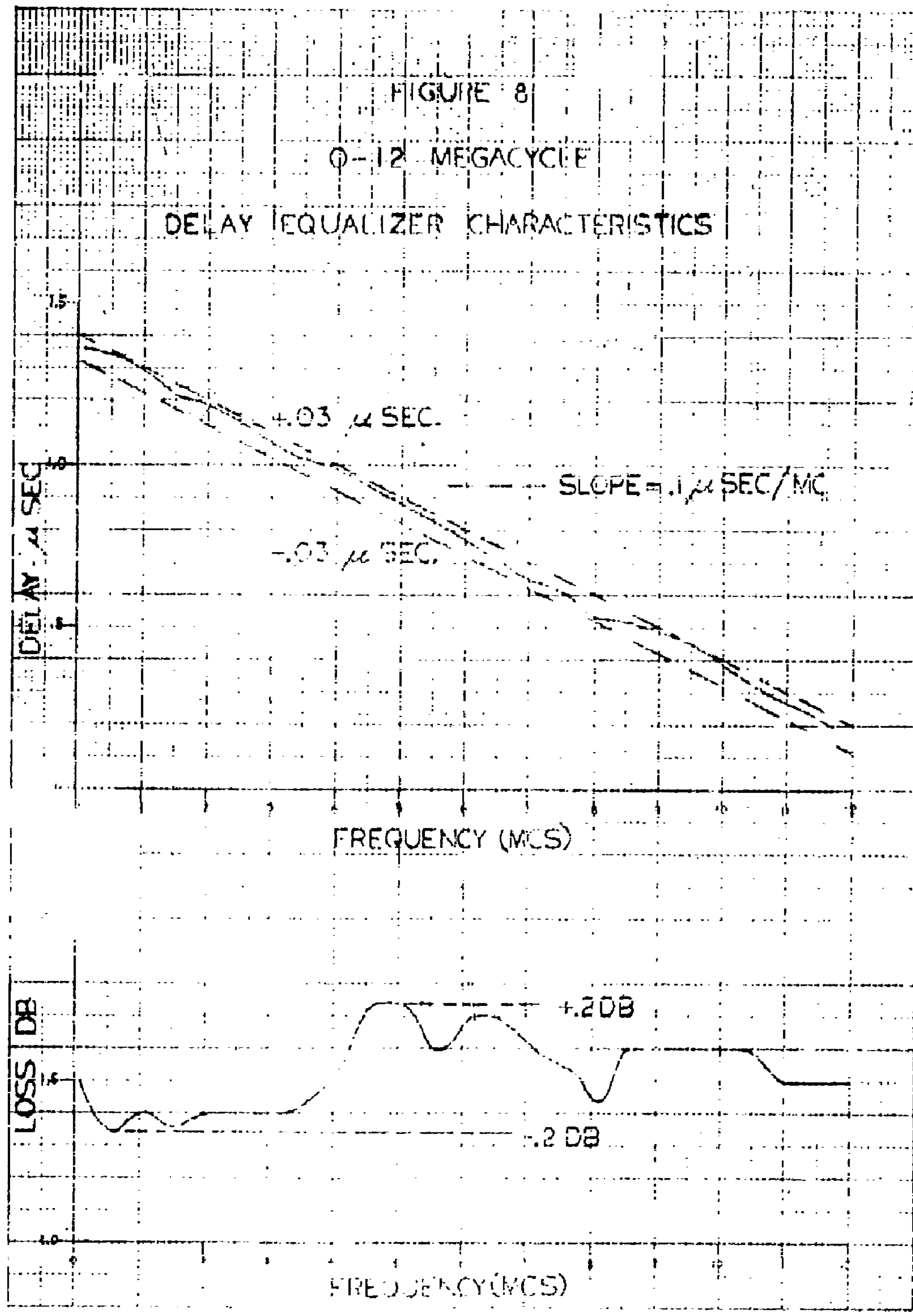
FIGURE 8
0-12 MEGACYCLE
DELAY EQUALIZER CHARACTERISTICS
+.03 μ SEC.
SLOPE = .1 μ SEC/MC
-.03 μ SEC.
DELAY - μ SEC
FREQUENCY (MCS)
+.2DB
-.2 DB
LOSS DB
FREQUENCY (MCS)

SECRET

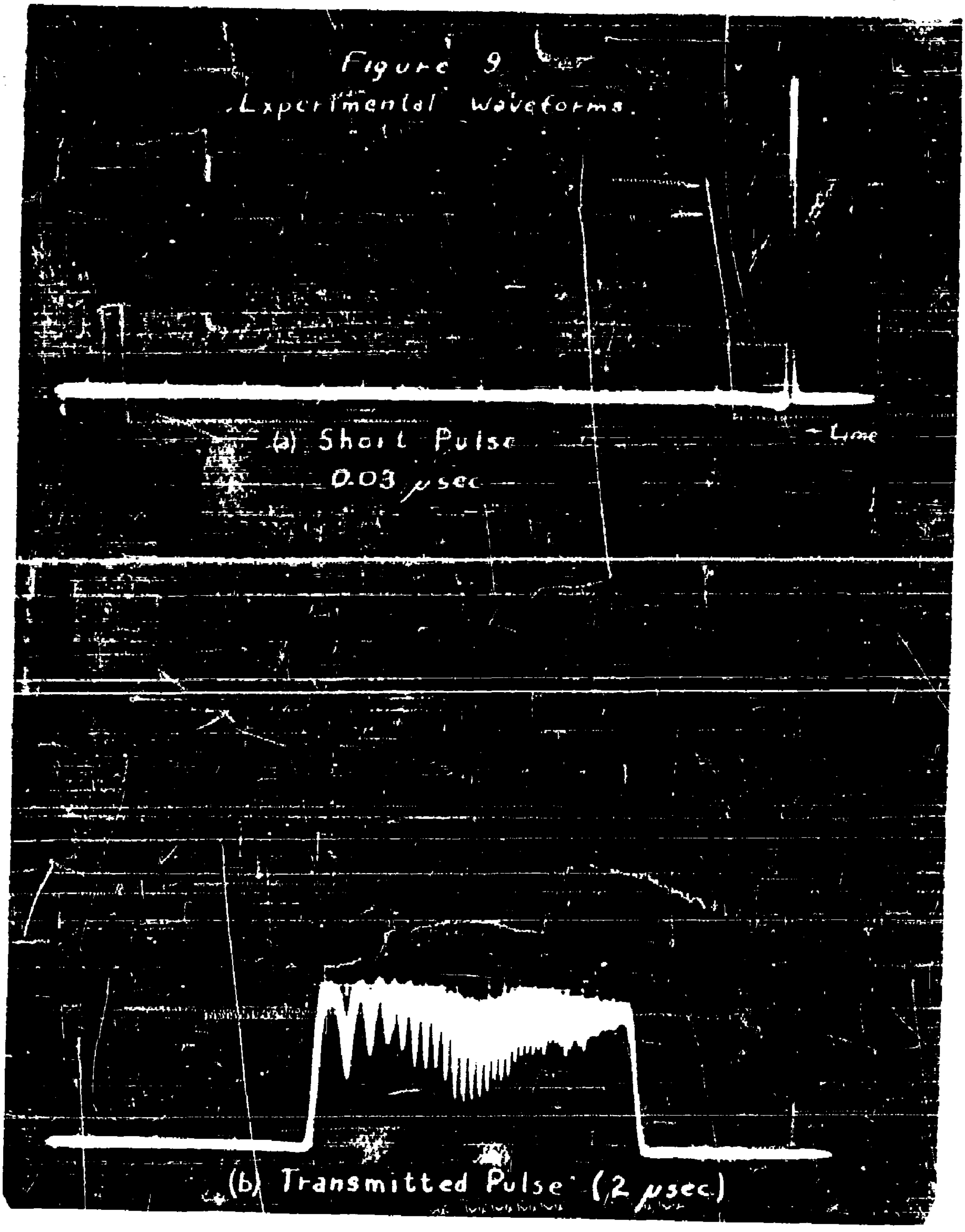
Figure 9
Experimental Waveforms.
(a) Short Pulse
0.03 μsec
Time
(b) Transmitted Pulse (2 μsec)

SECRET

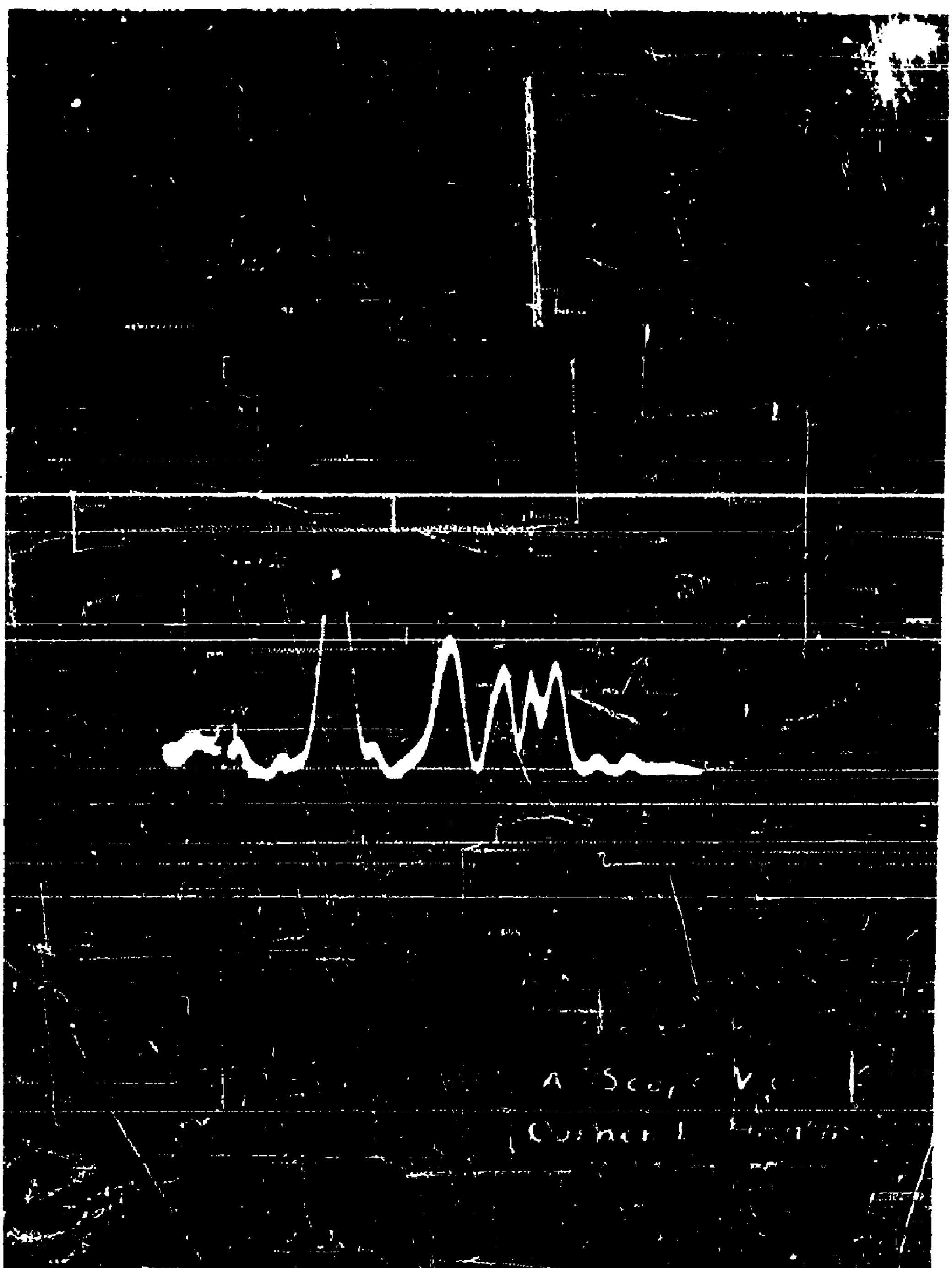

Figure 11
Weighting Effects on the Collapsed Main ...

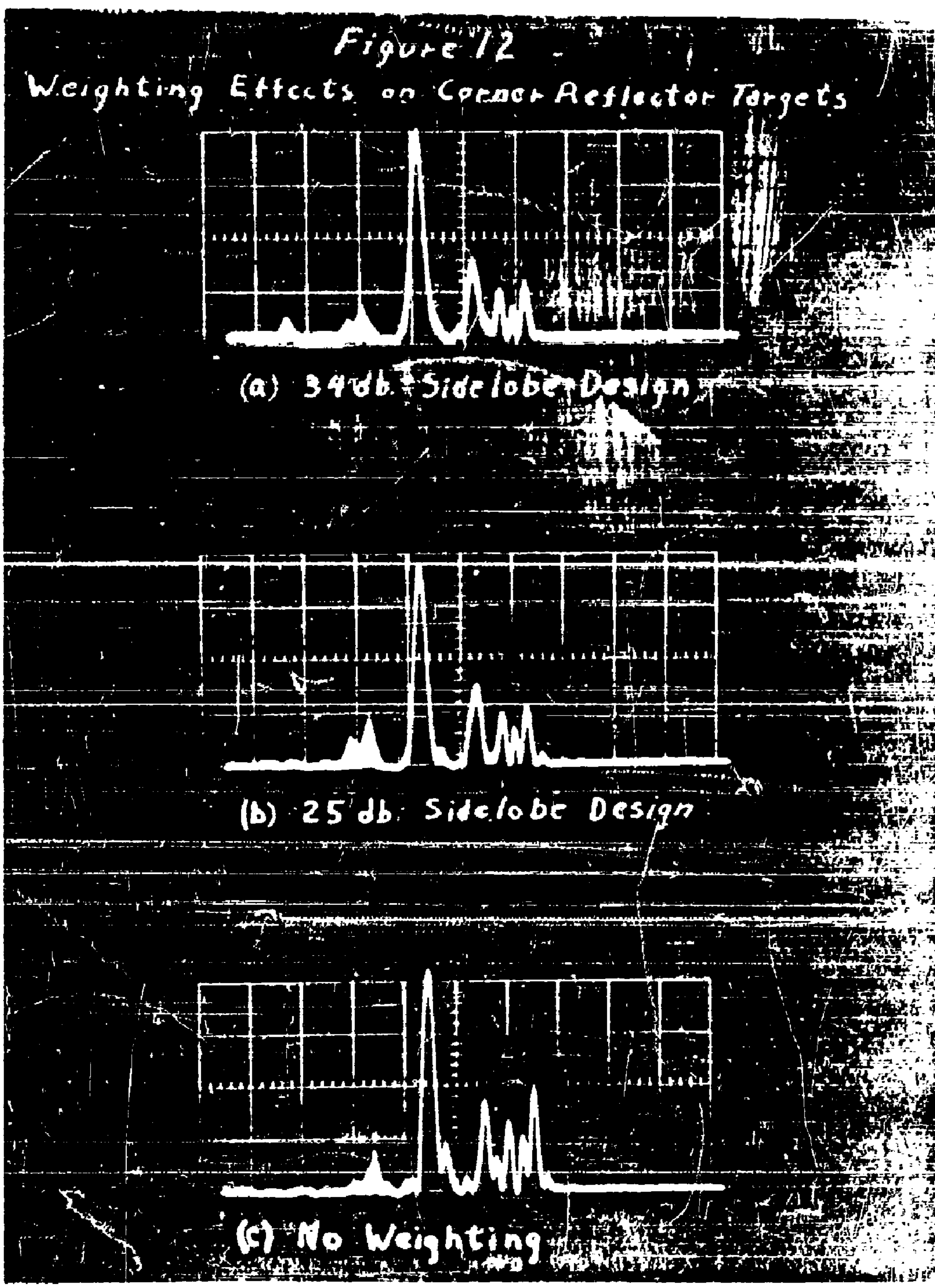

Figure 12
Weighting Effects on Corner Reflector Targets

CONFIDENTIAL

PULSE COMPRESSION AT S-BAND

by

G. P. Ohman

The Radar Division of the Naval Research Laboratory has built a number of experimental high resolution radar systems utilizing pulse lengths of the order of 10 millimicroseconds. A serious limitation of these radar systems has been their relatively short range resulting from the inability to generate high pulse energy by conventional means. Consequently, we have looked to the pulse-compression method with the hope of increasing the pulse energy available in the very short r-f pulses we require.

Before describing our experimentations with pulse compression it would, perhaps, be useful as a background to mention briefly some of the pertinent characteristics of our radar systems, especially with regard to short pulse generation and pulse power. Systems have been built at 3.2 cm. and at 8.6 mm. At both wavelengths the primary signal source was a magnetron. Two methods of short pulse generation have been used. The first is direct modulation of the magnetron by a short video pulse. Only a few magnetrons were found with sufficient bandwidth to be modulated successfully by a 10-millimicrosecond pulse. Among them were the 2J42A at 3.2 cm. and the 5789 at 8.6 mm. Peak power obtained was between 10 Kw and 20 Kw at 3.2 cm. and about 30 Kw at 8.6 mm, with average powers of the order of only a watt. A second method used successfully to obtain a short r-f pulse is pulse length clipping by gas tubes. The requirement here is an r-f pulse with a very rapid rise. Gas tubes placed in waveguide permit only the leading edge of the pulse to pass through before they become ionized after which they greatly attenuate the remainder of the pulse. Eight-millimicrosecond pulses have been produced at X-band at peak powers of about 100 Kw. Although an improvement over the direct modulation method, the increase in peak and average power obtained by pulse length clipping is not very great. Even if higher peak powers were obtainable by the methods mentioned, or by other direct methods, our prospects of a sizeable increase in radiated power at X-band and higher would not be very good because of voltage breakdown difficulties. Pulse compression, therefore, coupled with current developments in high-powered traveling-wave tubes, klystron amplifiers, and similar devices seems to offer us the only hope of a really significant increase in radiated pulse energy at the present time.

In our experimentation with pulse compression, we set the rather modest initial goal of a ten-to-one compression ratio. That is to say, we hoped to be able to start with a 100-millimicrosecond pulse and compress it to 10 millimicroseconds with a ten-to-one increase in peak power. Our plan was to generate a 100-millimicrosecond pulse of approximately gaussian shape and linearly frequency modulated 100 Mc, which according to theory, permits a compression to 10 millimicroseconds by a filter whose delay varies directly with frequency at the proper rate.

Although the realization of greater compression ratios has been reported by others working with pulse compression, their work was not directly applicable to ours because we were concerned with much shorter pulses and correspondingly wider bandwidths. Their methods of generation of frequency-modulated pulses and their methods of pulse compression, consequently, did not appear suited to our requirements. It seemed likely that in order to achieve the required frequency modulation rate of 100 Mc in 100 millimicroseconds, pulse generation would have to take place at a comparatively high frequency, probably at r-f rather than at the comparatively low frequencies used by others. Similarly, pulse compression would have to take place at a relatively high frequency since the compression network would have to be at least 100 Mc. wide. The bandwidth requirement alone suggested that a lumped-constant compression network would be difficult, if not impossible; accordingly, we felt that a distributed-constant compression network used directly at r-f would probably be desirable.

Our first thought on the generation of the frequency-modulated pulse was to sweep a klystron through a mode. To obtain the differential delay, we planned to take advantage of the dispersive properties of waveguide operating near cutoff. Waveguide though certainly not representing a really practical solution to the compression filter problem due to the bulk involved, as well as due to some theoretical limitation, would at least provide a relatively inexpensive and simple compression device to test. In order to keep waveguide losses at a reasonable level, it appeared that the operating frequency could not be much higher than S-band. RG-49/U waveguide which cuts off at 2155 Mc. was, therefore, selected. Actually, the choice of S-band as an operating frequency fitted well with our other radar work since our experimental radar systems were designed with an S-band i-f frequency utilizing traveling-wave tubes as i-f amplifiers.

Unfortunately, no S-band klystron could be found which had a 100-Mc wide mode so that direct generation of the frequency-modulated pulse by sweeping through a klystron mode did not appear possible. There was also some question whether a klystron could be swept in frequency as rapidly as required. An attempted solution to our pulse-generation problem consisted of starting with a klystron in the 6000-Mc. region sweeping it through a 50-Mc. wide mode, doubling to 12,000 Mc. and beating the signal down to S-band. Although a pulse was obtained, the system was beset with considerable instability and suffered the additional disadvantage of low power output. After other variations of this scheme were tried without more success the attempt to use klystrons was abandoned.

A more fruitful approach to our pulse-generation problem turned out to be the backward-wave oscillator (BWO). This device is capable of extremely high frequency-modulation rates over wide frequency-ranges. With a BWO as a signal source and waveguide as a compression filter a system fulfilling our initial objective of a ten to one compression was accomplished. Figure 1 shows a block diagram of equipment used to generate the frequency-modulated pulse, compress it and to view it both before and after compression.

The primary signal source is a Raytheon QK-518 backward-wave oscillator (BWO) which is voltage tunable. An increase in the BWO delay-line voltage from 150 to 1400 volts d.c. changes the frequency of oscillation from 2000 Mc to 4000 Mc, the change in frequency with voltage being most rapid at the low-voltage end. Output power is also a function of delay-line voltage. As far as our experiments were concerned, the range of frequencies of interest was 3300 Mc to 3400 Mc. Over this range the change in BWO frequency was very nearly proportional to change in BWO delay-line voltage, and the power output nearly constant at 340 mw.

 57-9048

The frequency-modulated pulse is formed through the combined action of a bandpass filter and a video-pulse generator. The filter which is of the iris-waveguide type is about 100-Mc wide and passes the band of frequencies normally between 3300 Mc and 3400 Mc. A fixed d-c voltage applied to the BWO delay-line causes a continuous fixed-frequency oscillation which is below the pass of the filter. The video-pulse generator produces a positive, low-impedance, bell-shaped pulse which is superimposed on the d-c BWO delay-line voltage. During the rise of this pulse, the BWO is swept in frequency through the passband of the filter causing an approximately gaussian-shaped frequency-modulated pulse to appear at the filter output. A second pulse frequency modulated in the other direction, generated on the fall of the video pulse is blanked out by applying a negative pulse to the BWO control grid at the proper time. The length of the output pulse is controlled by adjustment of the amplitude and rise time of the video pulse. Adjustment of the d-c BWO delay-line voltage is made so that the oscillator is swept in frequency through the passband of the filter on the linear part of the rise of the video pulse. Actually, it may be desirable to introduce a moderate amount of non-linearity in the rise to compensate for non-linearities in the frequency-versus-delay-line-voltage characteristics of the BWO, as well as in the differential-delay characteristics of the waveguide. To a certain extent this may be done by adjustment of the d-c level of the delay line and by changing video-pulse length and amplitude. The isolation attenuator is placed between the BWO and the filter to improve the match since the BWO output is quite sensitive to mismatch.

In order to be able to view both the uncompressed and the compressed pulses simultaneously, the filter output is split into two parts. About 30 percent is fed to a wideband high-level detector whose output is the envelope of the uncompressed pulse, and this is displayed on a Tektronics Type 545 oscilloscope. The remaining 70 percent of the power is sent through 145 feet of RG-49/U waveguide whose differential-delay characteristics produces pulse compression. Waveguide output is detected, amplified, and displayed on a high-speed oscilloscope as the compressed-pulse envelope.

Figure 2 is a pair of photographs, one showing the uncompressed pulse, the other the compressed pulse. The time scale on the former is 100 millimicroseconds per major division, and on the latter, a 50-Mc. timing wave, or 10 millimicroseconds between successive axis crossing. Since the detectors were approximately square law (actually the law is approximately 1.8) half amplitude corresponds roughly to half power. On this basis, it can be seen that the pulse has been compressed from 100 millimicroseconds to 10 millimicroseconds.

Measurement of peak power into and out of the waveguide showed a gain of approximately 5 db. Since the waveguide exhibited an average attenuation of approximately 6 db between 3300 Mc. and 3400 Mc, there was an intrinsic gain of about 11 db in power which agrees, within the limits of probable experimental error, with the expected value of 10 db based on a ten-to-one compression ratio.

Amplitude measurement of secondary pulses following the main pulse was complicated by video-amplifier ringing, the effects of which can be seen following the compressed pulse. Making allowance for the ringing, we estimate that all secondary pulses are at least 20 db below the main compressed pulse.

57-9048

The small "wiggles" preceding the uncompressed pulse are due to trigger-pulse leakage.

Figure 3 is a universal curve by which the length of waveguide required to produce a given differential delay may be calculated. The ordinates are proportional to the derivative of waveguide transit-time and, consequently, represent only an approximation which is good for frequency dispersions up to a few percent. As would be expected for a given percentage dispersion, the error increases as the center frequency approaches cutoff. In order to keep the required length small it is necessary to operate close to cutoff. The band from 3300 Mc to 3400 Mc used in our experiments runs from 95.6 percent to 92.8 percent of cutoff, which corresponds to a dispersion of just under 3 percent. Even for the 3 percent bandwidth the differential-delay-with-frequency deviates from linear by about ten percent. It seems reasonable to suppose that a certain amount of this non-linearity can be compensated for by tailoring the rate of frequency modulation over the uncompressed pulse length to correspond to the delay characteristics of the waveguide, and this was undoubtedly done to some extent since the d-c voltage on the BWO delay line was adjusted along with the video-pulse amplitude and rise-time to optimize the compressed-pulse shape. We have no quantitative information, however, on how far one can go in this direction.

By operating even closer to cutoff it would be theoretically possible to reduce the length of waveguide required for a given differential delay. Several difficulties arise in so doing; greater non-linearity in the differential delay characteristics was already mentioned; another is the greater change in attenuation over the frequency band, as well as the overall increase in attenuation. The latter if kept within reasonable bounds would not be a serious limitation since it could be overcome by a preamplifier which would undoubtedly be a required adjunct to any compression network which might be used. A large change in attenuation over the band would require equalization and might cause some difficulties.

The presence of noise should, of course, have no effect on the pulse-compression process. To show this we generated wide-band noise by amplifying the output of a "noisy" traveling-wave tube and mixed this with the pulse to be compressed. Figure 4 is a block diagram of the equipment used. As stated, the noise generator is a noisy traveling-wave tube followed by a traveling-wave tube amplifier. BWO output is attenuated to reduce it to the level of the noise with which it is mixed in a directional coupler, and then the combination is amplified up to the level of a watt by a third traveling-wave tube. Next, the combined signals are sent through the pulse-forming filter which serves the dual purpose of pulse formation and of limiting the bandwidth of the noise spectrum to that of the pulse. As before, the filter output is divided into two parts, the smaller of which is detected directly and the larger part being detected after passage through the waveguide. In order to preserve constant bandwidth a single oscilloscope which can be connected to either detector was used.

Figure 5 is a series of paired photographs comparing the uncompressed and compressed pulse in noise. In the first pair, the attenuator following the BWO is adjusted to cause an uncompressed-pulse amplitude-to-noise ratio of approximately unity. The corresponding photograph of the compressed pulse very clearly indicates the expected increase in pulse-amplitude-to-noise ratio.

57-4048

Because of this increased ratio it was necessary to reduce the relative gain of the oscilloscope to prevent overload by the pulse; consequently, the noise level here appears less than on the uncompressed-pulse photograph.

The remaining pairs of photographs illustrate the effect of reducing signal level relative to noise. Compression takes place even when noise is greater than signal. Because of the relatively long exposures required to take these pictures, some photographic integration of signal occurred and that, coupled with some deficiencies in printing, makes the uncompressed pulse more easily detectable on the oscilloscope screen photographically than visually.

Our work with pulse compression has been largely exploratory with the ultimate objective of increasing the range of our millimicrosecond radar-systems. The results to date are largely qualitative. Nevertheless, we feel that some useful information has been gained. With the possible exception of the differential-delay filter the pulse-compression scheme at S-band should be extendable to much higher frequencies, and, as such, has several advantages. Pulse generation and compression take place at transmitter frequencies rather than at some lower i-f frequency, thus eliminating the need for frequency conversions. Pulse shape and frequency are controlled essentially by a passive network; only a video pulse with a reasonably stable leading edge is required. By using the r-f pulse as it appears at the output of the pulse-forming filter as the time reference for the system, it would not be necessary to synchronize the frequency sweep of an f-m signal generator to prevent range error.

Although no attempt was made in the experiments described to increase the uncompressed-pulse energy to a level useful for radar purposes, we have shown for the case of 10-millimicrosecond pulses, as others have for longer ones, that the uncompressed pulses may be amplified and combined with noise without disturbing compression capabilities.

The ten-to-one compression-ratio achieved is rather modest and probably less than would be desirable for a practical radar system. Actually, we have achieved as much as a fifteen-to-one compression-ratio by increasing the waveguide length. This further emphasized what appears to be our major problem - the design of a more practical differential-delay pulse-compression device. The waveguide was already very long at 145 feet for the ten-to-one compression-ratio. Some thought has been given to the feasibility of filling waveguide with a low-loss high-dielectric material so that all waveguide dimensions can be reduced by a substantial amount. It may also be possible to find some slow-wave structure which has a highly dispersive frequency range. At any rate, on the basis of our experiments we feel that pulse compression holds promise for improving the performance of our 10-millimicrosecond radar-systems.

The work described in this paper is summarized in NRL Report 4971 entitled, "Pulse Compression at S-band," by L. L. Atkinson, G. P. Ohman, and F. H. Thompson.

57-9048

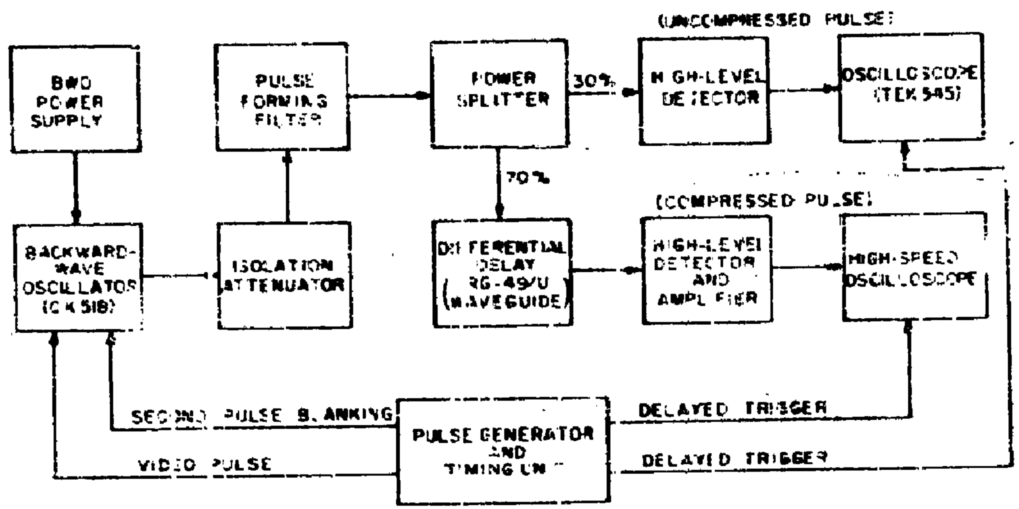

FIGURE I.

SETUP FOR GENERATING AND COMPRESSING PULSE

CONFIDENTIAL

FIGURE 2

COMPARISON OF UNCOMPRESSED AND COMPRESSED PULSES

CONFIDENTIAL

57-9048

CONFIDENTIAL

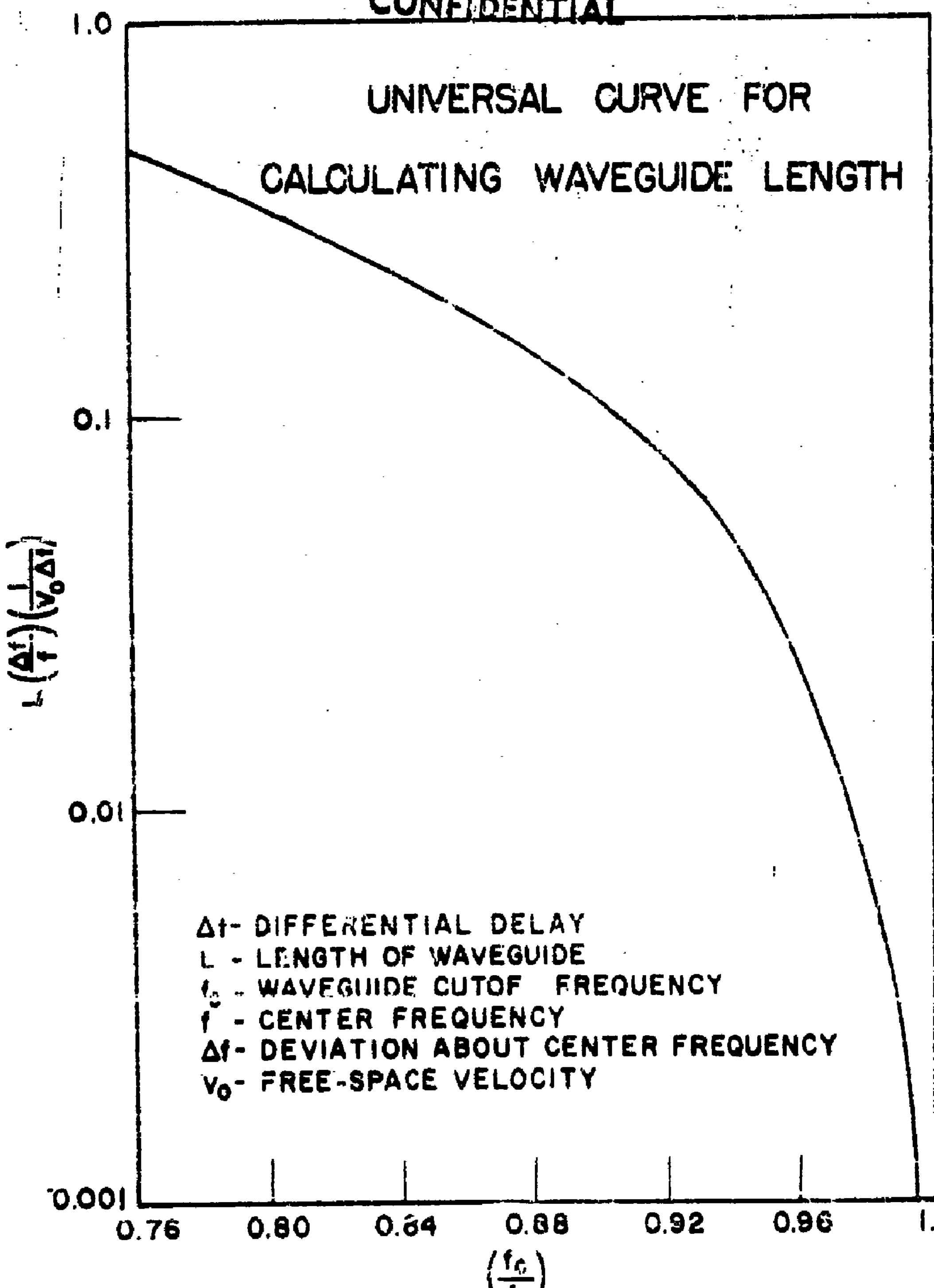

CONFIDENTIAL

FIGURE 3.

57-9048

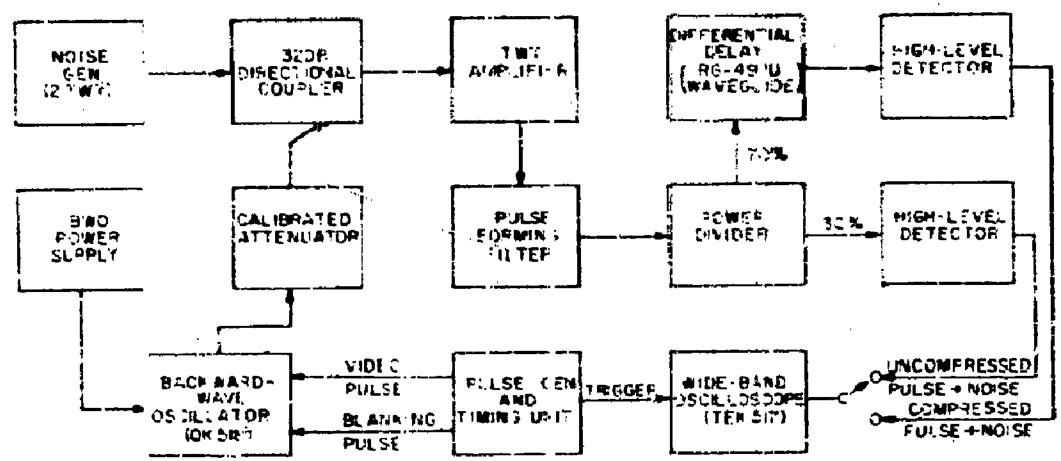

FIGURE 4. SETUP FOR COMBINING NOISE WITH PULSES

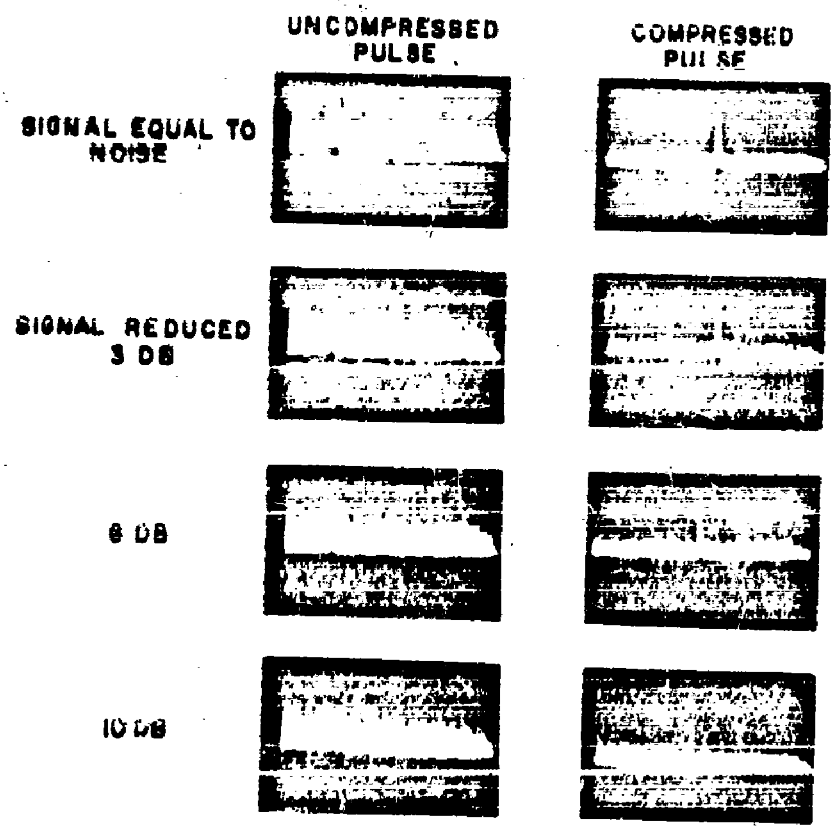

FIGURE 5. RELATIVE EFFECT OF COMPRESSION ON PULSE AND NOISE

CONFIDENTIAL

THEORY OF MATCHED-FILTER PULSE COMPRESSION

by
R. F. Schreitmueller
Microwave Electronics Division
Sperry Gyroscope Company
Division of Sperry Rand Corporation
Great Neck, New York

Summary. A brief explanation of matched filter theory is followed by a derivation of the output of a compression filter passing a frequency-modulated pulse. A matched compression filter is assumed, and a time-domain approach is used. Results include an expression for the envelope, compression ratio and residue values, and the lack of FM on the output pulse.

INTRODUCTION

Pulse compression radar systems transmit a wide pulse, and convert the received signal into a narrow pulse. This technique can be accomplished, among other means, by frequency-modulating the pulse to be transmitted, and passing the received signal through a network having a time delay which varies with frequency. This paper is concerned with the linear FM type of pulse compression. Zero Doppler shift is assumed.

Computing the performance of such a radar can be a length task. It may require tables of Fresnel integrals, and numerical evaluation of Fourier transforms. Instead of this complicated frequency-domain approach, a simpler analysis can sometimes be carried out in the time domain. To use the time-domain approach, the receiver is assumed to be a matched filter. This assumption is often closely realized in practice, so that the results have physical meaning.

The results of this time-domain analysis are preceded by a brief explanation of matched-filter theory. Detailed derivations are given at the end of the paper.

CONFIDENTIAL 57-9048

THE MATCHED-FILTER CRITERION

A matched filter optimizes the detection of weak signals in white noise. Suppose there is a signal of known waveform in white noise, and its peak signal-to-noise ratio should be maximized. The linear filter that best accomplishes this was first specified by North[1]. He showed that the frequency response of the filters and the spectrum of the signal must be complex conjugates of each other (except for a linear phase shift). In other words, the filter must be matched to the signal.

Expressed in the time domain, the time response of the filter to an impulse must be the reverse of the signal waveform. Quantitatively, if $f(t)$ is the signal and $F(\omega)$ its spectrum, the filter frequency response is

$$H(\omega) = F^*(\omega)$$

and the filter impulse response is

$$h(t) = f(-t)$$

For applications such as detection and time measurement, peak S/N is more important than waveform preservation. The matched filter may be regarded as a device which essentially transforms the shape information of the signal into amplitude information.

APPLICATION TO PULSE COMPRESSION

If a pulsed carrier having frequency modulation is transmitted, and is received with a matched filter, the transmitted signal will be

$$f(t) = \cos\left[\omega_0 t + \frac{1}{2}at^2\right] \quad \frac{T}{2} < t < \frac{T}{2}$$

 57-9248

The pulse characteristics of this signal are:

carrier frequency = $\omega_o/2\pi$ cycles/sec

rate of frequency change = $a/2\pi$ cycles/sec^2

pulse width = T sec

frequency deviation = a $T/2\pi$ cycles/sec

The matched filter impulse response may be written

$$h(t) = F(-t) = \cos\left[\omega_o t - \frac{1}{2}at^2\right] \quad -\frac{T}{2}<t<\frac{T}{2}$$

The output pulse may then be formed by convolution of f and h:

$$r(t) = \int_{-\infty}^{\infty} f(x)\, h(t-x)\, dx$$

This may be carried out directly in the time domain using ordinary trigonometric integrals to yield the solution

$$r(t) = \frac{1}{at}\sin\frac{1}{2}at(T-|t|)\cos\omega_o t \quad -T<t<T$$

(A second term, containing Fresnel integrals, is small enough to be neglected, provided $\omega_o >> a^{1/2}$ and $\omega_o >> at$).

The pulse compression filter output is now in closed form. A number of interesting observations can be drawn from this expression:

1. The envelope approaches the form (sin 1/2 at T)/at when $aT^2 >> 1$. On the other hand, for $a = 0$, the envelope becomes simply $1/2\ (T-|t|)$, for $-T < t < T$, i.e., a triangular pulse of duration 2T. This agrees with the result obtained for a conventional rectangular pulse passed through a matched filter.

2. The carrier is $\cos \omega_o t$. This is a constant-frequency carrier which is not frequency modulated. The absence of FM is not

too surprising since the output spectrum of a matched filter has zero phase characteristic, i.e.,

$$R(\omega) = F(\omega)\ F^*(\omega)$$

While no FM is present for this case, the result does not contradict other analyses which show FM to exist, but which do not assume a matched filter characteristic.

3. The peak power compression ratio can be calculated as

$$\text{P.P.C.R.} = \left[\frac{\text{output amplitude}}{\text{input amplitude} \times \text{filter gain}}\right]^2$$

$$= \frac{r^2\ (0)}{f^2\ (0)\ H(\omega_0)^2} = \frac{T^2}{4} \times \frac{2a}{\pi} = \frac{aT^2}{2\pi}$$

This is in agreement with the relation for compression ratio: compression ratio = pulse width (sec) x frequency deviation (cps) $= T \times aT/2\pi = aT^2/2\pi$

4. The pulse width compression ratio is defined as input pulse width/output pulse width. The definition of pulse width can be somewhat arbitrary. Consider a pulsed carrier with an envelope of form (sin t)/t. This has a rectangular spectrum of bandwidth B. A pulse width may be arbitrarily defined as 1/B for this case. This is the pulse width at 4 db down for the (sin t)/t envelope. It is also half the width between the first nulls of the envelope. Let the 4 db level be used to define widths of other pulses. If a 4 db definition is used, the pulse width of the output wave-form is 6.28/a T (for $aT^2 \gg 1$). Then the pulse width compression ratio is

$$\frac{T}{6.28/aT} = \frac{aT^2}{2\pi}$$

57-9048

This gives the same compression ratio as is obtained for peak power. The pulse width definition is somewhat arbitrary, but does have some justification and results in an agreement with the peak power compression ratio. If 3 db pulse width is used, the pulse-width compression is $aT^2/5.6$.

5. The output envelope is not "clean," but has residues, or spurious signals, analogous to antenna side lobes. This appears to be characteristic of rectangular pulse compression since some portion of the waveform, which has a total duration of twice the input pulse width, is present to some extent.

The magnitude of the residues can be readily determined from the envelope function. For high compression ratios, the envelope approaches the form (sin t)/t in the region of interest. This function has residues of 13.3 db down.

For moderate compression ratios, the residues are slightly better. For example, at a compression ratio of 10, the resides are 14.9 db down.

These relatively high residues are characteristic of matched filter pulse compression but do not represent the best possible residue performance. They can be reduced by techniques such as bandpass-shaping as will be discussed in the paper by Messrs. Cook, Chin, and Sadler[2].

APPLICATIONS

A closed-form expression for output of matched pulse compression filter simplifies computation of the performance of some non-matched pulse compression filters. Other linear filters can be regarded as a cascade combination of a matched filter and a second network. If the

57-9048

second network can be specified, only the response of the matched filter output to the second network need be determined. For very high compression ratios (greater than 100), the approximations of a (sin t)/t waveform and a rectangular spectrum further simplify the computation.

The matched-filter pulse compressor also sets a standard for signal detectability. The radar system engineer, as a user of pulse compression, wants to know what performance can be expected in terms such as signal detection, resolution, and ambiguity. If the receiver contains a predetection filter matched to the transmitted signal, the same peak signal-to-noise ratio per pulse is obtained at the filter output for a given pulse energy and a given noise level per unit bandwidth, independent of pulse waveform.

Therefore, for a given transmitted pulse energy, and a matched filter, signals in noise will be detected equally well whether or not pulse compression is used. Any other compression filter results in poorer signal detectability. The difference in decibels between the output signal-to-noise ratios for the two cases can be called "compression loss." This is the penalty in db that a radar system engineer pays for pulse compression. The difference between the matched-filter case and another case can be easily calculated in many instances.

Similar, but less clear-cut, criteria can be established for resolution and for ambiguity, i.e., residues. For the latter, the matched-filter case may not be optimum but it can be used as a conveniently determined standard.

57-9048

CONCLUSION

The assumption of a matched-filter receiver for a pulse compression radar transmitting a rectangular pulse with FM results in a closed-form expression for the output waveform. This can be approximated by (sin t)/t for high compression ratios. Compression ratio is determined as pulse width times frequency deviation. No frequency modulation is present and the output residue level is readily calculated.

The matched-filter compressor may be used as an aid in analyzing the behavior of other pulse compression systems, and as a standard for evaluating radar performance.

57-9048

APPENDIX

Derivation of output waveform

It has been shown that the output waveform can be obtained by convolution:

$$r(t) = \int_{-\infty}^{\infty} f(x)\, h(t - x)\, dx$$

$$= \int_{A}^{B} \cos\left(\omega_o x + \frac{1}{2}a x^2\right) \cos\left[\omega_o (t - x) - \frac{1}{2}a (t - x)^2\right] dx$$

For $-T<t<0$, $A = -T/2$ and $B = t + T/2$ and for $0<t<T$, $A = t-T/2$ and $B = T/2$

$$r(t) = \frac{1}{2}\int_{A}^{B} \cos\left[\omega_o t + \frac{1}{2}a\,(2tx - t^2)\right] dx + \frac{1}{2}\int_{A}^{B} \cos\left[\omega_o (2x - t) + \frac{1}{2}a\,(t^2 - 2tx + 2x^2)\right] dx$$

The second term is an average of a carrier frequency $x = 2\omega_o/2\pi$ and can be neglected if $\omega_o >> a^{1/2}$ and $\omega_o >> at$.

Then

$$r(t) = \frac{1}{2a} \sin\left[\omega_o t + atx - \frac{1}{2}at^2\right] \Big|_{x = A}^{x = B}$$

For

$$-T<t<0, \quad r(t) = \frac{1}{2at} \sin\left[\omega_o t + \frac{1}{2}at^2 + \frac{1}{2}at\,T\right]$$

$$- \frac{1}{2at} \sin\left[\omega_o t - \frac{1}{2}at^2 - \frac{1}{2}at\,T\right]$$

$$= \frac{1}{at} \sin\frac{1}{2}at\,(t + T) \cos \omega_o t$$

57-9048

For

$$0<t<T, \quad r(t) = \frac{1}{2at} \sin\left[\omega_o t - \frac{1}{2}at^2 + \frac{1}{2}at\ T\right]$$

$$-\frac{1}{2at} \sin\left[\omega_o t + \frac{1}{2}at^2 - \frac{1}{2}at\ T\right]$$

$$= \frac{1}{at} \sin\frac{1}{2}at\ (T - t) \cos \omega_o t$$

Thus, for $-T<t<T$,

$$r(t) = \frac{1}{at} \sin\frac{1}{2}at\ (T - |t|) \cos\omega_o\ t$$

<u>Derivation of Peak Power Compression Ratio</u>

To find the peak power compression ratio, it is first necessary to find the gain of the matched filter. At the center frequency this is given by the Fourier transform

$$H(\omega_o) = \int_{-\infty}^{\infty} h(t) e^{j\omega_o t}\ dt = \int_{-T/2}^{T/2} \cos\left(\omega_o t - \frac{1}{2}at^2\right) e^{j\omega_o t}\ dt$$

$$H(\omega_o) = \int_{-T/2}^{T/2} \cos\left(\omega_o t - \frac{1}{2}at^2\right) \cos\omega_o t\ dt$$

$$+ j \int_{-T/2}^{T/2} \cos\left[\omega_o t - \frac{1}{2}at^2\right] \sin\omega_o t\ dt$$

$$= (\text{for } \omega_o\ T>>1)\ \frac{1}{2} \int_{-T/2}^{T/2} \cos\frac{1}{2}at^2\ dt + \frac{1}{2}\ j \int_{-T/2}^{T/2} \sin\frac{1}{2}at^2\ dt$$

$$= \int_{o}^{T/2} \cos\frac{1}{2}at^2\ dt + j \int_{o}^{T/2} \sin\frac{1}{2}at^2\ dt$$

57- 9.48

Let

$$\frac{1}{2}at^2 = \frac{1}{2}\pi V^2 \text{ and}$$

$$K = (a/\pi)^{1/2}$$

Then

$$H(\omega_o) = \frac{1}{K}\int_o^{KT/2} \cos\frac{\pi}{2}V^2\,dv + \frac{j}{K}\int_o^{KT/2} \sin\frac{\pi}{2}V^2\,dv$$

$H(\omega_o)$ can then be represented as $1/K$ times a vector drawn from the origin to a point on the Cornu spiral at $V = KT/2$.

As

$$K \to \infty,\ H(\omega_o) \to (1 + j)/2K$$

and

$$|H(\omega_o)| \to \frac{1}{\sqrt{2K}} = \sqrt{\frac{\pi}{2a}}$$

(In addition, the phase shift approaches 45°.)

The approximation of $|H(\omega_o)|$ is accurate ±10 per cent for $aT^2/2\pi > 40.5$, and accurate ±20 per cent for $aT^2/2\pi > 9.7$. The filter "gain" is even more exactly equal to $\sqrt{\pi/2a}$ if one takes the average in the pass band, rather than only the value at ω_o.

For $aT^2/2\pi < 1$, the approximation is not valid. A series expansion gives $H(\omega_o) = T/2 + j\ aT^3/48$ for the first two terms.

The peak values of the pulse envelopes are:

$$f(o) = 1$$

$$r(o) = \lim_{t \to o} \frac{\sin\frac{1}{2}at\ (T - t)}{at} = \lim_{t \to o} \frac{\left[\frac{1}{2}aT - at\right]\cos\frac{1}{2}at\ (T - t)}{a} = \frac{T}{2}$$

57-9048

The peak power compression ratio is:

$$\frac{1}{|H(\omega_o)|^2} \frac{r^2(o)}{f^2(o)} = \frac{2a}{\pi} \frac{T^2}{4} = \frac{aT^2}{2\pi}$$

REFERENCES

1. North, D.O., "An analysis of the factors which determine signal/noise discrimination in pulsed-carrier systems," RCA Report PTR-6C, June 25, 1943.
2. Chin, J.E., Cook, C.E., and Sadler, L.R., "Pulse Compression Spectra," presented at RADC Pulse Compression Symposium, June 26, 1957.

CONFIDENTIAL

PULSE COMPRESSION SPECTRA

by
C.E. Cook
J.E. Chin
L.R. Sadler
Air Armament Division
Sperry Gyroscope Company
Division of Sperry Rand Corporation
Great Neck, New York

Summary. Linear FM pulse compression techniques lead to spectrum functions which are expressable as Fresnel integrals and a time function which is (sin x)/x in nature. Multiple target environments preclude use of a time signal that has such high "sidelobes" or "residues." Spectrum shaping (i.e. phase and/or amplitude) can be used to modify the time function to a more useable shape. Some examples of spectrum shaping are considered to indicate the types of improvements that can be achieved.

INTRODUCTION

The Sperry Gyroscope Company has supported a pulse compression investigation and development program for a number of years. This technique has number of interesting applications in the area of extending radar performance. It is recognized that what is here termed "pulse compression" is one of a number of matched filter or quasi-matched filter approaches that may be used to achieve similar results. This paper will briefly cover some areas of the analytical work by one of the groups at Sperry that has been concerned with basic pulse compression investigation, and will indicate some of the pulse compression problems that may be related to spectrum properties in a linear FM pulse compression system.

GENERAL DISCUSSION

Fig. 1 shows in its simplest block diagram form the basic ingredients of the pulse compression used by Sperry engineers and also by a number of

29-9648

CONFIDENTIAL

other investigators. It can be seen from the illustration that the time delay of the filter is matched to sweep function of the input pulse. For the rectangular input pulse shown, the compression filter output pulse is narrower in width and higher in peak power by the compression ratio factor. By making use of the 0.64 amplitude point one obtains a figure for compressed pulse width that is the inverse of the frequency deviation of the uncompressed pulse (i.e., $\tau = 1/\Delta f$). This is, of course, purely arbitrary, but it does provide an easy method for calculating the pulsewidth and is consistent with the amplitude ratio definition of pulse compression. Associated with the compressed pulse are ripples, shown in Fig. 1, which we have termed "residues". These extraneous signals are one of the problems that result from the use of a linear FM pulse compression technique.

The time domain integral solution for this arrangement shows that the form of the compressed pulse is (sin x)/x and that, in addition, the carrier of the compressed pulse is frequency swept in a sense opposite to that of the input, or uncompressed, pulse. Both of these effects are undesirable, although for high compression ratios the FM effect is largely negligible. The presence of the residue signals are of particular interest if we are anticipating the use of pulse compression in a multi-target environment where large signals may be present whose residues are of greater amplitude than those of other signals we are seeking. A partial solution to these residue and FM phenomena may be found by treating in some detail the spectra of the various signals used.

When the actual spectrum of a compressed pulse is evaluated, it is found to be a function of Fresnel integrals. Table I briefly summarizes the time and spectrum functions involved. The spectrum is that of the

57-9548

compressed pulse output from the linear time delay compression filter. The Fresnel integrals are seen to be functions of the compression ratio T_o/T as defined previously. Fig. 2 shows one half of the symmetrical amplitude and phase spectra computed from the Fresnel integrals for compression ratios of 13:1, 52:1 and 130:1. The spectra tend to become more rectangular as the compression ratio increases. When these spectra are integrated to obtain the compressed pulse time function, the (sin x)/x form is obtained. Referring again to the spectrum diagrams, one might suspect that the phase function, which is highly non-linear at the band edges, is contributing to the high level of ripples, or residue signals. Since a rectangular amplitude spectrum is normally associated with the (sin x)/x shape, it can be seen that this pulse form is not to be expected on an amplitude distribution basis alone until fairly high compression ratios are used.

Assuming optimum phase matching to obtain either a flat or linear spectrum phase, the compressed pulse shapes are recalculated with the results shown in Fig. 3. It is seen that in all cases the residues are reduced, with the biggest gains at the lower compression ratios. In addition optimum phase matching increases pulse resolution to a degree, this also being more pronounced at the lower compression ratios. Fig. 4 plots the comparative signal-to-residue ratios as a function of compression ratio, and Fig. 5 plots the peak signal change when optimum phase matching is assumed.

The results shown are caused by providing a complete phase match for the signal phase spectrum, which incidentally eliminates the residual FM

57-9048

at the compressed pulse carrier as pointed out by Schreitmueller[1] in his paper. If a spectrum amplitude match is provided in the compression filter, the residues tend to increase. Fig. 4 shows that, for compression ratios of less than 30 or 40 to 1, the additional phase equalization may be desirable. The advantage here is that residues may be reduced in this manner before other techniques of residue reduction are applied. In addition, improved resolution and peak signal amplitude also result. Since this additional phase equalization must be done before the second detector, its use would not be compatible with large doppler shifts, for the compensating network will have to work in a specific band. No such limitation need apply to the linear time delay equalization method since the delay characteristic of the compression filter can be kept linear over the expected interval of doppler frequency shifts.

The conventional approach to residue reduction involves weighting the amplitude portion of the spectrum, either over the whole band or on a selective basis. Examples of these will be given for the 52:1 compression ratio. The weighting function used as an example for modifying the entire spectrum is the single tuned bandpass function, various bandwidths being applied and phase compensation being assumed. Other functions can be employed and may be preferable although differences should be small for monotonic functions.

Fig. 6 shows the 52:1 compression ratio amplitude spectrum and the bandpass weighting functions which have been applied to it. For purposes

---

[1] Schreitmueller, R.F., "Theory of Matched-Filter Pulse Compression", presented at RADC Pulse Compression Symposium, June 26, 1957.

57-9048

of calculation the unshaped spectrum is cut off when the amplitude is 20 db down from the average midband level. We define the shaping ratio of the shaping filter as the bandwidth at its 3 db points divided by the frequency deviation of the uncompressed pulse. Fig. 7 illustrates the effect of this type of spectrum weighting on the compressed pulse shape. The trade-off of resolution vs. residue reduction is clearly illustrated. For small ratios of shaping bandwidth to spectrum bandwidth the pulse shape tends to become very unsatisfactory. Our definition of signal-to-residue ratio is the ratio of peak signal amplitude to the first relative maximum following the first relative minimum.

This definition is open to question if one has a case such as shown for a bandshaping ratio of 0.25 where the waveform does not go to zero amplitude before a residue builds up. The first relative minimum could be taken as a reference for calculating residues which would yield a better signal-to-residue ratio for the very low bandshaping ratio. The given definition has been chosen since we are interested in the maximum interference with another i-f signal. Fig. 8 plots the signal-to-residue ratio for this case making use of the definition given above. For a bandshaping ratio of 0.5 the signal-to-residue ratio is 32 db and the resolution loss is approximately 10 per cent over the linear time delay compressed pulse which produces the (sin x)/x pulse shape. Fig. 9 plots increase in pulse width vs. the shaping ratio. Fig. 10 plots the increase in signal-to-noise ratio obtained when the band shaping function in this example is used (linear spectrum phase is assumed). This increase can be attributed to the fact that the pulse compression filter originally specified is "matched" only as far as phase characteristic is concerned and not in the North matched filter sense.

57-9048

A somewhat different approach to residue reductions is the concept of selective attenuation of certain portions of the amplitude spectrum. An example of this is given in Fig. 11. The dashed line represents the modification to the spectrum caused by inserting narrow band filters at the band edges. The basic idea behind this is that certain portions of the spectrum contribute more to building up residue signals than to signal resolution. The pulse shape associated with this form of spectrum shaping is shown in Fig. 12. The residues are uniformly below 20 db, the first residue being 21 db below the peak of the desired portion of the signal. There is noticeably less loss in resolution for this residue level than for the bandshaping discussed previously.

Combinations of selective attenuation and other weighting functions may produce improved results and are being studied.

CONCLUSION

The type of spectrum associated with a linear FM pulse compression leads to certain pulse shape problems that are undesirable in a radar application. These may be attacked in a number of ways, as has been outlined, and the general area of results has been indicated. The particular utility of any method of pulse shape improvement will depend somewhat on factors that are determined by tactical considerations. Further study in this area is being pursued by Sperry and, undoubtedly, others in the field to achieve optimum utilization of the linear FM type of pulse compression.

CONFIDENTIAL

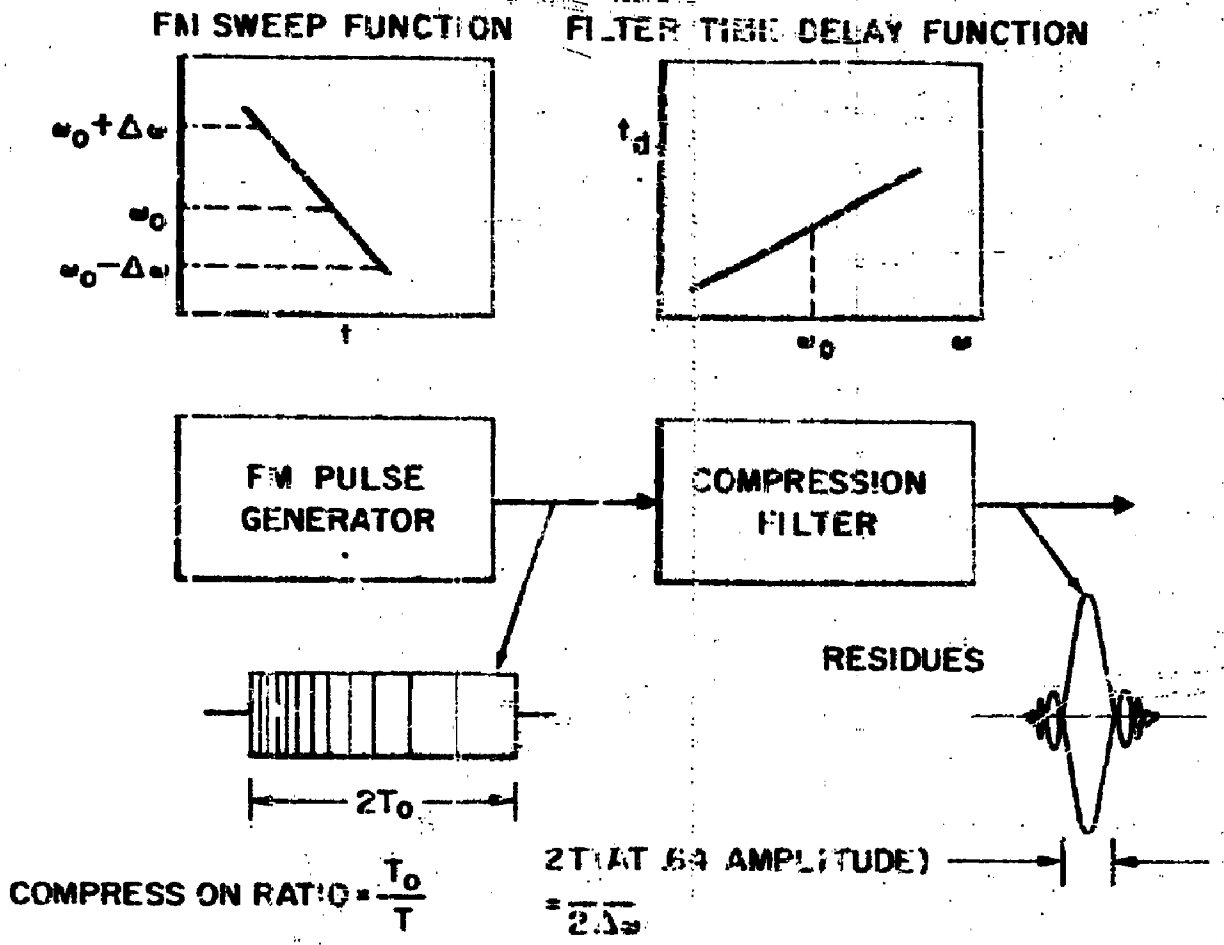

FIG I SIMPLIFIED DIAGRAM
OF LINEAR FM PULSE COMPRESSION

CONFIDENTIAL

57-9048

CONFIDENTIAL

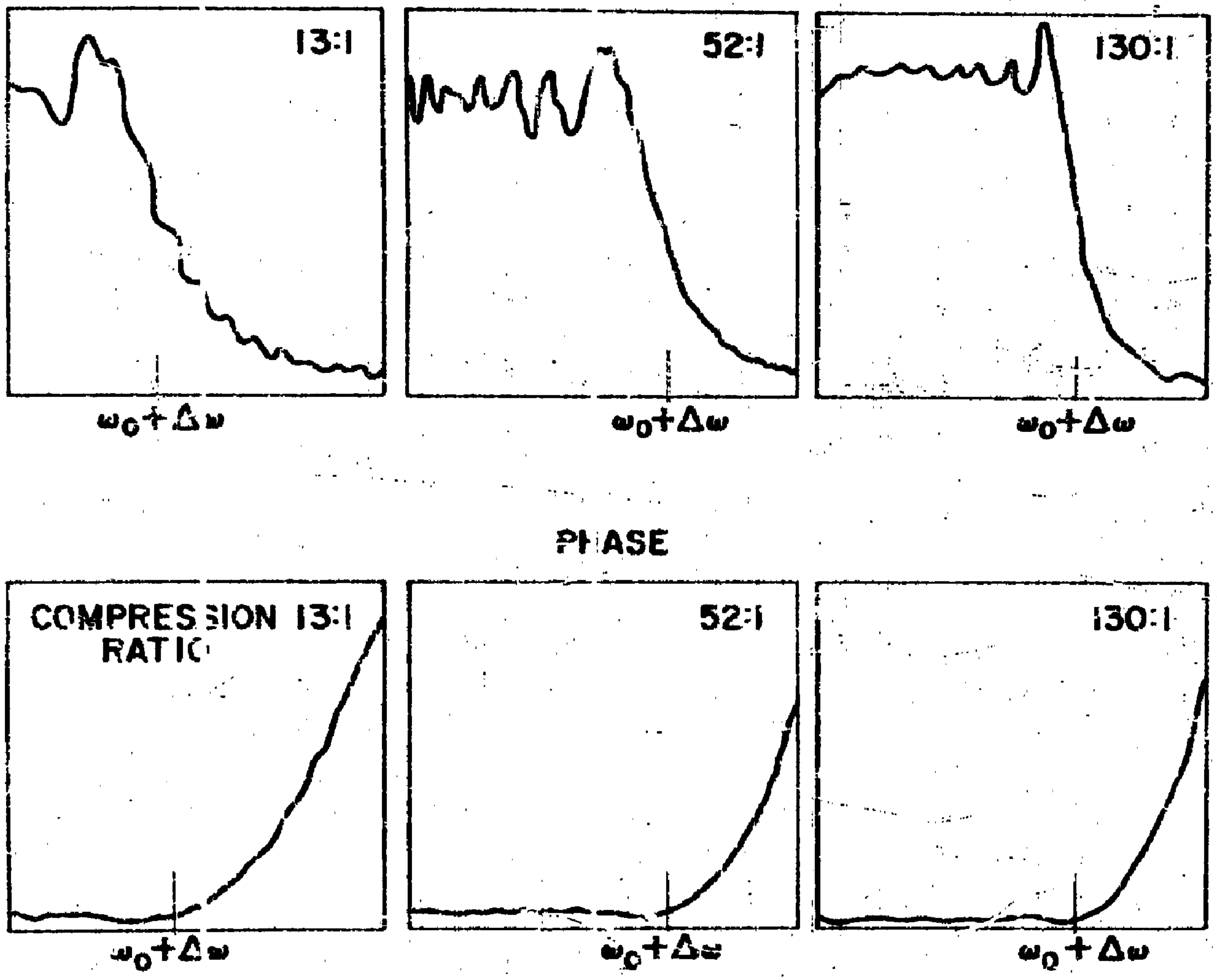

FIG 2 PULSE COMPRESSION SPECTRA

CONFIDENTIAL

CONFIDENTIAL

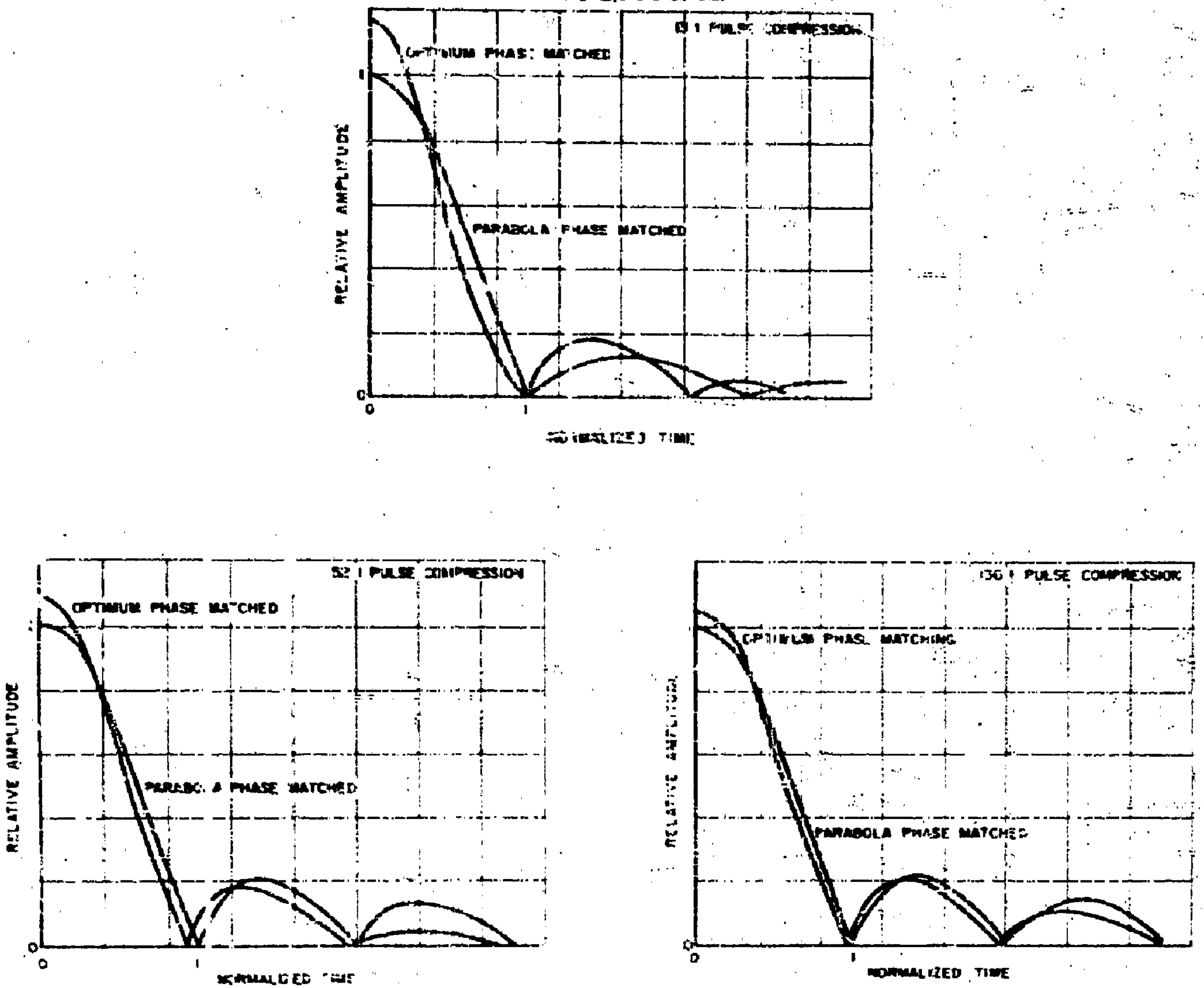

FIG. 3 EFFECT OF OPTIMUM PHASE MATCHING ON THE COMPRESSED PULSE SHAPE

CONFIDENTIAL

67-9048

CONFIDENTIAL

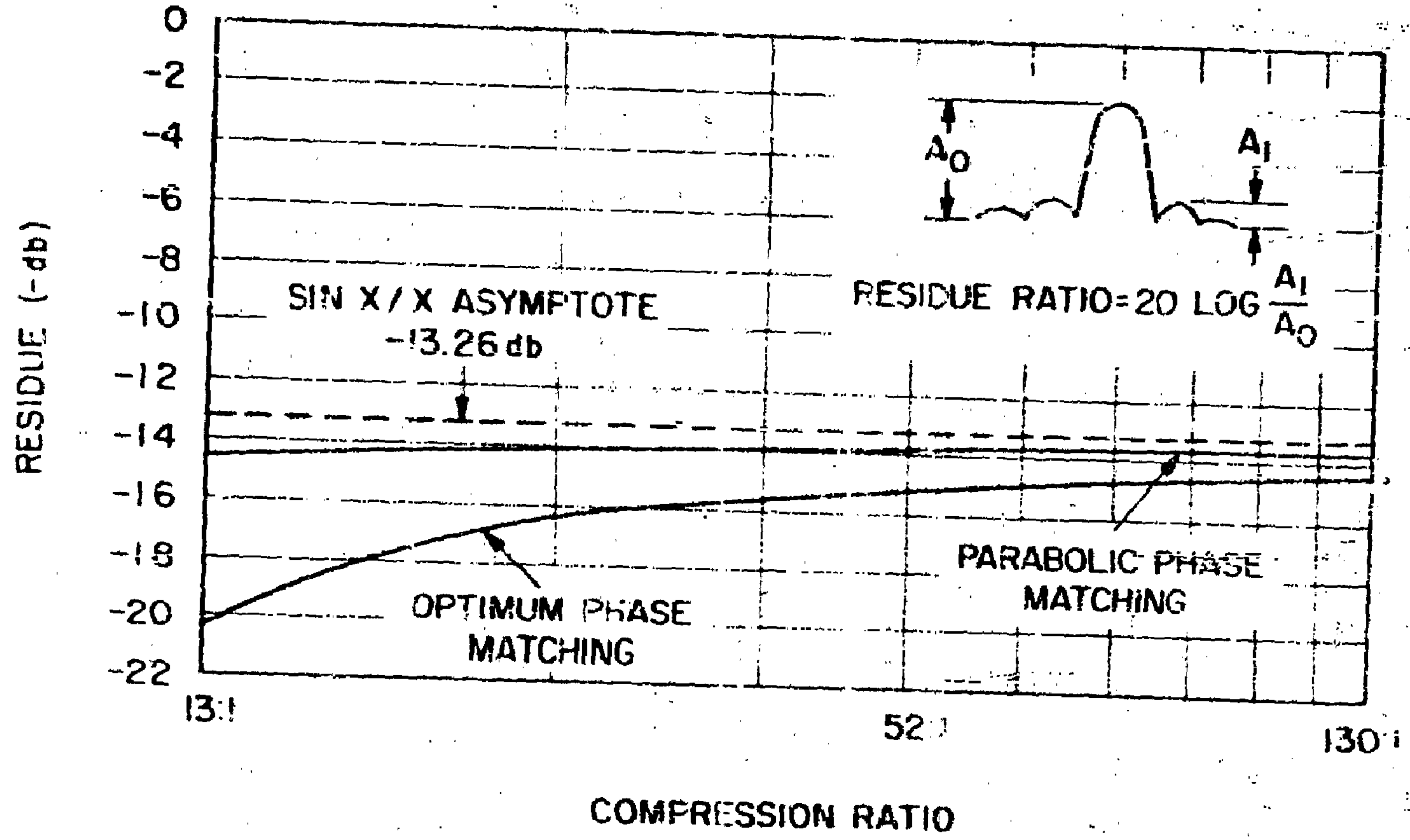

FIG. 4 RESIDUE IMPROVEMENT FOR OPTIMUM PHASE MATCHING

57-9048

CONFIDENTIAL

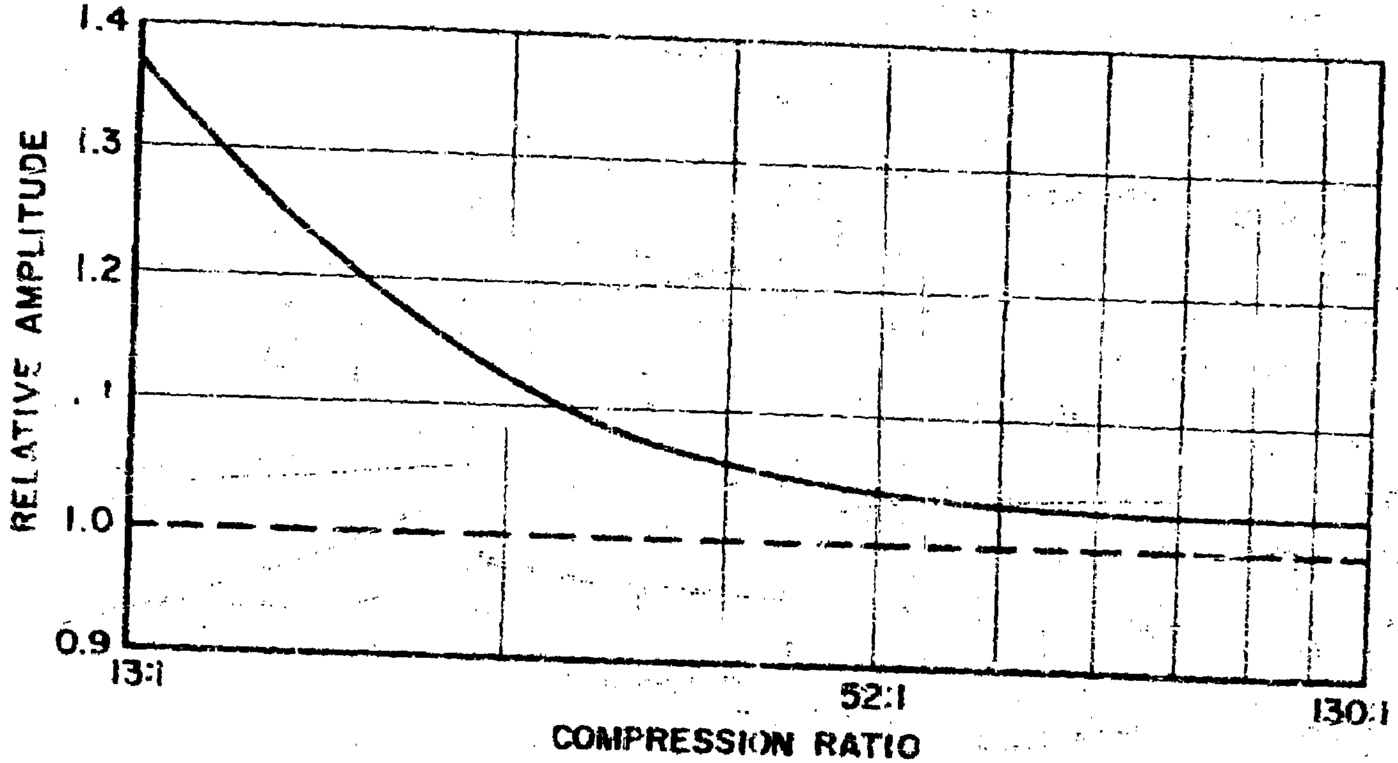

FIG. 5 AMPLITUDE INCREASE FOR OPTIMUM PHASE MATCHING

57-9048

CONFIDENTIAL

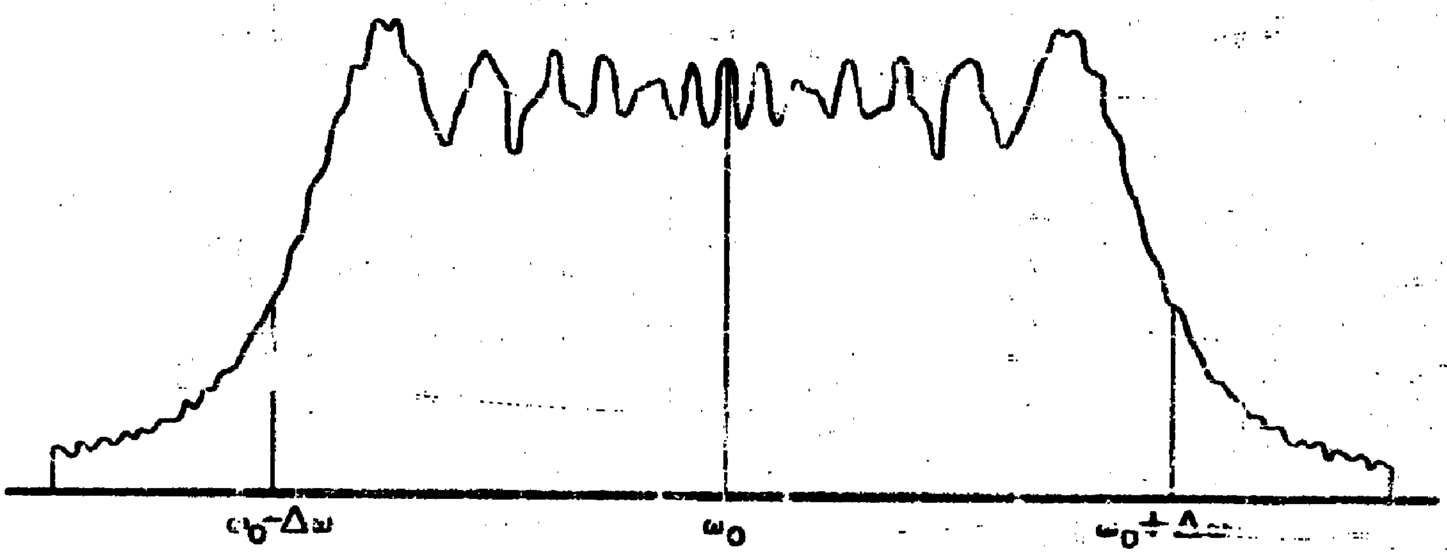

FIG 6 AMPLITUDE SPECTRUM 52:1 COMPRESSION RATIO

57-9048

CONFIDENTIAL

CONFIDENTIAL

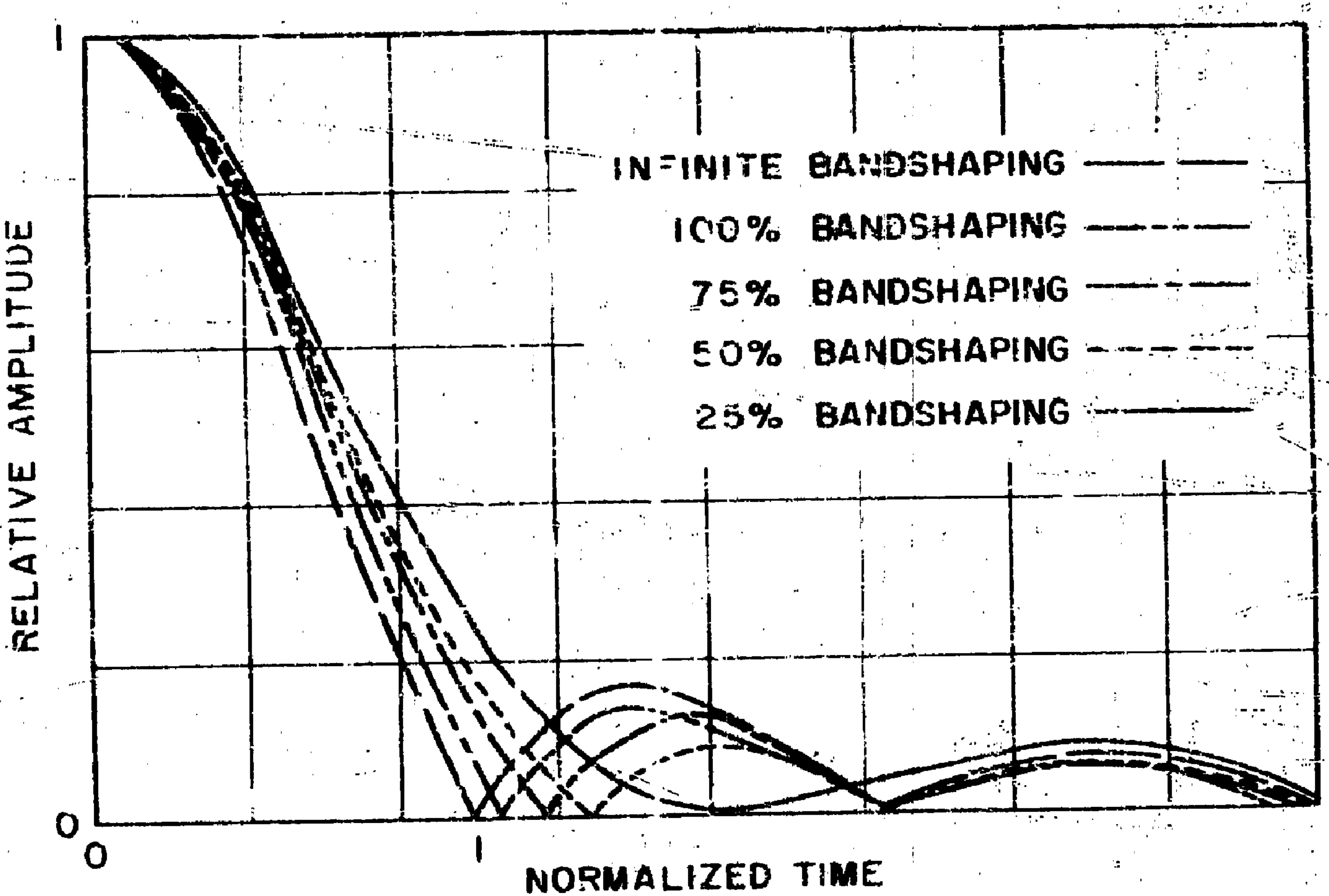

FIG. 7 EFFECT OF BANDSHAPING ON THE COMPRESSED PULSE SHAPE 52:1 COMPRESSION RATIO

57-9048

CONFIDENTIAL

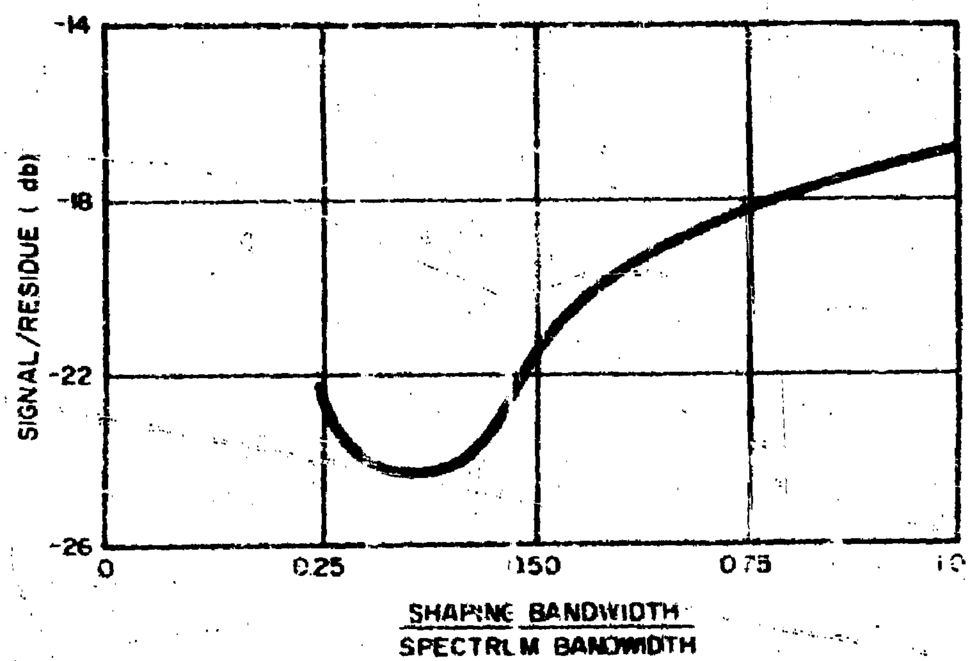

FIG. 8 SIGNAL/RESIDUE RATIO VS BANDSHAPING RATIO
52:1 COMPRESSION RATIO

CONFIDENTIAL

57-9048

CONFIDENTIAL

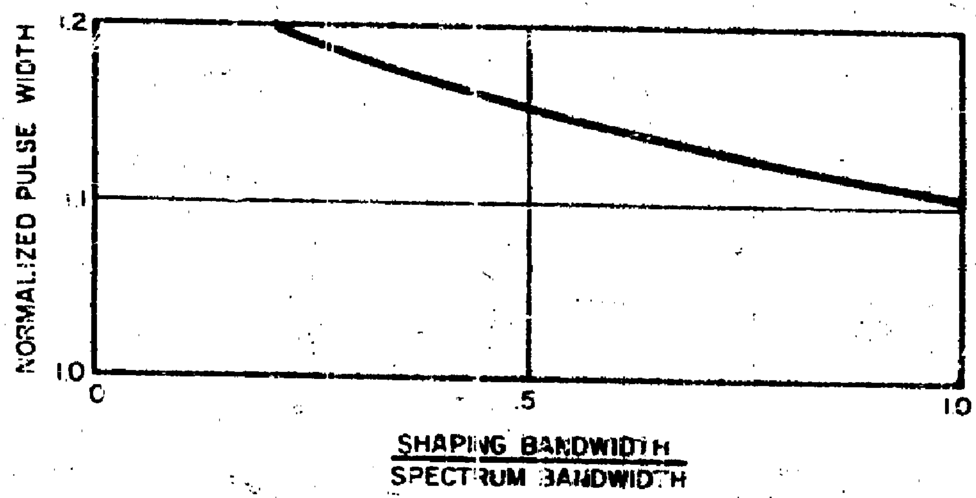

FIG. 9 EFFECTS OF BANDSHAPING ON PULSE SHAPE
52:1 COMPRESSION RATIO

CONFIDENTIAL

57-8048

CONFIDENTIAL

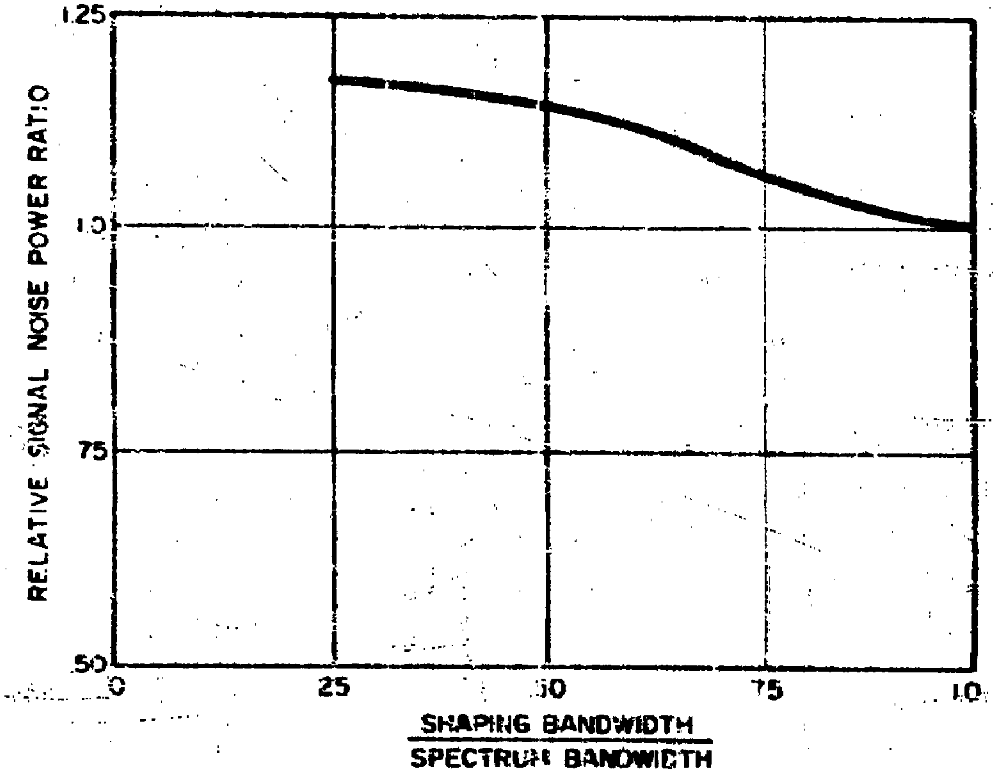

FIG. 10 OPTIMUM PHASE MATCHING ASSUMED
52:1 COMPRESSION RATIO

CONFIDENTIAL

57-9048

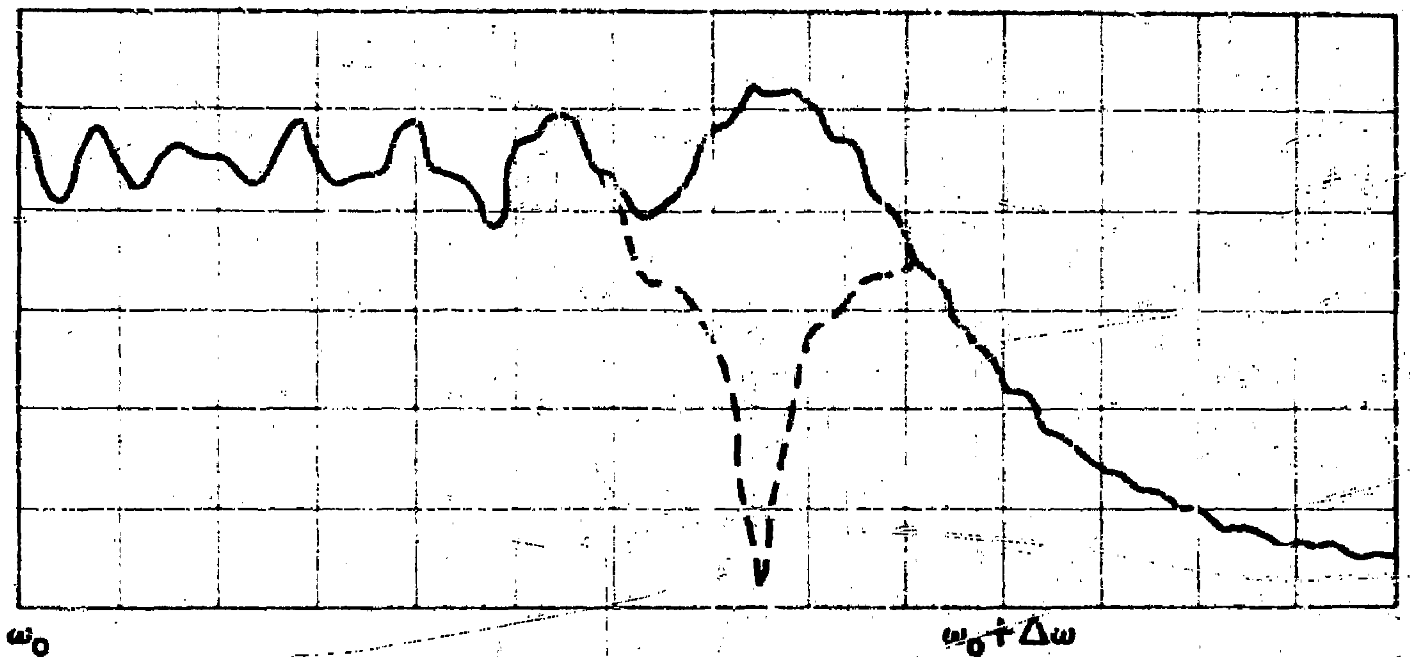

FIG. 11 EFFECT OF SELECTIVE ATTENUATION ON IF SPECTRUM
52:1 COMPRESSION RATIO

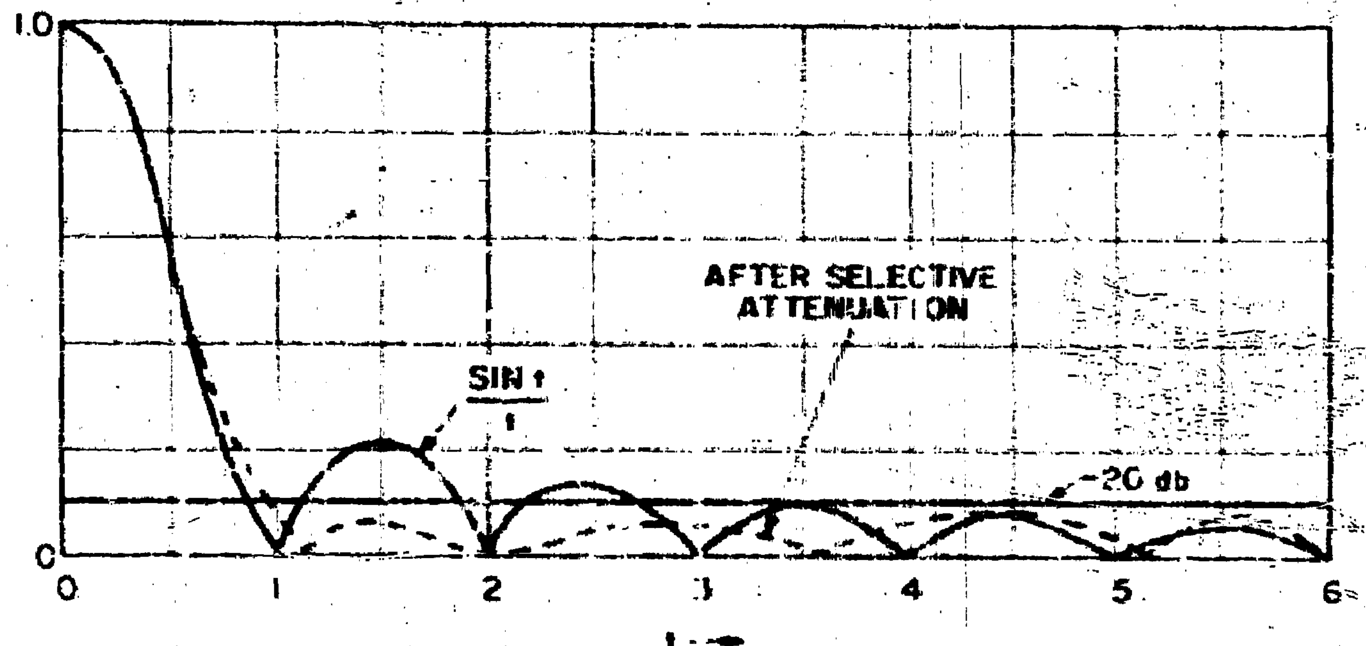

FIG. 12 EFFECT OF SELECTIVE ATTENUATION ON COMPRESSED PULSE SHAPE 52:1 COMPRESSION PULSE

57 9048